

Investigating neurodegenerative diseases with small molecule modulators

Reka Rebecca Letso

Submitted in partial fulfillment of the
requirements for the degree of
Doctor of Philosophy
in the Graduate School of Arts and Sciences

COLUMBIA UNIVERSITY

2011

©2011

Reka Rebecca Letso

All Rights Reserved

Abstract

Investigating neurodegenerative diseases with small molecule modulators

Reka Rebecca Letso

Elucidation of the mechanisms underlying cell death in neurodegenerative diseases has proven difficult, due to the complex and interconnected architecture of the nervous system as well as the often pleiotropic nature of these diseases. Cell culture models of neurodegenerative diseases, although seldom recapitulating all aspects of the disease phenotype, enable investigation of specific aspects of these disease states. Small molecule screening in these cell culture models is a powerful method for identifying novel small molecule modulators of these disease phenotypes. Mechanistic studies of these modulators can reveal vital insights into the cellular pathways altered in these disease states, identifying new mechanisms leading to cellular dysfunction, as well as novel therapeutic targets to combat these destructive diseases.

Small molecule modulators of protein activity have proven invaluable in the study of protein function and regulation. While inhibitors of protein activity are relatively common, small molecules that can increase protein abundance are quite rare. Small molecule protein upregulators with targeted activities would be of great value in the study of the mechanisms underlying many loss of function diseases. We developed a high-throughput screening approach to identify small molecule upregulators of the Survival of Motor Neuron protein (SMN), whose decreased levels cause the neurodegenerative disease Spinal Muscular Atrophy (SMA). We screened 69,189 compounds for SMN

upregulators and performed mechanistic studies on the most active compound, a bromobenzophenone analog designated cuspin-1. Mechanistic studies of cuspin-1 revealed that increasing Ras signaling upregulates SMN protein abundance via translation, an effect which may be associated with the translational regulator mammalian target of rapamycin (mTOR). These findings suggest that controlled modulation of the Ras signaling pathway may benefit patients with SMA.

Small molecule modulators of a disease phenotype, such as cell death, have the potential to reveal novel mechanisms regulating disease processes. This was exemplified by a screen for small molecule inhibitors of cell death caused by a pathogenic, misfolded mutant huntingtin protein in a cell culture model of Huntington's Disease (HD). These cell death inhibitors were found to target protein disulfide isomerase (PDI), an oxidoreductase known to be important in endoplasmic reticulum quality control of protein folding. However, our studies utilizing the small molecule PDI inhibitors determined that the cell death observed in this system was due to a pro-apoptotic function of PDI involving proteins of the mitochondrial outer membrane. We have begun studies aimed at identifying the binding mode of these novel small molecule inhibitors of PDI, in efforts to develop more potent and efficacious analogs for testing in animal models of HD. These studies have helped defined a novel mechanism linking protein misfolding to cell death, and may prove to be relevant to a broader range of protein misfolding diseases.

Table of contents

List of Figures and Tables.....	v
Acknowledgements.....	vii
Chapter 1: Spinal Muscular Atrophy.....	1
I. Treating inherited neurodegenerative diseases.....	1
a. Gain of function neurodegenerative diseases.....	2
b. Loss of function neurodegenerative diseases.....	5
II. Spinal Muscular Atrophy Disease.....	7
a. SMA disease pathogenesis.....	8
b. SMA disease phenotypes.....	9
c. Genetics of SMA.....	10
d. Animal models of SMA.....	15
III. Survival of Motor Neuron protein: Structure and Function.....	23
a. SMN expression and localization.....	23
b. SMN domain structure and functions.....	25
c. SMN interacting partners.....	28
i. The SMN Complex.....	29
ii. SMN interacts with hnRNP Q/R and β -actin mRNA.....	30
iii. SMN and profilin.....	32
iv. The possible role of actin dynamics in Spinal Muscular Atrophy.....	33
d. Neuronal function(s) of SMN.....	34
IV. Current state of small molecule therapeutics for SMA.....	46

V.	References.....	65
Chapter 2: Small molecule upregulator reveals regulation of SMN protein levels by Ras.....79		
I.	High-throughput screen for small molecule upregulators of SMN protein levels.....	79
II.	Screen development and optimization.....	81
III.	Screening and hit validation.....	83
IV.	Structure activity relationship of cuspin-1.....	86
V.	Cuspin-1 reveals link between Ras signaling and SMN protein levels....	88
VI.	Mechanistic studies of Ras-mediated upregulation of SMN protein levels.....	93
VII.	The Raf-MEK-Erk pathway is not responsible for Ras-mediated upregulation of SMN.....	96
VIII.	Mammalian target of rapamycin modulates SMN protein levels.....	101
IX.	The starvation response downregulates SMN protein levels.....	102
X.	SMN downregulation is stimulated by serum deprivation.....	102
XI.	Inhibition of mTOR by the small molecule rapamycin reduces SMN protein levels.....	104
XII.	SMN downregulation is mediated by the proteasome.....	109
XIII.	Discussion.....	114
XIV.	Methods.....	117
	a. Cell culture.....	117
	b. Small molecule libraries selected for screening.....	118

c.	Preparation of compound libraries for screening.....	120
d.	Primary screen.....	120
e.	Cytoblot fixation, permeabilization and antibody staining.....	121
f.	Cytoblot signal detection.....	121
g.	Dose-response experiments.....	122
h.	Robotic scripts and settings.....	123
i.	Analog synthesis.....	123
j.	Western blot analysis.....	123
k.	Retroviral preparation and transduction.....	125
l.	RT-qPCR of <i>SMN</i> transcripts.....	126
m.	³⁵ S-methionine/cysteine translation rate assay.....	126
IX.	References.....	128
Chapter 3:	High-throughput screening hit validation for Huntington’s Disease.....	133
I.	Phenotypic small molecule screening in neurodegenerative diseases....	133
II.	Pathogenesis of Huntington’s Disease.....	133
III.	Huntingtin protein.....	134
IV.	Protein misfolding and chaperones in neurodegenerative disease.....	135
V.	Protein disulfide isomerase in Huntington’s Disease.....	138
VI.	Validation of PDI as a mitochondrially-mediated pro-apoptotic stimuli.....	140
a.	Rescue of mutant Htt-induced cell death by Bcl-2.....	140
b.	Overexpression of PDI isoforms A1 and A3.....	144
c.	Mitochondrial outer membrane permeabilization (MOMP).....	146

d.	Crystallization condition screening for the a domain of PDI isoforms A1 and A3.....	146
VII.	Discussion.....	151
VIII.	Methods.....	152
a.	Cell lines and reagents.....	152
b.	Q103 PC12 plate-based viability assay.....	153
c.	PDI overexpression.....	153
d.	Bcl-2 overexpression.....	154
e.	Mitochondrial isolation.....	154
f.	MOMP assay.....	155
g.	Expression and purification of PDI A1 and A3 a domains.....	155
h.	Crystallization condition screening.....	157
IX.	References.....	158
Chapter 4. Conclusions and Future Directions.....		163
I.	Spinal Muscular Atrophy.....	163
a.	Summary.....	163
b.	Significance.....	164
c.	Future Directions.....	164
II.	Huntington’s Disease.....	169
a.	Summary.....	169
b.	Significance.....	170
c.	Future Directions.....	170
III.	References.....	172

Figures and Tables

Figure i. Low levels of SMN protein lead to SMA.....	13
Figure ii. SMN protein domain architecture.....	26
Figure iii. SMN knockdown results in axonal pathfinding defects in zebrafish.....	44
Figure iv. The pathogenic events occurring in motor neurons in SMA.....	47
Figure 1. Schematic of primary screening workflow.....	82
Figures 2. Dose-response of the SMN-upregulating compounds 72 and 81	84
Figure 3. Cuspin-1 upregulates SMN protein levels in SMA patient fibroblast cells.....	85
Figure 4. Structure-activity relationship of cuspin-1.....	89
Figure 5. Increased Ras signaling upregulates SMN protein abundance.....	91
Figure 6. Increased Ras signaling enhances SMN translation rate.....	94
Figure 7. SMN upregulation due to increased Ras signaling is not mediated by the Raf- MEK-Erk effector pathway.....	97
Figure 8. Small molecule inhibition of downstream Ras effector kinases does not inhibit oncogenic Ras-mediated upregulation of SMN protein levels.....	100
Figure 9. Serum starvation downregulates SMN protein levels.....	101
Figure 10. Treatment with the mTOR inhibitor rapamycin decreases SMN protein levels.....	105
Figure 11. Ras activation inhibits rapamycin-mediated downregulation of SMN protein levels.....	108
Figure 12. Inhibitors of autophagy cannot rescue starvation-mediated downregulation of SMN protein levels.....	110

Figure 13. Starvation-mediated downregulation of SMN protein levels is prevented by proteasome inhibitors.....	113
Figure 14. Cell based (PC12) model of mutant huntingtin protein misfolding and cell toxicity.....	136
Figure 15. Dose-response curves for hit compounds that suppress Q103-induced apoptosis.....	137
Figure 16. Overexpression of the anti-apoptotic protein Bcl-2 rescues from mutant Q103-HTT induced cell death.....	141
Figure 17. Overexpression of the anti-apoptotic protein Bcl-2 rescues morphology as well as viability from mutant Q103-HTT induced cell death.....	143
Figure 18. Overexpression of PDI leads to loss of cell viability in Q103-PC12 cells....	145
Figure 19. Overexpression of Bcl-2 rescues from PDI-induced MOMP in isolated mitochondria.....	147
Figure 20. Expression and purification of the PDI A1 a domain for crystallization trials.....	149
Table 1. Summary of small molecule screen.....	87
Table 2. Genotype-specificity testing of cuspin-1.....	87

Acknowledgements

I would very much like to thank my advisor, Dr. Brent Stockwell, for all the direction and advice he has given me during my graduate studies. His guidance brought focus to my work, while his willingness to follow the data to wherever it may lead gave me the freedom to engage in an abundance of (informative and educational) trial with the occasional error. Perhaps not every part of this project went in exactly the direction we were expecting, but the twists and turns sure have led to some interesting results, and I have learned a great deal along the way.

I would like to thank all the Stockwell Lab members, past and present, who have been a joy to work with and continue to teach me on a daily basis about what it means to be a good scientist. I will truly miss our lunchtime conversations. Special thanks belong to Mitch Lunn, who got me into this project in the first place, to Andras Bauer, who got me through it, and to Hemant Varma, who always pointed me in the right direction to keep moving forward.

There are many collaborators I would like to thank. Their willingness to share knowledge and reagents has brought great insights into my work and broadened by scientific horizons. I would like to kindly thank Dr. Christopher Henderson, Katisha Gopaul, Gist Croft and Mathieu Desacleux for the experiments involving human and mouse primary and embryonic stem cell-derived motor neurons. I would like to thank Dr. Barrington Burnett for confirmatory testing of cuspin-1, which reassured me that my compound really was active. I would also like to thank Dan MacDougall and Dr. Rubin Gonzalez for their expert assistance with polysome fractionation, exciting work which is

still underway. I would like to thank Dr. Liang Tong and the Tong Lab members Gabe Amodeo and Christine Huang for their help with our PDI purifications and crystallization trials. Although we never got a crystal, if you ever need a solubilizing fusion protein, boy do I have a domain for you. I would also like to thank the Columbia Motor Neuron Center and their lecture series, which have taught me just how many facets there are to truly understanding disease.

I am very grateful to Dr. Liz Miller and Dr. Liang Tong for their helpful discussions on my work, as well as Dr. Kenneth Olive and Dr. Ron Liem for their time serving on my committee.

Thanks belong also to my family and friends, who have always supported my decision to remain a near-eternal student and who have refrained (mostly) from asking the dreaded: “So, when are you graduating?” Look! The day is near!

I would like to give a big shout out to grad school for introducing me to a great group of friends and fellow scientists, and most importantly, to my fiancé, David Recinos. My biggest proponent, he has always believed in me far more than I could believe in myself, supported and encouraged me, and has quantifiably improved every aspect of my existence. Without David, and his delicious cooking repertoire, I would likely have starved to death long ago, and I therefore owe him my life.

So, Dave: “When are you graduating?” ;)

Chapter 1. Spinal Muscular Atrophy

Treating inherited neurodegenerative diseases

The development of pharmacological therapeutics for neurodegenerative diseases has been impeded by their complex etiology and the intricately entwined nature of the cells of the central nervous system¹. However, understanding the genetic alterations resulting in inherited neurodegenerative diseases, as well as the cellular pathways affected, may define new avenues for treatment. Monogenic diseases are particularly valuable as research tools, as animal models of monogenic diseases are generally straightforward to produce. These animal models can provide a wealth of information concerning the pathology of disease, as well as the underlying biochemical alterations resulting in cellular dysfunction.

Monogenic inherited neurodegenerative disorders can be further classified into two groups based on their proposed mechanisms of action: neomorphic and hypomorphic disorders. Neomorphic mutations are generally dominant, as they result from an “activated” mutant form of the defective protein. Hypomorphic mutations tend to be recessive, as they are normally caused by a severe decrease or loss of protein activity. Therapeutic strategies for these two types of diseases generally differ greatly, as one is aimed at inhibiting an active aberrant process, while the other requires substitution for the protein activity which is lacking. Approaches for inhibiting active processes are generally more straightforward than searching for methods to replace a lost function, and this is often reflected in the level of success of drug discovery efforts. This section provides

examples of both types of inherited neurodegenerative diseases and discusses the therapeutic strategies employed for each.

Neomorphic neurodegenerative diseases

Neomorphic diseases are characterized by excessive or ectopic activity of a mutated protein, resulting in cellular dysfunction and disease. Classical examples of neomorphic neurodegenerative diseases are those caused by expanded tri-nucleotide repeats. A common tri-nucleotide repeat expansion is that of the codon CAG, which codes for glutamine, resulting in proteins with expanded polyglutamine regions. Both Huntington's disease and Spinal Bulbar Muscular Atrophy (SBMA) result from expanded polyglutamine stretches in a single gene.

The genetic cause of Huntington's disease is an expansion in the CAG triplet repeat in the *huntingtin* (*htt*) gene, which results in a mutant Htt protein with an expanded polyglutamine stretch. Wild-type Htt contains between 6 and 35 glutamines in this region, however expansion greater than 36 repeats has been associated with development of Huntington's symptoms². Age of onset and severity of symptoms have been shown to be inversely correlated with the length of the polyglutamine stretch. 'Genetic anticipation' has been observed caused by further expansion of the polyglutamine stretch with successive generations, with a corresponding increase in severity and decrease in age of onset³. The pathogenic effect of mutant Htt is correlated with its degree of aggregation and therapeutic strategies against HD have been aimed at preventing polyQ-Htt

aggregation⁴ or enhancing clearance of the aggregated protein by stimulation of autophagy^{5,6}.

Spinal Bulbar Muscular Atrophy (SBMA) results from an expanded glutamine repeat in the first exon of the androgen receptor⁷. The mutant androgen receptor (mAR) accumulates in the nucleus in a testosterone-dependent manner, potentially explaining why only males show the degenerative phenotype. mAR causes adult-onset, progressive degeneration of the lower motor neurons, though other tissues have also shown to be affected. Loss of neuronal input from the lower motor neurons results in atrophy of the innervated muscles, leading to the phenotype of weakness and eventual paralysis. The testosterone-lowering hormone agonist leuprorelin has been studied for its ability to reduce the levels of pathogenic mAR, however the results of human trials have been somewhat conflicting^{8,9}. Additionally, the small molecule ASC-J9 has been demonstrated to increase the clearance of the androgen receptor¹⁰, providing another compound that can prevent the accumulation of the pathogenic mAR.

The CAG triplet is not the only codon in which expansion can result in pathogenic effects. Diseases involving other tri-nucleotide repeats include Fragile X Syndrome and Friedreich's Ataxia. Fragile X Syndrome is caused by expansion of a CGG triplet repeat, coding for a polyarginine tract, in the fragile X mental retardation 1 gene (*FMR1*) on the X chromosome. Mutations in *FMR1* result in cognitive impairments and increased likelihood of childhood seizures. FMR1 protein is highly expressed in the brain and is believed to play a role in cortical synapse development¹¹ and negative regulation of protein synthesis at neuronal synapses¹². Synaptic protein synthesis has been suggested to be positively regulated by the group 1 metabotropic glutamate receptors (Gp1 mGluR),

and inhibition of mGluR5 has been shown to be beneficial in animal models of Fragile X Syndrome¹³.

Friedreich's Ataxia (FRDA) is an autosomal recessive disease characterized by progressive sensory loss and loss of coordinated muscle movements, known as ataxia. FRDA is caused by an expansion of an intronic GAA triplet repeat in the frataxin (*FXN*) gene¹⁴. *FXN* is a mitochondrially-targeted protein involved in biogenesis of mitochondrial iron-sulfur cluster proteins, which are especially important for proper function of the electron transport chain¹⁵. The mutant *FXN* is expressed at lower levels, causing accumulation of mitochondrial iron and increased susceptibility to oxidative stress¹⁶. Therefore, the treatment strategies for FRDA have been mainly aimed at scavenging the reactive oxygen species produced by the mitochondrial damage¹⁷.

Amyotrophic lateral sclerosis (ALS) provides an example of a gain of function neurodegenerative disease not attributed to expansion of triplicate repeats. Approximately 1% of ALS cases have a discernable mutation in the *superoxide dismutase 1 (SOD1)* gene¹⁸. Mutations in *SOD1* result in degeneration of the upper and lower motor neurons, though the sensory neurons and cognitive functions are generally unimpaired. Selective motor neuron death has been attributed to increased reactive oxygen species as a result of *SOD1* mutation, and pharmacological treatments have focused on development of antioxidant SOD mimetics¹⁹.

Although differing in the exact nature of the mutation and gene affected, these neomorphic diseases share a common feature in that therapeutic interventions are generally aimed at preventing the toxic effects of the mutants, either by reducing the accumulation of the offending protein or directly inhibiting their gain of function effects.

Therefore, in some ways pharmacological development is simplified, as it does not always require a complete understanding of the effector pathways leading to cellular dysfunction and disease.

Hypomorphic neurodegenerative diseases

Development of treatments for hypomorphic diseases are generally not quite as straightforward as for neomorphic diseases, as they are not caused by a pathogenic gain of function mutation that can be “shut down”. Countering the loss of a protein’s activity generally requires a thorough understanding of the underlying pathology. Metabolic diseases provide a good example of how understanding the biochemical pathways affected can lead to management of the disease state. Metabolic diseases are generally caused by a mutation in a single gene encoding an enzyme required for the synthesis of a key cellular metabolite. Disease can occur by a toxic buildup of the metabolic precursor or due to loss of the enzymatic product. In the case of toxic accumulation, a diet restricted in the precursor can resolve the condition. In Phenylketonuria (PKU) a mutation in phenylalanine hydroxylase prevents conversion of phenylalanine to tyrosine. Elevated levels of phenylalanine reduces the CNS levels of methionine and tyrosine, resulting in decreased levels of dopamine²⁰. PKU requires a strict diet low in phenylalanine in order to prevent the mental degeneration caused by these unbalanced metabolic processes.

When the problem is loss of a metabolite, supplementation can markedly improve the course of the disease. Biotinidase deficiency, in which mutations in the biotinidase (*BTD*) gene prevent absorption of biotin (vitamin H or B7), results in seizures and ataxia

due to the body's inability to properly process fats, carbohydrates and the amino acids leucine and isoleucine ²¹. Supplementation with biotin can completely prevent all symptoms of BTD deficiency.

The negative consequences of these diseases are preventable due to a thorough understanding of the metabolic pathways affected. However, there are many other diseases for which the underlying pathology is unclear, often those involving non-enzymatic proteins. This lack of understanding often results in a lack of effective treatment options for these conditions. However, understanding the underlying condition can only get you so far. For many of these currently untreatable diseases, it is difficult to conceive of how one could pharmacologically remediate the absence of a protein function. An example of this is Duchenne muscular dystrophy (DMD), which is characterized by progressive degeneration of skeletal muscle, due to impairment of dystrophin. Dystrophin is required for proper attachment of the cytoskeleton to the basal lamina in skeletal muscle cells ²². In the absence of functional dystrophin, the extracellular membrane becomes more fragile, intracellular calcium levels increase and muscle cells undergo necrosis. Despite significant funding and decades of research, resulting in nearly 7,000 articles listed in PubMed under the search "Duchenne muscular dystrophy", the concept of a drug target in this disease remains untenable.

Another such disease is Spinal Muscular Atrophy ²³, an autosomal recessive neuromuscular disorder that is unusual in the realm of neurodegenerative diseases, as it is monogenic and demonstrates simple Mendelian inheritance patterns. Approximately 98% of SMA cases can be identified by a deletion or inactivating mutation in the Survival of Motor Neuron 1 (*SMN1*) gene ^{24,25}. Complete loss of SMN protein is embryonic lethal,

however, due to a gene duplication event, there exists a nearly identical copy of *SMN1*, termed *SMN2*. Due to a mutation in *SMN2* affecting splicing, it only produces a small fraction of the protein produced by *SMN1*. This small amount of SMN rescues the embryonic lethality, but results in degeneration of a subset of motor neurons and progressive atrophy of the innervated muscles ²⁶. Although the genetic alterations underlying SMA have been known since 1995 and are relatively straightforward, the mechanism resulting in the pathology of SMA is still unknown. The development of candidate therapeutics has focused on increasing the levels of SMN protein within the motor neuron, as without further knowledge of the underlying alterations in cellular pathways resulting in disease, this remains the only conceivable method of pharmaceutical intervention.

This thesis focuses on Spinal Muscular Atrophy, and the efforts made by ourselves and others at identifying candidate therapeutics and revealing novel molecular targets.

Spinal Muscular Atrophy Disease

Spinal Muscular Atrophy ²³ is an autosomal recessive neurodegenerative disease characterized by progressive degeneration of lower motor neurons. SMA presents clinically as atrophy of the proximal muscles, while later stages of the disease often result in quadriplegia. SMA is the most common autosomal recessive genetic disease that is lethal in infancy, with an incidence rate between 1 in 6,000 and 1 in 10,000 (0.02% to 0.01% of the population, respectively) ²⁷. This rate is comparable to more well-known

disorders such as Duchenne Muscular Dystrophy ²⁸. The carrier frequency has been estimated at 1 in 48 (approximately 2% of the population) ²⁹. SMA is found within all ethnic groups. However, a study of North American populations found that the carrier rates varied somewhat between ethnic backgrounds. Hispanic ethnicities had the lowest carrier rate at 0.8%, followed by African American at 1.1%, Asian at 1.8%, Ashkenazi Jew at 2.2% and Caucasians carrying the highest rate at 2.7% ³⁰. These values generally agree with the 2% carrier rate estimated previously, and demonstrate a relatively even pan-ethnic distribution.

SMA disease pathogenesis

In SMA, the primary step in disease progression is degeneration of the alpha motor neurons projecting from the anterior horn of the spinal cord ²⁶. Alpha motor neurons innervate skeletal muscles and are responsible for conducting action potentials initiating skeletal muscle contracture. Alpha motor neurons contact their corresponding muscle at a region termed the neuromuscular junction (NMJ). At the NMJ, motor neurons provide neurotransmitters to stimulate the muscle, and also provide the muscle with trophic support. Loss of normal motor neuron-to-muscle communication, via physical damage or neurodegenerative diseases such as SMA, results in atrophy of the corresponding muscle ^{31,32}.

Therefore, although the alpha motor neurons are the tissue directly affected in SMA disease pathogenesis, the primary physical manifestation is muscle weakness. The muscle groups most commonly affected are the proximal muscles, such as the shoulders

and hips ²⁶. Also affected are the intercostal muscles, which assist in breathing, although the diaphragm is generally spared. The facial muscles are unaffected, as are all sensory neurons, interneurons, upper motor neurons and alpha motor neurons projecting from the ventral horn of the spinal cord. Disease-specific targeting of sub-populations of neurons is not uncommon and is seen in several other neurodegenerative diseases such as Huntington's disease ³.

SMA is diagnosed first by general weakness and lack of muscle tone. In infants, it is often noted when the child does not reach its developmental milestones, such as being unable to hold up the head. Additionally, children with SMA have difficulty feeding and often develop a characteristic bell-shaped torso, due to the compensatory use of abdominal muscles for breathing as the intercostal muscles atrophy. In the clinic, additional tests used to confirm the diagnosis are electromyography, which records the electrical output capacity of a muscle group, as well as polymerase chain reaction (PCR) to determine whether there are mutations in the disease gene.

SMA disease phenotypes

SMA demonstrates a wide range of clinical severity, from the most severe Type 0 to the mildest form, Type IV. SMA Type 0 demonstrates prenatal onset with a median neonatal survival period of 7 months ³³. SMA Type I, also called Werdnig-Hoffman disease (OMIM 253300), is the most common form of SMA, making up approximately 50% of SMA cases. The onset of disease is usually prior to six months of age, and these patients generally do not ever acquire the ability to sit or stand independently. In addition to the weakness and muscle hypotonia observed in all forms of SMA, Type I patients also

display tongue fasciculation (twitching of the tongue due to spontaneous contraction of the muscles), hyporeflexia (lack of normal reflexes), and have difficulty eating and breathing. Most patients develop moderate to severe respiratory problems, often requiring support by a breathing apparatus. These breathing difficulties often lead to recurrent respiratory infections, such as pneumonia, which are the most common cause of death. The majority of SMA Type I cases do not survive past age two, although significant respiratory and nutritional support can prolong life span.

Type II patients (OMIM 253550) have an average age of onset between six months and two years, and also demonstrate a reduced life expectancy. They are normally confined to a wheelchair, as they can sit unaided but are unable to walk. These patients may also require respiratory support. Patients with Type III SMA, also known as Kugelberg-Wlinder disease (OMIM 253400), usually develop symptoms after 18 months of age, and can often learn to walk, but often develop the need for assistance within a few years after onset. Type III patients can have a normal life span. The least common Type IV form (OMIM 271150) is termed ‘adult-onset’ as symptoms develop normally after age 30³⁴. Type IV patients can usually sit and walk unaided, although they lose their ability for more strenuous exertion, such as continuing to participate in sports that they played prior to the onset of symptoms.

Genetics of SMA

The three common types of SMA, Types I-III, were determined to be genetically homogenous via linkage analysis studies which mapped the SMA-determining gene to

the chromosomal region 5q11.2-5q14 in 1990^{35,36}. It is of worth to note that the efforts aimed at identification of the gene mutated in SMA were a significant undertaking, due to the laborious nature of the gene mapping techniques available prior to whole genome sequencing. The region of interest was further refined in 1992, to the chromosomal region 5q13³⁷, and deletions within this region were noted to be a statistically significant occurrence in SMA patients²⁷. In 1995, Lefebvre, *et al.*, identified a 500kb inverted duplication within the 5q13 region, which contained a duplication of a little-studied gene that was disrupted in a large percentage of SMA patients²⁴. This gene was the aptly-named *survival of motor neuron (SMN)* gene.

In the 5q13 region, there are two copies of *SMN*. The gene that is mutated in the majority of SMA cases is the telomeric gene, *SMN1*. The disease modifying gene is the centromeric copy, *SMN2*. The two *SMN* genes are nearly identical, with only eleven nucleotide changes, five within the coding region²⁴. The nucleotide alterations within the coding sequence are all silent³⁸. The promoters of the two genes share common regulatory elements^{39,40} and the pre-mRNA sequences are 99.9% identical⁴¹. Additionally, both demonstrate ubiquitous expression of mRNA and protein^{24,42}. However, Monani *et al.* demonstrated that the single cytosine (C) to thymine (T) transition at position 6 in exon 7 in the *SMN2* gene resulted in alternative splicing of the majority of *SMN2* pre-mRNA's⁴¹. The alternatively spliced form of *SMN2* is truncated, missing exon 7⁴³. Loss of exon 7 is denoted as *SMNΔ7*. Although the loss of exon 7 has no affect on *SMNΔ7* mRNA, the truncated protein translated from the mRNA, termed SMNΔ7, is extremely unstable and does not accumulate to a quantifiable degree in cells⁴⁴⁻⁴⁶. It is important to note that the *SMN2* mRNA's that contain exon 7, termed *SMN-FL*

for full-length, generate the same protein produced in larger quantities by the *SMN1* gene. However, the *SMN2* gene does not produce enough full-length SMN protein to rescue from homozygous loss of the *SMN1* gene (Figure i).

There has been some debate over the mechanism by which the C/T transition in *SMN2* results in skipping of exon 7. Cartegni, *et al.*, first suggested that the nucleotide transition disrupted an exonic splicing enhancer (ESE) sequence required for inclusion of exon 7⁴⁷. This ESE motif was identified by computational analysis, which predicted binding by the serine/arginine-rich⁴⁸ proteins SF2/ASF, SC35, SRp40 and SRp55. *SMN1* was predicted to have a heptamer motif which was predicted to be strongly recognized by the splicing factor SF2/ASF. *In vitro* and *in vivo* splicing assay demonstrated that while the *SMN1* sequence was efficiently recognized by SF2/ASF, the sequence divergence of *SMN2* reduced its splicing efficiency greater than two-fold in these assays.

However, it has also been argued that rather than disrupting an ESE, the C/T transition in the *SMN2* gene created an exonic splicing suppressor (ESS) element⁴⁹. In this study, modulation of the levels of the SR protein SF2/ASF demonstrated only very mild effects on *SMN2* mRNA splicing, which did not agree with the previous report implicating SF2/ASF as the major protein regulating exon 7 inclusion. Instead, the authors hypothesized that *SMN2* mRNA contained an ESE, and demonstrated that this putative ESE is efficiently recognized by the splicing repressor protein, heterogeneous nuclear ribonucleoprotein A1 (hnRNP A1). Additionally, RNAi knockdown of hnRNP A1 as well as mutating the ESS resulted in inclusion of exon 7 in spliced *SMN2* transcripts. Cartegni, *et al.*, attempted to reconcile these results by proposing that hnRNP

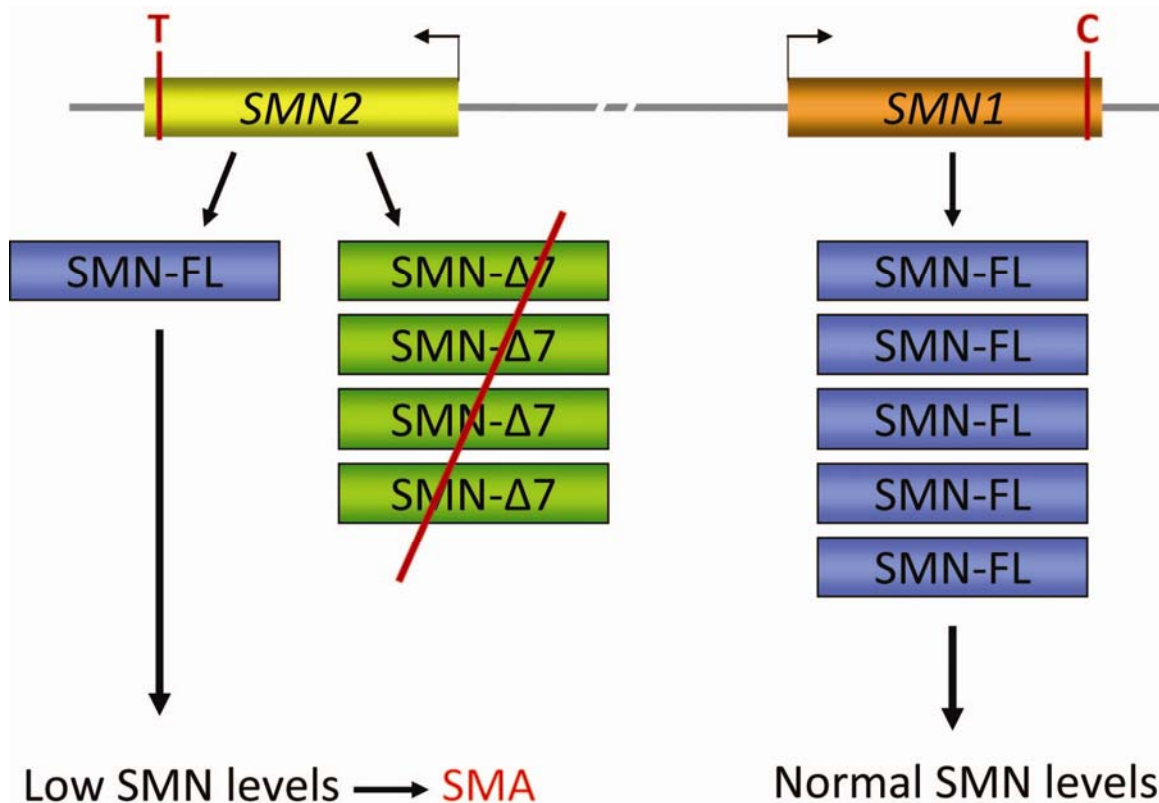


Figure i. Low levels of SMN protein lead to SMA.

The genomic organization of the *SMN* locus is depicted above. A 500kb inverted duplication in the *SMN* locus resulted in a near-exact copy of the *SMN1* gene, termed the *SMN2* gene. However, a C to T transition in exon 7 of the *SMN2* gene causes the majority of the transcripts to be alternatively spliced to exclude exon 7. This transcript is translated into a mutant SMN protein lacking exon 7, termed SMN-Δ7. SMN-Δ7 is unstable and quickly degraded. Therefore, the *SMN2* gene produces significantly less functional SMN protein compared to the *SMN1* gene. Upon homozygous loss of the *SMN1* gene, as is seen in many SMA patients, the low level of full length SMN protein produced by the remaining *SMN2* gene(s) is not sufficient to rescue motor neuron viability, resulting in Spinal Muscular Atrophy.

A1 antagonized SF2/ASF binding⁵⁰, however the validity of this model is still under debate.

The majority of SMA patients (over 98%) have homozygous deletions or mutations of the *SMN1* gene^{24,25}. As these patients express SMN protein only from their *SMN2* gene, this results in the patients' cells producing a significantly decreased quantity of SMN protein. However, patients can have more than one copy of the *SMN2* gene, due to the instability of the 5q13 chromosomal region. The clinical range of SMA severity has been strongly correlated with gene copy number⁵¹⁻⁵³. One to two copies of *SMN2* correlate with the most common form of SMA, type I, while increasing the *SMN2* copy number to four or five correlates with the less severe Type III cases. No patients have been reported with homozygous loss of both the *SMN1* and *SMN2* genes, suggesting that complete loss of SMN protein is lethal during embryonic development in humans. This hypothesis has evidence in numerous SMN knockout animal models, which demonstrated that the *smn* null background is non-viable in organisms ranging from yeast to mice⁵⁴⁻⁵⁷.

SMN1 is the only gene in which mutations have been associated with SMA to date. However, a recent comprehensive analysis of SMA patients identified 92% of patients had homozygous deletions of *SMN1*, 3.4% had intragenic mutations, while 4.6% had no identifiable mutation in the *SMN1* gene⁵⁸. As approximately 5% of SMA patients do not have an identifiable mutation of the *SMN1* gene, this may indicate that mutations in yet-undefined genes can result in SMA. Alternatively, these cases may be misdiagnosed as SMA, for example resulting from an environmental toxin mimicking the symptoms of SMA. Toxic insults leading to or imitating neurodegenerative phenotypes have been implicated in other neurodegenerative diseases, such as Parkinsons disease⁵⁹ and has

been suggested in the elevated incidence of ALS observed in professional Italian soccer players⁶⁰.

It is of interest to note that only *Homo sapiens* carry the *SMN2* gene. Even species as genetically similar as chimpanzees lack *SMN2*⁶¹, indicating that the gene duplication event occurred after the Homo-Pan (chimpanzee) split, which last shared a common ancestor circa 5-7million years ago⁶². However, as the *SMN2* gene is relatively evenly dispersed within all ethnic groups worldwide, the duplication event must have occurred prior to the *Homo sapiens* species migration from Africa, approximately 60,000 years ago⁶³. The rather high carrier rate of SMA (approximately 2%) suggests that it may have been selected for to remain within the population, however, no evolutionary advantage has been identified for SMA carriers to date. One hypothesis is that it may be involved in viral infection, as it has been demonstrated that the SMN complex interacts functionally with several viruses. The Lymphotropic Herpesvirus saimiri has been shown to co-opt the SMN complex for assembly of their own ribonucleoproteins⁶⁴. The mouse Minute virus has been shown to utilize SMN for activation of viral promoters⁶⁵. Additionally, components of the SMN complex have been shown to be important for HIV-1 infection⁶⁶. Therefore, it is possible that reduction in SMN protein levels could result in increased resistance to viral infection or reproduction, although there is no direct evidence to support this hypothesis.

Animal Models of SMA

In efforts to gain a better understanding of the cellular functions of SMN and the pathogenesis of Spinal Muscular Atrophy, animal models of SMA have been developed in several diverse model organisms, including *Schizosaccharomyces pombe* (fission yeast), *Drosophila melanogaster* (fruit fly), *Danio rerio* (zebrafish) and *Mus musculus* (mouse). Complete loss of SMN has been demonstrated to be lethal across all species tested^{54,57,67}, highlighting the evolutionary conservation of the essential function(s) of SMN.

SMN in Schizosaccharomyces pombe (fission yeast)

The yeast protein Yab8 was identified as the yeast orthologue of human *SMN* in *S. pombe*⁵⁴. Other yeast species, including the laboratory workhorse *S. cerevisiae*, lack an orthologue of human *SMN* (*hSMN*). Yab8 is an essential yeast protein, and is found in the yeast nucleus and cytoplasm. The yeast orthologue has 24% sequence similarity to human *SMN*, with the highest similarities clustered near the N and C terminus. However, despite these similarities *hSMN* cannot rescue loss of Yab8 in yeast, indicating incomplete replacement of an essential function. These regions have shown to be important for the self-oligomerization of hSMN as well as its interaction with its binding proteins⁶⁸⁻⁷⁰. The high level of conservation in these regions permits Yab8 to oligomerize with *hSMN* and bind to human Sm proteins, however Yab8 binds significantly more strongly with itself than with *hSMN*. Yab8 is found to be highly oligomerized by HPLC gel filtration, generally eluting in the range of 100-440kDa with no detectable monomer (32kDa). While the knockout of Yab8 is lethal, overexpression of Yab8 under a strong

promoter also had a negative effect on yeast growth rate and colony size, indicating that an overabundance of Yab8 is deleterious. This effect has not been observed in mouse models of SMA⁵⁶, suggesting it may be a yeast-specific effect.

Hannus, *et al.* also identified Yab8 as the *S. pombe* orthologue, and demonstrated that conditional knockdown of Yab8 inhibited splicing and lead to nuclear accumulation of polyadenylated mRNA⁷¹. The authors additionally characterized Yip1 as the orthologue of human *SIP1*. A yeast two-hybrid screen was utilized to detect proteins interacting with Yab8, which identified Yip1 as a binding partner. Yip1 has 45% sequence similarity with the human SIP1/Gemin2, a known binding partner of SMN⁷², and the authors suggest that Yip1 is the *S. pombe* orthologue of Gemin2. *In vitro* binding studies confirmed this interaction, as well as the ability of Yab8 to self-oligomerize. However, unlike Paushkin⁵⁴, Hannus did not observe efficient binding between the *S. pombe* Yab8 and human SMN, nor with the orthologous *SIP1*/Yip1, or the human Sm proteins, indicating the conservation of binding domains may not be as high as previously thought. While complete knockout of Yab8 prevented cell growth, conditional knockdown of Yab8 under a thiamine-repressible promoter demonstrated a severe splicing defect. Unspliced poly(A) mRNAs were shown to accumulate in the nucleus, demonstrating that Yab8 activity is required for splicing.

SMN in Caenorhabditis elegans (worm)

The *C. elegans* orthologue of *SMN*, CeSMN, was characterized by Miguel-Aliaga and colleagues⁶⁷. CeSMN is localized mainly to the nucleus, with diffuse cytoplasmic

staining, though CeSMN is excluded from the nucleus of blastomeres during mitosis. In order to determine the pattern of SMN expression in the adult worms, a CeSMN-GFP construct was created which included 3.5kb of the region upstream of the CeSMN promoter. GFP expression was observed in the nucleus of hypodermal, gut, muscle and germ cells, which the authors claimed was unusual, as the *C. elegans* germline is known to normally silence transgene expression within the germline cells⁷³. Interestingly, the excretory cell and neurons demonstrated cytoplasmic staining, in particular in the neuronal processes, suggesting that CeSMN may have an important alternative function in these cells. RNAi knockdown of CeSMN caused late embryonic developmental arrest in the majority of the F1 progeny. Those progeny which continued development demonstrated paralysis and sterility. The most prevalent phenotype was sterility, which was observed even in the least affected individuals. The sterility was due to an inability of the germ cells to mature, due to loss of the maternally provided spliced mRNA's normally packed into the maturing germ cells, indicating that knockdown of CeSMN had a strong negative effect on splicing in *C. elegans*. Overexpression of CeSMN resulted in a similar phenotype as knockdown, including locomotor defects and decreased number of progeny. This deleterious effect of overexpression has also been shown upon overexpression of the yeast SMN orthologue Yab8 in *S. pombe*⁵⁴.

Burt and colleagues utilized a yeast two-hybrid assay to identify additional binding partners of CeSMN⁵⁵. This screen identified 16 putative CeSMN interacting proteins, many of which demonstrated similarity to proteins involved in RNA processing and metabolism. The interaction with RNA processing proteins suggests that many of the functions observed in human SMN may be conserved across species. Additionally, the

authors identified the *C. elegans* orthologue of human Gemin2, which they termed SMI-1, for SMN interacting protein-1 (40% similarity). The expression of a SMI-1-GFP transgene was observed throughout entire lifespan of the worm, in the gut, some nerve cells in the head, ventral nerve cord cell bodies and body-wall muscle cells. Knockdown of SMI-1 resulted in locomotor defects, paralysis and sterility in adults, and complete embryonic lethality, demonstrating the essential nature of this protein.

SMN in Drosophila (fruit fly)

A *Drosophila* model of SMA was generated by creating animals with a missense mutation in the *Drosophila* SMN orthologue⁷⁴. This missense mutation (*smn*^{73A0}) resides within the YG-box, a region which is important for self-oligomerization and proper function of human SMN protein⁶⁸. Homozygous mutants demonstrated lethality at late larval stages, rather than the early embryonic lethality seen in mammalian models⁵⁷, due to maternally-contributed *smn* mRNA. This mutant also displayed motor defects, suggesting that the *Drosophila* SMN orthologue was also required for neuronal health. The motor defects were determined to be due to dysfunctionality of the neuromuscular junction (NMJ). The NMJ is made up of a motor neuron on the pre-synaptic side, which, upon being stimulated by an action potential, will release a neurotransmitter acetylcholine (ACh) in humans, glutamate in *Drosophila*) across the synaptic cleft. Binding of the neurotransmitter by the post-synaptic receptors located on the muscle cause excitatory postsynaptic currents (EPSCs), resulting in muscle contracture. The defects in the SMA model *Drosophila* caused reduced amplitude of the excitatory postsynaptic currents

(EPSCs), indicating that the signaling beginning in the pre-synaptic neuron was not being properly translated into contraction signaling at the post-synaptic side of the neuromuscular junction (NMJ). Additionally, although gross architecture of both the motor neuron and muscle were preserved, mild defects in synapse structure were evident, such as reduced clustering of the glutamate receptor. This model of SMA displayed significant SMA-like deterioration of motor function, which were determined to be due to defects at the neuromuscular junction. This defect was later shown to be rescued by modulation of the bone morphogenic protein (BMP) signaling pathway⁴⁸, suggesting a potential new therapeutic target, which has yet to be investigated in humans.

SMN in Danio rerio (zebrafish)

Similar axonal defects were observed in SMA model developed in zebrafish⁷⁵. Antisense morpholinos, which have been demonstrated to be effective at knocking down the levels of target mRNAs in zebrafish⁷⁶, were utilized to selectively decrease the levels of zebrafish SMN protein. Knockdown of zebrafish SMN in the embryo resulted in defects in axonal outgrowth and pathfinding, mainly in the form of truncated and improperly branched motor neuron axons. Other neuronal subtypes were unaffected, demonstrating a similar tissue-specific pattern as observed in SMA patients.

Expression of a human *SMN* transgene in the morpholino-decreased background resulted in partial rescue of the axonal defects, while expression of a pathogenic human *SMNΔ7* transgene did not, indicating that the axonal defects were due directly to loss of SMN activity. To determine whether SMN functioned cell-autonomously in the motor

neurons, zebrafish *smn* was specifically knocked down in individual motor neurons. Reduction of SMN protein levels in the motor neuron alone was sufficient to reproduce the axonal defects observed upon SMN knockdown in the whole organism, indicating that other cell types are not involved in SMA disease pathogenesis. However, as the invertebrate models of SMA each produced some species-specific effects that are not recapitulated in the human disease state, the development of mouse models were required in order to gain a more thorough understanding of disease pathogenesis in a mammalian system.

SMN in Mus musculus (mouse)

Mouse models have now been developed modeling from the most severe types of SMA to more mild forms. As mice have only the single murine *smn* (*mSmn*) gene, corresponding to human *SMN1*, homozygous knockout of *mSmn* results in early embryonic lethality⁵⁷. Mouse models of SMA are generated by replacing *mSmn* with a pathogenic human transgene. Mice with 1-2 copies of the human *SMNΔ7* transgene survive up to four days after birth, however they generally show progressive weakness and loss of motor neurons by postnatal day 2⁵⁶. Mice with eight or more copies of the human *SMNΔ7* transgene are phenotypically normal, providing strong evidence that upregulation of the human *SMN2* gene could be therapeutically beneficial.

Through the use of a severe mouse model of SMA, it was observed that loss of muscle function predates motor neuron loss⁷⁷. This was explained by the identification of significant defects in the neuromuscular junctions (NMJ) of the severe mice. These mice

show poor terminal arborization and immature acetylcholine receptor clusters, indicative of inadequate maturation of the NMJ⁷⁸. Defects in the NMJs have also been reported in human SMA patients⁷⁸, indicating that these mouse model faithfully recapitulate the disease pathogenesis of SMA.

To determine the temporal onset of NMJ defects, McGovern and colleagues expressed the HB9:GFP motor neuronal marker in the *hSMN2/mSmn*^{-/-} mouse model⁷⁹, to allow visualization of the axonal outgrowth. The gross morphology of the motor neurons (MNs) appeared intact, and no defects in axonal pathfinding or branching were observed indicating these defects are specific to the zebrafish model of SMA⁷⁵. In this study, approximately half of the intercostal synapses were shown to be deinnervated, however less severe denervation have been observed in human studies⁷⁸ as well as in other mouse models of SMA.

One such study was performed by Kong and colleagues, in which they utilized the severe *hSMN2/SMNΔ7/mSmn*^{-/-} mouse model to investigate perturbations at the NMJ⁸⁰. In this mouse model, the authors found a very low degree of denervation, even late in disease progression. Rather, they found that the primary deficiency was functional deficits in synaptic transmission, caused by defects at both the pre- and post-synaptic sites.

To determine whether defects due to decreased SMN expression occur cell autonomously in a mammalian model of SMA, Gavrilina and colleagues performed experiments to determine the spatial need for SMN⁸¹. Utilizing a severe mouse model of SMA (*hSMN2;mSmn*^{-/-}), they expressed SMN in either exclusively in the nervous system (using a prion promoter) or exclusively in the myofibers (using a human skeletal actin

promoter). Neuronal expression of SMN rescued the phenotype while muscular expression did not, agreeing with the zebrafish studies that decreased levels of SMN result in cell autonomous degeneration of motor neurons⁷⁵.

A serious question relevant to the treatment of SMA is the temporal requirement for SMN. Or in other words, how late in disease progression can the phenotype be rescued? To address this question, Hammond and colleagues created a mouse model with inducible alleles of murine *Smn*⁸². The induction of SMN production during early gestation could rescue the embryonic lethality seen in these mice, however induction during late gestation could not rescue the pups. This strongly suggests that there is a window of opportunity for treatment of SMA before the neuronal degeneration and consequent downstream defects become unable to be reversed. In theory, this ‘point of no return’ would be earlier in life for the Type I patients and later for the milder Type III patients.

Altogether, animal models of SMA have demonstrated that SMN is an evolutionarily conserved and essential gene. SMN is required for pre-mRNA splicing, and decreased levels of this protein result in axonal defects in both invertebrate and mammalian systems. Mouse models have been the most faithful in replicating disease phenotypes, and continue to be useful in therapeutics studies.

The Survival of Motor Neuron Protein: Structure and Function

SMN expression and localization

SMN mRNA and protein are expressed in all tissues of metazoan organisms^{83,84}, indicating that the activity of SMN is essential to cell function. The expression of SMN protein is developmentally regulated, with the highest expression levels observed during embryogenesis⁸⁵⁻⁸⁷, declining postnatally to low levels in most adult tissues^{84,85}. However, some tissues, including the CNS, the kidney and liver retain high levels of SMN expression into adulthood⁴², suggesting they may be more dependent on SMN activity. A study comparing the levels of SMN protein in Type I patients compared to phenotypically normal individuals found that SMN protein levels are reduced between 96-99% in spinal cords⁴², with a more moderate difference (70-90%) in fibroblasts, suggesting there may be cell type-specific pathways regulating SMN protein levels, and these pathways may be differentially regulated in the disease state.

SMN has been shown to be localized to the nucleus and cytoplasm in all cell types⁸⁸, although the fraction localizing to each region varies by cell type. Within the nucleus of some tissues, SMN can be found concentrated in punctate structures termed gems. The term gems stands for gemini of coiled bodies, as the two structures are often found in close proximity^{88,89}. Coiled bodies, also known as Cajal bodies, are nuclear sub-organelles involved in assembly of components of the RNA splicing machinery⁹⁰. The interaction between gems and Cajal bodies appears to be developmentally regulated as the two structures do not colocalize strongly in fetal tissues, however this interaction increases with age, with nearly complete colocalization in adult tissues⁹¹. This proximity first suggested a role for SMN in RNA splicing.

Since the discovery of gems in 1996, a great deal of progress has been made towards understanding the connection between SMN and gems and their role in pre-RNA

splicing. SMN has been identified to be a necessary component for the formation of gems, as RNAi knockdown of SMN in HeLa cells results in complete loss of gems⁹² and the number of gems has been demonstrated to be correlated with SMN protein levels and disease severity⁴². Although gems are seen in all fetal tissues⁹¹, they appear to be disassembled in some cell types upon maturation. Adult tissues of humans, pigs and rabbits were stained for SMN, however gems were not observed in blood vessels, cardiac and smooth muscle, stomach or spleen across all species⁸⁹. This suggests that gems are not absolutely required for formation of the pre-mRNA splicing machinery, and may serve as repository for excess spliceosomal assembly proteins.

SMN domain structure and functions

Human *SMN* mRNA contains eight exons (1, 2A, 2B and 3-7), and is translated into a 294 amino acid, 38kDa protein with no significant homology to other proteins. The tertiary structure of the SMN protein is poorly understood, with the exception of the Tudor domain in exon 3, which has been crystallized^{93,94}. Notable secondary structures within the SMN protein include the lysine-rich (K-rich) exons 2A and 2B, the extended proline-rich domain (P-rich) in exons 5 and 6 and the tyrosine/glycine rich region (YG box) in the C-terminal end of exon 6 (Figure ii).

The Tudor domain in exon 3 has been identified as the Sm protein binding region⁶⁹. The missense mutations E134K and W92S, which have been identified in SMA patients lacking the more common homozygous *SMN1* deletion pattern, reside within the Tudor domain and have been demonstrated to significantly reduce the ability of the SMN

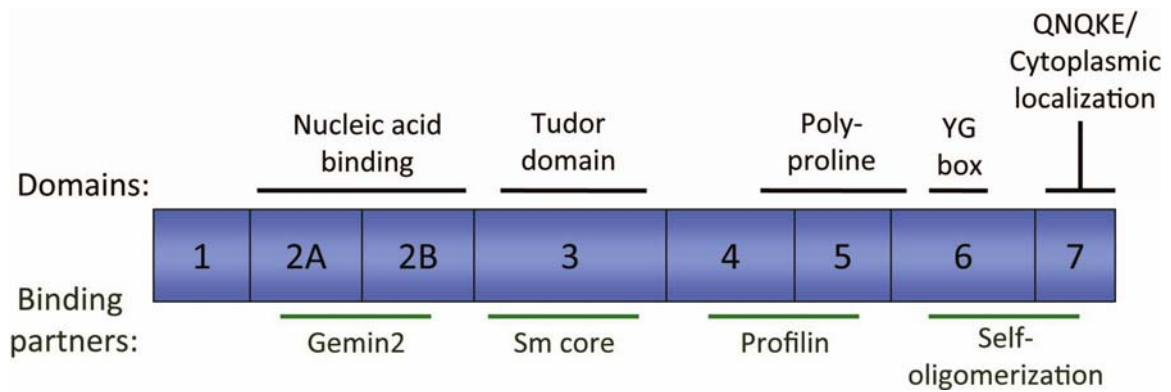


Figure ii. SMN protein domain architecture.

SMN protein is 294 amino acids long, and the relative exon sizes are diagrammed with the exon number within. Identified protein domains and an abbreviated list of SMN protein interacting partners.

complex to bind Sm proteins^{70,95}. The E134K mutation, as well as the I116F and Q136E mutations also identified within the Tudor domain, have been shown to negatively affect U snRNP assembly^{69,96,97}. Although these SMA-causing mutations suggest that the primary cause of SMA is a defect in spliceosome assembly, a hypothesis with several proponents^{69,98-100}, there exist other SMA-causing mutations within this domain that do not affect Sm protein binding⁷⁰ or snRNP assembly⁹⁶. At this time it is unclear how strong a role the Tudor domain plays in the development of SMA, and mutations resulting in SMA have been identified in other domains as well.

The SMA missense mutations D30N and D44V have been identified in the K-rich exon 2A⁷⁰. Together with exon 2B, this region is required for binding Gemin2/SIP1, a major component of the U snRNP-assembling SMN complex^{72,101}. However, these mutations do not show a defect in SMN binding to Gemin2⁷⁰, nor do they significantly affect Sm protein binding or snRNP assembly^{70,96}, indicating that this region may have additional functions that have yet to be identified.

Animal model studies have demonstrated that these mutant forms of SMN are not functional alone, as they cannot rescue survival in the absence of a human *SMN2* transgene¹⁰². Instead, these partially functional mutants require a limiting amount of wild-type SMN in order to assemble snRNPs *in vitro*, as demonstrated by complementation studies⁹⁸; *in vivo* the small amount of wild type SMN would be provided by the *SMN2* gene. This suggests that SMN functions as an oligomer, and that the heteromers made up of the mutant and wild type SMN proteins restore sufficient function for survival of the organism, but not enough to prevent degeneration of the motor neurons. There is strong *in vitro* evidence for SMN's ability to self-associate,

including observed oligomerization of SMN^{103,104} and gel filtration studies which have estimated that SMN is stably organized as an octamer¹⁰⁵.

The C-terminal region of SMN has been shown to be important for self-oligomerization. Mutations in the C-terminal exons 6 and 7 generally affect the ability of SMN to self-oligomerize, and the YG box in exon 6 has been shown to be vital for this self-association⁶⁸. The severe oligomerization defects associated with the SMA mutations Y272C and G279C/V significantly affect SMN activity, as demonstrated by decreased U snRNP assembly^{96,103,104,106,107}. These mutants also result in severe Type I SMA in patients with one to two copies of *SMN2*. The exon 7-deleted SMN protein (SMN Δ 7) mainly produced by *SMN2* also falls into this category, as it demonstrates a reduced capability for self-oligomerization¹⁰³, making it unable to compensate for the decreased levels of full-length SMN due to homozygous *SMN1* deletion.

SMN interacting partners

In addition to self-association, SMN has been shown to interact with a diverse array of proteins involved in many cellular functions, such as apoptosis¹⁰⁸⁻¹¹⁰, assembly of U snRNPs^{72,101}, and axonal transport of mRNAs^{111,112}. The ability of SMN to interact with both the RNA and protein components of many RNP complexes have led some to suggest it is an assemblyosome for RNPs^{113,114}. The most well-defined RNP assembly function of SMN is its construction of the U snRNPs, which is performed by the macromolecular structure termed the SMN complex.

The SMN Complex

The SMN complex is responsible for assembly, fidelity and transport of uridine-rich small nuclear ribonucleoproteins (U snRNPs) ^{115,116}, which in part make up the mammalian spliceosome. U snRNPs are composed of a ring of seven Smith-class (Sm) proteins and a unique small nuclear RNA (snRNA) ¹¹⁷. The snRNA is responsible for recognition of their cognate splice sites on pre-mRNAs ¹¹⁸. The SMN complex has been shown to be necessary and sufficient for assembly of U snRNPs *in vitro*, and prevents the promiscuous association of Sm proteins with other RNAs ^{115,119}.

The SMN complex consists of multiple units of SMN in a large macromolecular complex with nine additional proteins: Gemin2/SIP1, Gemin3/DP103, Gemin4, Gemin5/p175, Gemin6, Gemin7, Gemin8 and UNR-interacting protein (UNRIP) ^{101,120-126}. Gemin3 and 5 contain notable protein motifs. Gemin3 contains the Asp-Glu-Ala-Asp DEAD-box motif ¹²⁰, and has been demonstrated to have ATP-dependent RNA helicase activity ¹²⁷, which may be required for the SMN complex's assembly of RNPs. Gemin5 contains 13 WD repeats ¹²², which may be involved in scaffolding of the many protein-protein interactions directed by the SMN complex.

The SMN complex is highly stable, remaining associated even in stringent *in vitro* conditions ¹¹³. Gemin 2, 3, 5 and 7 bind SMN directly, while Gemin4 binds via Gemin3 and Gemin6 binds via Gemin7. The Gemin proteins colocalize with SMN both in the cytoplasm and in nuclear gems ^{101,120,122,124}. The SMN complex assembles snRNPs in the cytoplasm, however the Sm proteins must first be dimethylated by the protein arginine methyltransferase complex (PRMT5) in order to be recognized by the SMN complex ¹²⁸⁻

¹³². The dimethylarginine-modified Sm proteins are then transferred to the SMN complex, which mediates their proper assembly onto their respective snRNAs ^{72,101,133} bound by Gemin5 ¹³⁴. The 7-methylguanosine cap of the snRNA is then hypermethylated by trimethylguanosine synthetase 1 (TGS1) ¹³⁵, and several 3' nucleotides on the 3' termini of the snRNPs are trimmed, which appear to increase the import kinetics of the snRNPs ¹³⁶. The snRNP-SMN complex is then imported into the nucleus via its interactions with snurportin ¹³⁷ and importin- β ¹³⁸. Within the nucleus, the SMN complex as well as the snRNPs are concentrated within the nuclear sub-organelles called Cajal bodies ¹³⁹, where the snRNPs undergo further maturation ¹⁴⁰.

Lack of functional SMN complex has been proposed to be the cause of SMA ^{98,99}, however many have voiced concerns over the ability of a ubiquitous and essential function to mediate motor neuron-specific cell death. Animal models of SMA have both supported ^{98,99} and opposed ^{107,141} the hypothesis that decreased snRNP assembly is the cause of SMA, however alternative hypotheses have begun to gain favor after the identification of additional, neuron-specific SMN-protein complexes.

SMN interacts with hnRNPQ/R and β -actin mRNA

A yeast two-hybrid study identified the heterogeneous nuclear ribonucleoproteins (hnRNP) R and Q as binding partners for SMN ¹⁴². The C-terminal ends of the hnRNPs R and Q are likely required for SMN protein binding, as they contain arginine-glycine-glycine (RGG) domains which have been shown to be important for Sm protein binding to SMN ¹⁴³. Of note, these hnRNPs bind wild-type SMN protein *in vitro*, but not the

various SMA mutants E134K, S262I, T274I, Y272C, G279V, Δ exon7, Δ exon5, Δ exon5+7, indicating this complex could be relevant to the disease state. Additionally, hnRNP R was demonstrated to be expressed most prominently in motor neurons, rather than other neuronal subtypes, such as sensory peripheral nerve and Schwann cells ¹⁴², suggesting it may have motor neuron-specific functions. Both hnRNP R and Q were determined to be developmentally regulated in mouse spinal cord, with high expression levels during late embryogenesis and significantly decreased postnatal levels, a temporal expression pattern similar to SMN. hnRNP R colocalized with SMN in the cytoplasm and axons of mouse spinal cord sections and embryonic motor neurons. Although it was present in the nucleus, it did not colocalize with nuclear SMN, suggesting that hnRNP R binding to SMN is independent of the snRNP assembly functions of the SMN complex. Due to difficulties with the antibody against hnRNP Q, only colocalization between hnRNP R and SMN could be determined in this study.

The complex of SMN bound to hnRNP R was later demonstrated to have vital neuronal functions as overexpression of either SMN or hnRNP R stimulated neurite outgrowth in neuronal-like PC12 cells in culture ¹⁴⁴. Neurite length was not affected upon expression of an hnRNP R mutant lacking the SMN interaction domain, indicating that the interaction of SMN and hnRNP R is necessary to mediate this function in the axon. Next, the authors tested the importance of the SMN-hnRNP R heterocomplex in motor neurons isolated from a severe mouse model of SMA ⁵⁶. These SMA motor neurons demonstrate reduced axonal outgrowth in culture, with smaller growth cones and decreased levels of *β -actin* mRNA and protein within the growth cone. hnRNP R contains two primary RNA recognition motifs (RRMs) ¹⁴², which can bind *β -actin*

mRNA via a 54 nucleotide zipcode sequence within its 3' UTR. This zipcode has been shown to be both necessary and sufficient for peripheral localization of *β-actin* mRNA¹⁴⁵.

Knockdown of hnRNP R in isolated mouse motor neurons demonstrated a similar defect in axonal outgrowth and *β-actin* mRNA translocation as was observed in the motor neurons isolated from the SMA model mice¹¹¹, suggesting that a SMN-hnRNP R heterocomplex is responsible for transporting *β-actin* mRNA to the growth cones. This model also suggest that defects in this function, via decreased levels of SMN or hnRNP R, lead to reduced axonal outgrowth and defects in presynaptic maturation¹¹¹. Deficiencies in pre-synaptic differentiation have been observed in SMA mouse models^{78,146}, strongly suggesting that this pathway may be affected in SMA patients.

SMN and profilin

Another SMN heterocomplex which has been shown to have neuron-specific effects is the SMN-profilin complex, providing another alternative hypothesis for the motor neuron-specific phenotype observed in SMA patients. The polyproline (P-rich) region in exons 5 and 6 of SMN have been shown to bind profilins¹⁴⁷, and colocalization has been observed in the growth cones of cultured PC12 cells¹⁴⁸. Profilins are actin-binding proteins which can regulate actin polymerization dynamics by sequestering β -actin monomers, preventing them from being added to growing actin microfilaments¹⁴⁹. BIAcore studies indicated a strong, specific interaction between SMN and profilin IIa¹⁴⁸, the major neuronal isoform of profilin in mammals¹⁵⁰. The observed interaction was

abolished when pathogenic mutants of SMN were utilized in the study. RNAi studies in PC12 cells demonstrated that reducing SMN protein levels resulted in increased expression of profilin IIA, and together with decreased availability of SMN, leads to increased formation of the profilin IIA/RhoA/ROCK complex¹⁵¹.

Activation of the Rho-associated kinase¹⁵² by the small GTPase RhoA is involved in cytoskeleton-mediated motility, polarity and gene expression¹⁵³. These effects are mediated by phosphorylation of myosin light chain (MLC) which inhibits neuronal outgrowth and differentiation¹⁵⁴. Regulation of neuronal outgrowth by ROCK has been shown to be mediated in part by profilin IIA's control of actin polymerization¹⁵⁵. Therefore, increased formation of the profilin IIA/RhoA/ROCK complex can result in inhibition of neuritogenesis, suggesting an alternative mechanism for the decreased axonal outgrowth observed in motor neurons isolated from SMA model mice¹⁴².

The possible role of actin dynamics in Spinal Muscular Atrophy

The studies identifying profilin IIA and hnRNP R as SMN binding partners suggested an important role for SMN in actin dynamics and regulation of the cytoskeleton. A study searching for SMA-modifying genes in discordant SMA families, (families with siblings who have the same genotype but display different severity of phenotypes) demonstrated 3-fold higher expression levels of the actin-bundling protein plastin 3 (PLS3/T-plastin) in unaffected individuals versus their affected counterparts¹⁵⁶. The unaffected *SMN1*-deleted siblings who expressed increased levels of PLS3 also had significantly increased levels of filamentous actin (F-actin), which has been shown to be

vital for axon outgrowth and pathfinding¹⁵⁷. These findings were validated in motor neurons isolated from an SMA model mouse, where overexpression of PLS3 rescued the axonal outgrowth defects of the SMN-deficient neurons, albeit not completely¹⁵⁶. However, another study utilizing an SMA mouse model demonstrated that increasing the levels of PLS3 could not rescue the SMA phenotype, even upon concomitant knockdown of profilin IIa, suggesting that additional factors may be involved in the dysregulation of actin dynamics in the disease state¹⁵⁸. However, as SMN and PLS3 were found to be colocalized in the axons and growth cones of wild-type mouse motor neurons, this study identifies yet another SMN binding protein involved in the regulation of actin dynamics.

The importance of the cytoskeleton in SMN-deficient motor neurons was highlighted in a recent study which demonstrated significantly increased survival in an intermediate mouse model of SMA¹⁵⁸ treated with the ROCK inhibitor Y-27632¹⁵⁹. The treated mice had improved motility and neuromuscular junction innervation, although surprisingly Y-27632 did not rescue the motor neuron loss seen in this mouse model. Additionally, treatment with the ROCK inhibitor in a severe mouse model of SMA showed no rescue, suggesting that the axonal defects in this model are either too multifaceted or too severe to be compensated by inhibition of ROCK alone. However, this study strongly supports an involvement of cytoskeletal dynamics in the pathogenesis of SMA.

Neuronal function(s) of SMN

SMN has been demonstrated to be highly expressed in neuronal tissues *in vivo*⁴², and has been shown to localized to neurites and growth cones in neuronal cells in culture¹⁴⁸. Within the CNS, *SMN* gene expression was found to be selectively enriched in specific cell populations. In the spinal cord, *in situ* hybridization revealed strong staining in the ventral horn, with little staining in the dorsal horn. Interestingly, SMN protein expression was found most highly expressed in the cytoplasm of neurons in the spinal cord and brain⁸⁶, as opposed to the strong, punctate nuclear staining generally observed in cells in culture. The authors propose that the difference in the localization of SMN is due to fully-differentiated, post-mitotic nature of the cells being studied within the tissues. However, other studies have reported gem-like nuclear staining within post-mitotic motor neurons¹⁶⁰. SMN protein expression was reported to be highly abundant in the neurons of the deep cerebellar nuclei, pallidal neurons in the basal ganglia, layer V pyramidal neurons of the neocortex and motor neurons in the brainstem and spinal cord⁸⁶. Defects in the development of these brain regions have been recently observed in a mouse model of severe SMA¹⁶¹.

Neuronal defects observed in animal models of SMA

SMN had also been proposed to have important functions in axonal outgrowth and formation and maturation of the neuromuscular junction (NMJ). Several animal models of SMA have been utilized to gain further understanding of SMN's role in neurons. Knockdown of *Smn* in zebrafish results in defects specifically in motor neurons, such as abnormally branched and truncated axons⁷⁵. As complete loss of SMN protein is

embryonic lethal, to better understand the developmental and long-term effects of decreased SMN protein levels, *SMN2* (*hSMN2*) transgene^{56,162}. These mice produce ~10% of the amount of SMN protein produced by wild-type animals, and display severe motor defects. Motor neurons extracted from these SMA model mice display reduced axonal outgrowth as well as decreased growth cone size¹⁴⁴, however these growth defects are not observed *in vivo*⁷⁹. This mouse model displays electrophysiological abnormalities, and show defects in calcium channel clustering of the subtypes Cav2.1 and Cav2.2¹⁴⁶. However, expression of the calcium channel subtypes found to be irregularly clustered in SMA is not restricted to motor neurons. These channels are also expressed in many other CNS neuronal populations, and it is therefore unclear why the altered, “immature” clustering pattern is only found in the motor neurons.

Additional deformities of the neuromuscular junction (NMJ) are evident in mouse models. Aberrant neurofilament (NF) accumulation has been repeatedly observed, both in the axons and in the NMJ^{79,163,164}. Decreased complexity of the NMJ morphology, including reduced NMJ folding and arborization, is consistent with the lack of maturation of the NMJ's suggested by improper calcium channel clustering^{78,80}. Denervation, as defined by a NMJ unoccupied by a motor neuron, is also a common finding. The extent of denervation generally correlates with the degree of severity in the SMA mouse models^{78,81,163}, although one study found no pre-synaptic abnormalities in pre- or post-synapses¹⁶⁵. A recent study in the severe *Smn*^{-/-}; *SMN2*^{+/+} mouse model also found mitochondria with disturbed cristae on both the pre- and post-synaptic sides of the NMJ, as well as vacuolization of the perisynaptic Schwann cells¹⁶⁶. Importantly, these changes were

observed in the diaphragm, a muscle affected in this animal model, but not in the soleus, a muscle mostly spared in this model.

Defects in neuromuscular junction morphology often result in altered neurotransmission, which is seen in both the most severe⁸⁰ and milder SMA mouse models⁷⁸. These defects range from reduced quantal content to facilitation, though not all defects are observed across all the SMA mouse models. A reduction in the synaptic vesicle (SV) quantal content (amount of neurotransmitter per vesicle) was observed in the *SMN2;SMNΔ7;Smn*^{-/-} severe SMA mouse model⁸⁰, and to a more modest degree in the *SMNΔ7;Smn*^{-/-} mouse model¹⁶⁷. The severe SMA mouse model also demonstrated additional SV defects, such as reduced SV release probability and decreased SV density, however the milder SMA mouse model *SMN2*^{+/+}; *Smn*^{-/-}; *SMNA2G*^{+/+} did not confirm this phenotype¹⁶⁷. The milder mouse model demonstrated intermittent neurotransmission failure, although in this model innervation was retained well into the disease course. The neurotransmission failure and reduced SV release probability have been proposed to be a result of the defects in Ca²⁺ channel clustering. The results from these animal models demonstrate a vital role for SMN in motor neurons, however the question remains as to the exact nature of SMN's function in the axon, and how the lack of this activity results in the SMA phenotype.

How can decreased activity of a ubiquitous protein result in a tissue-specific disease?

The question of how a defect in a ubiquitous housekeeping gene could result in neurodegenerative disease targeting a specific subset of neurons has been asked many

times, by many researchers. However, SMA is not alone in this category, as several other ubiquitously expressed genes have been implicated in CNS disorders. These genes include spastin, aminoacyl tRNA synthetases and parkin. Spastin (*SPG4*) is an AAA family ATPase with a role in regulating microtubule stability ¹⁶⁸. Mutations in spastin cause the most common form of autosomal dominant hereditary spastic paraplegia (AD-HSP) ¹⁶⁸. AD-HSP is a neurodegenerative disease characterized by spasticity and weakness in the lower extremities and degeneration of axons ¹⁶⁹.

Aminoacyl tRNA synthetases (ARSs) are responsible for loading tRNAs with their correct amino acid during translation, however mutations in these essential proteins lead to a multitude of diseases including the neurodegenerative disorders Charcot-Marie-Tooth disease type 2D and Leukoencephalopathy ¹⁷⁰. Rare familial forms of Parkinson's have been connected to pathogenic mutations in parkin (*PARK2*), a subunit of an E3 ubiquitin ligase complex ¹⁷¹. Each of these proteins, including SMN, are expressed ubiquitously in all tissues.

In general, three mechanisms can be conceived in which impairment in a ubiquitous protein could result in a tissue-specific disease. The simplest mechanism would be that the tissue in question is more sensitive to alterations in the levels of activity of the ubiquitous protein. Alternatively, it is possible that the pathway(s) regulated by the disease-protein are different in the specific cell type. Lastly, the protein of interest may have additional tissue-specific functions, due to e.g. tissue-specific expression of a binding partner, or tissue-specific splicing of the disease gene.

The most conservative hypothesis proposed suggests that motor neurons are more sensitive to alterations in splicing efficiency ^{98,99}. In this scenario, impaired snRNP

biogenesis leads to defects in splicing resulting in decreased levels of proteins required for motor neuron homeostasis⁹⁹. Alternatively, as motor neurons have extremely long processes, the discovery that SMN is involved in axonal transport of RNP particles lead to the hypothesis that the motor neuron degeneration is due to deficient local synthesis of proteins required for axonal outgrowth and maintenance^{142,148}.

To round out the potential hypotheses, a tissue-specific splicing isoform of SMN was identified by Setola *et al.*, however their findings remain controversial to date. The authors reported the discovery of an alternatively spliced isoform of *SMN1* which is selectively expressed in motor neurons¹⁷². This isoform, termed axonal-SMN or a-SMN, retains intron 3 in the spliced transcript. However, as intron 3 contains an in-frame stop codon, a-SMN is significantly smaller than full-length SMN, and was identified as a ~20kDa band, utilizing antibodies developed by the lab. Additionally, a-SMN was reported to be expressed solely in the axons of motor neurons within the spinal cord, and to be maximally expressed during initial development of the neuromuscular system. Transfection of *a-SMN* into NSC-34, a mouse motor neuron-like cell line, stimulated production of filipodia-like extensions. These extensions developed into a single, long axon by 72 hours post-transfection, similar to what is seen in motor neurons. In comparison, transfection of full-length *SMN* had no effect. The authors suggest that a-SMN has a vital role in axonogenesis, a neuronal function which has been shown to be impaired in SMA animal models. However, SMA patients have been identified with mutations in exon 6, which is not included in this isoform¹⁰⁶. Therefore, although it is tempting to ascribe a tissue-specific disease to tissue-specific expression of an isoform of the disease-gene, it is unlikely that a-SMN has a role in SMA.

Neuromuscular disorders with similarities to SMA

A rare, yet interesting finding was the report of a single SMA patient with an increase in serum anti-acetylcholine receptor antibodies (α -AChR-Ab). The presence of α -AChR-Ab in the blood is usually an indicator of the neuromuscular disorder myasthenia gravis (MG). MG is characterized by muscle fatigability and predominantly affects the muscles of the eyes and limbs, as well as those involved in swallowing or breathing¹⁷³. MG is an autoimmune disease caused by auto-antibodies against the nicotinic acetylcholine receptor (nAChR) or muscle specific kinase (MuSK). These proteins are found in the neuromuscular junction (NMJ) and have important roles in neurotransmission. Although the patient's diagnosis was confirmed as SMA, not MG, the identification of auto-antibodies in the blood suggested that there may be sufficient trauma or degeneration at the neuromuscular junction to hyper-activate the immune system.

A neuromuscular disorder closely related to MG is Lambert-Eaton myasthenic syndrome (LEMS). LEMS is of special interest, as the symptoms of LEMS are strikingly similar to those of SMA. In both disorders, patients develop progressive weakness of the proximal muscles of the limbs, with facial and respiratory muscles usually remaining unaffected. LEMS, however, is an autoimmune disorder usually identified by the presence of auto-antibodies against the neuromuscular junction proteins P/Q-type voltage gated calcium channels (VGCCs), synaptotagmin 1 (Syt1) or the M1-type presynaptic muscarinic ACh receptor (M1-AChR)¹⁷⁴. Syt1 and M1-AChR are functionally associated

with the P/Q-type VGCCs, suggesting a common mechanism. The appearance of these auto-antibodies is usually temporally associated with malignant neoplasms, most often small cell lung carcinoma, in which the tumor cells express one or more of these proteins¹⁷⁵. The immune response against the neoplastic cells is speculated to result in the NMJ proteins becoming antigenic. Auto-antibodies against any of the three proteins (VGCCs, Syt1 or M1-AChR) are released into the bloodstream, bind to protein at the NMJ, resulting in impaired acetylcholine signaling and consequent muscle weakness.

The involvement of Syt1 in LEMS was of interest, as mice bearing a homozygous loss of function mutation of Syt1 or modeling a severe form of SMA are phenotypically similar^{56,176}. Both mouse models are phenotypically indistinguishable from their normal littermates at birth, but demonstrate progressive skeletal muscle weakness, poor suckling and abnormal synaptic vesicle release prior to dying within 48 hours after birth. The similarity in phenotype could suggest an association between SMN and Syt1. In fact, there is the possibility of a physical interaction between SMN and Syt1, as they share a binding partner in hnRNP Q (also known as SYN-CRIP, standing for synaptotagmin-binding cytoplasmic RNA interacting protein). Syt1 and hnRNP Q/SYNCRIP have been shown to interact *in vitro*¹⁷⁷.

Syt1 is an abundant, neuron-specific synaptic vesicle transmembrane protein whose N-terminal region cycles between vesicular and extracellular during synaptic vesicle fusion¹⁷⁸. Syt1 is believed to be a calcium sensor for regulation of synchronous neurotransmitter release via synaptic vesicle (SV) fusion¹⁷⁹, as mutations which modulate binding to Ca²⁺ ions directly affect the Ca²⁺-dependent SV release probability¹⁸⁰. Additionally, Syt1 has been implicated in clathrin-mediated SV recycling^{181,182}. The

activity of Syt1 may be relevant to SMA, as several researchers have demonstrated defects in neurotransmission in SMA animal models^{183,184} although there have been conflicting reports stating that decreased levels of SMN have no effect on electrophysiological activity of motor neurons¹⁸⁵. Future studies investigating the potential interaction between SMN and proteins involved in synaptic vesicle release and recycling could identify a direct correlation between SMN levels and the robustness of neurotransmission.

Axonal defects in animal models of SMA

It has been suggested that the motor neuron degeneration observed in SMN is due to decreased activity of its housekeeping function: assembly of the spliceosome for pre-mRNA splicing. Jablonka *et al.* investigated the importance of splicing activity for motor neuron health by creating a double heterozygous mouse model for *Smn* and *Gemin2*¹⁸⁶. SMN and Gemin2 are required subunits for the macromolecular complex, termed the SMN complex, which is the assemblyosome for the spliceosomal uridine-rich small nuclear ribonucleoproteins (U snRNPs). In the double heterozygote mouse model *Smn*^{+/-}; *Gemin2*^{+/-}, spliceosome assembly was further decreased compared to the *Smn*^{+/-} mice, as determined by a reduction in the nuclear pool of Sm proteins. The *Smn*^{+/-}; *Gemin2*^{+/-} mice also demonstrated an 34% decrease in the number of lumbar motor neurons, in comparison to the 9% reduction observed in the single heterozygous *Smn*^{+/-} mice. This enhancement of motor neuron loss in the double heterozygote suggests that motor

neurons are extremely sensitive to reductions in the level of spliceosomal activity, and that defects in splicing can result in the loss of motor neurons observed in SMA patients.

In support of the hypothesis that SMA pathogenesis resulted from deficient spliceosomal activity, Gabanella *et al.* demonstrated that SMA severity correlated with snRNP assembly potential⁹⁹. The authors show a preferential decrease in the assembly of a subset of U snRNPs, especially U11 snRNP, indicating that the decrease in SMN does not affect all U snRNPs uniformly. The U11 snRNP is part of the minor spliceosome, which is responsible for splicing between four hundred and seven hundred genes in the human genome^{187,188}. This small subset of genes may include protein products vital to the health of motor neurons, and could contribute to SMA disease pathogenesis.

In another study of snRNP activity in a SMA mouse model, Workman *et al.* demonstrated that expression of an SMN isoform containing a missense mutation seen in SMA patients, *SMN(A111G)*, can rescue a *hSMN2^{+/-};mSmn^{-/-}* severe SMA mouse model⁹⁸. The *SMN(A111G)* allele retains the ability to assemble U snRNPs. Its ability to complement *hSMN^{+/-}* correlates with an increase in the level of snRNP activity in the spinal cord, suggesting that elevation of snRNP levels is critical to rescuing motor neuron degeneration.

To directly assess the role of U snRNPs in motor neurodegeneration, Winkler *et al.* knocked down *Smn* in *Danio Rerio* (zebrafish) and *Xenopus laevis* (African clawed frog) and demonstrated defects in U snRNP assembly and degeneration of motor axons, comparable to the pathology seen in SMA¹⁰⁰ (Figure iii). Similar results were observed upon knockdown of *Gemin2* and *pICln*, the chloride conductance regulatory protein, two additional proteins required for snRNP biogenesis. The axonal defects observed upon

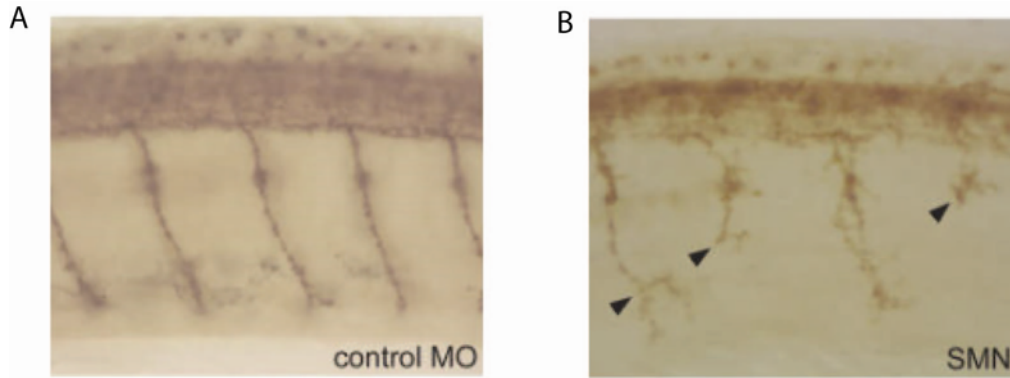


Figure iii. SMN knockdown results in axonal pathfinding defects in zebrafish.

Lateral views of zebrafish trunk with stained motor neurons. (A) Motor neuron phenotype in zebrafish injected with a control morpholino versus, (B) injected with a morpholino against *smn* mRNA. Arrowheads indicate truncated or abnormally branched motor neurons. *Images reproduced from* Winkler, C., *et al.* (2005) *Genes Dev.* **19**(19):232030⁹⁹.

Smn or *Gemin2* knockdown could be rescued by injection of purified U snRNPs into the *Smn*- or *Gemin2*-deficient embryos, suggesting that the motor neuron defects observed upon knockdown of SMN resulted directly from decreased splicing efficiency.

Despite the strong evidence linking deficiencies in snRNP activity to SMA pathogenesis, several other studies have failed to find any correlation between snRNPs and SMN's function in axons. Carrel *et al.* utilized morpholinos, nuclease-resistant phosphorodiamidate antisense oligomers, to knock down the levels of *Smn* in zebrafish¹⁰⁷. Reducing the levels of SMN protein in zebrafish results in motor neuron-specific defects, such as truncated axons and irregular axonal branching⁷⁵. Various human *SMN* mRNAs, including wild-type and SMA-causing mutants, were then co-injected in order to determine their effects on the axonal defects observed upon *Smn* knockdown. Although several of these mutant SMN proteins retain the ability to assemble snRNPs, only wild-type *SMN* was able to rescue the axonal outgrowth defects, suggesting that motor neuron-relevant function of SMN is independent of snRNP biogenesis.

McWhorter *et al.* performed a similar examination to investigate the role of *Gemin2* in motor neurons¹⁴¹. The authors knocked down *Gemin2* in zebrafish, however, while knock down of *Gemin2* resulted in abnormal development of the zebrafish embryos, the motor neuron axons were unaffected. Motor neuron-specific knockdown of *Gemin2* additionally had no effect on motor neuron morphology or function. The authors conclude that since *Gemin2* is required for proper snRNP biogenesis and knockdown of *Gemin2* has no effect on motor neurons, the neuronal defects seen upon *Smn* knockdown suggest a neuronal role for SMN aside from snRNP biogenesis.

Splicing defects have also been investigated in mouse models of SMA. Baumer, *et al.* investigated whether SMN decrease leads to splicing defects early in the disease course, which would suggest a direct role in disease pathogenesis. Utilizing exon arrays, the authors demonstrated that the SMA model mice show progressive alterations in splicing, but these defects only become readily apparent late in the disease course, suggesting that alternative splicing events are unlikely to be causative for degeneration of the motor neurons¹⁸⁹. However, as SMA model mice have been shown to be selectively deficient in components of the minor spliceosome, it cannot be ruled out that defects in the splicing of a small number of genes, while going unnoticed in this screen, result in SMA disease pathogenesis.

Despite our advances in understanding the disease pathogenesis of SMA utilizing animal models, it remains unclear how reduced levels of SMN protein result in motor neuron-specific degeneration (Figure iv). Previous studies have shed light on several potential neuron-specific functions of SMN, however it has yet to be conclusively shown whether any of the proposed mechanisms, or a yet unidentified function, is the causative agent in SMA.

Current state of small molecule therapeutics for SMA

Small molecule screening has proven indispensable for the identification of compounds inhibiting enzymes or cellular functions of interest. These bioactive compounds have provided us with tools to dissect the molecular mechanisms underlying biological processes, and are also lead therapeutics that have on occasion been developed

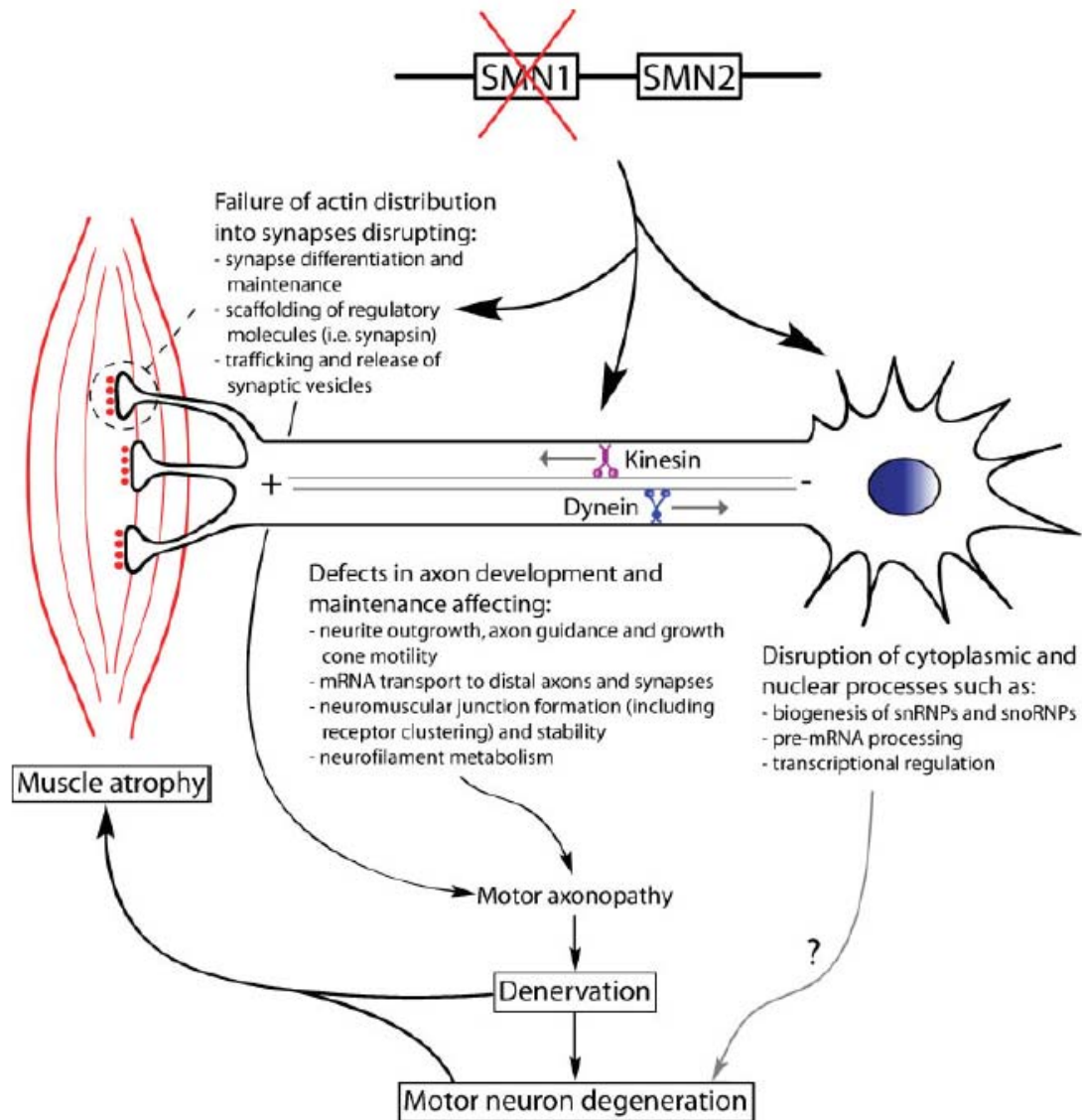


Figure iv. The pathogenic events occurring in motor neurons in SMA.

The homozygous loss of the *SMN1* gene results in neurons being forced to rely on the decreased levels of functional SMN protein produced by the *SMN2* gene. This results in a myriad of negative effects on motor neurons, including defects in U snRNP biogenesis, axonal pathfinding and synaptic vesicle release. Each of these could be the root cause of the motor neuron degeneration observed in Spinal Muscular Atrophy. *Image reproduced from Briese, M., et al. (2005) BioEssays 27: 946-957*¹⁹⁰.

into extremely valuable drugs. Drugs such as AZT (azidothymidine), the anti-retroviral that changed HIV infection from a fatal disease to a manageable chronic condition in the late 1980's¹⁹¹, are important inhibitors that were discovered through high-throughput small molecule screens.

However, not all cellular functions or diseases of interest are best addressed by an inhibitor. In certain cases, an activator of an enzyme or cellular process could provide more information on the process being studied, or perform an action necessary for a diseased organism to reestablish homeostasis. Small molecule activators can be categorized into one of three groups. The first and most common type of activator is the 'inhibitor of an inhibitor', which generally follow the adage 'the enemy of my enemy is my friend'. Compounds that fall into this category include many of the small molecules that induce cell death pathways, such as the classical activators of apoptosis: camptothecin (topoisomerase I inhibitor)¹⁹², staurosporine (broad spectrum kinase inhibitor)¹⁹³ and cycloheximide (protein synthesis inhibitor)¹⁹⁴.

The second, and more rare, type of activator could be considered an 'enabler'. One mechanism of actions for these molecules is to bind allosterically to their target enzyme, lowering the activation energy of the enzymatic reaction. Examples of this type of activator mainly include endogenous small molecule ligands, such as the secondary metabolite inositol hexakisphosphate, an activator of RTX cysteine proteases¹⁹⁵. However, exogenous 'enablers' have also been identified, such as the non-ligand small molecule which was recently identified in a high-throughput screen as an activator of pro-caspase 3¹⁹⁶. These particular compounds function by increasing the likelihood of

auto-proteolytic processing of pro-caspase 3 to the active form, caspase 3, 'enabling' the activation of downstream pro-apoptotic pathways.

A third type of activator is an 'upregulator'. This type of compound increases the intracellular levels of a target protein or proteins. The advantage of this type of activator is that it is protein-class independent. While the activity of most inhibitors and allosteric activators are restricted to proteins with enzymatic activity and/or binding pockets for endogenous ligands, an 'upregulator' could in theory increase the activity, via an increase in intracellular level, of any class of protein. Spinal Muscular Atrophy exemplifies the type of disease in which an upregulator could be of great use, as it is caused by decreased levels of a single protein, Survival of Motor Neuron (SMN)²⁴. Despite years of research, attempts at small molecule modulation of the pathways affected by decreased levels of SMN protein have not proven fruitful. The complexities of the neuronal system, and the difficulties of studying the system in whole organisms, have limited the understanding of the mechanisms resulting in disease pathogenesis. Without understanding the pathways being affected, the only option available for therapeutic intervention is to increase the concentration of the affected protein.

There has been a strong drive to discover small molecule upregulators for SMA since the genetic basis of the disease was identified in 1995²⁴. In SMA, the *survival of motor neuron 1 (SMN1)* gene is mutated or deleted. However, there exists a nearly identical gene copy, the *SMN2* gene, which produces SMN protein, albeit at significantly lower levels than *SMN1*, due to alternative splicing⁴¹. The existence of the gene copy opens up new avenues for pharmaceutical intervention not available in most genetic conditions. The idea that the disease phenotype could be ameliorated or even resolved by

a drug that increased the amount of full-length SMN protein produced by the *smn2* gene has interested researchers and pharmaceutical companies alike for over a decade.

Several pharmaceutical companies have become involved in efforts to identify and develop potential therapeutics for SMA. In conjunction with the Families of Spinal Muscular Atrophy (FSMA) Foundation, Aurora Biosciences (now Vertex Pharmaceuticals) participated in the high-throughput screen which identified the quinazoline backbone as an upregulator of the *SMN2* promoter¹⁹⁷. The structure-activity relationship³¹ and medicinal chemistry required to improve the potency and efficacy of the compound class to a level where therapeutic testing would be feasible were performed in partnership with deCODE Genetics (Reykjavik, Iceland)¹⁹⁸. The clinical candidate resulting from the SAR received Orphan Drug Designation from the FDA and was licensed to Repligen Corporation (Waltham, MA) for human trials (<http://www.repligen.com/products/pipeline/rgsma>), providing hope for families affected by this devastating disease. In addition to the quinazoline program, FSMA has partnered with Paratek Pharmaceuticals (Boston, MA) to develop non-toxic analogs of Aclarubicin A, which was identified as a modulator of *SMN2* splicing in 2001 (http://www.paratekpharm.com/pt_tet_tc.html)¹⁹⁹.

HDAC inhibitors in SMA therapy

Histone deacetylase (HDAC) inhibitors were the first small molecule pharmaceuticals identified to affect the levels of SMN protein in patient cells. HDAC inhibitors inhibit the activity of deacetylating enzymes which cleave acetyl groups from

the ϵ -amino of lysines in the amino terminal tails of histones²⁰⁰. The histone substrates of the HDAC enzymes make up the nucleosomes around which the genomic DNA is wrapped. Addition of an acetyl group onto a lysine neutralizes the positive charge of the residue. This diminishes the interaction of the positively charged lysine groups with the negatively charged DNA, resulting in decreased packing density of the nucleosomes²⁰¹. This 'relaxation' provides access for the gene transcription machinery to the DNA and is generally associated with increased gene transcription^{202,203}. Histone acetylase⁸ enzymes perform antagonizing functions, utilizing acetyl-coenzyme A to transfer acetyl groups onto the N-terminal tails of the lysines, resulting in condensation of the DNA and reduced gene transcription.²⁰⁰

Therefore, small molecule inhibition of HDAC enzymes results in globally decreased levels of histone acetylation as well as decreased chromatin condensation. This has been shown to increase expression of approximately 2% of the genome, or approximately 400-500 gene products²⁰³. In addition to its effects on gene transcription, HDAC enzymes can cleave acetyl groups from non-histone proteins as well, modulating their level of activity. Non-histone substrates identified for HDAC's include transcription factors²⁰⁴, alpha-tubulin^{205,206}, signaling regulators and metabolic proteins²⁰⁷. Due to the ability of HDAC enzymes to alter the activity of a wide range of substrates, inhibitors of these enzymes have been utilized for the treatment of a wide range of disorders, from psychiatric conditions such as epilepsy^{208,209} to treatments for various cancers^{152,210}.

In 2001, Chang *et al.* identified sodium butyrate, a simple aliphatic acid known to inhibit HDAC enzymes, as a compound able to affect the splicing of the *SMN2* gene in Epstein-Barr virus transformed lymphoid cell lines derived from SMA patients²¹¹.

Treatment with sodium butyrate significantly increased the ratio of *SMN* transcripts containing exon 7 to those lacking exon 7. Western blots of the sodium butyrate-treated SMA lymphoid cell lines showed an approximately 130-150% increase in SMN protein level. To determine the effect on an SMA mouse model, mice models of Type II and Type III SMA were administered sodium butyrate *ad libitum* in drinking water for 1-12 weeks or left untreated as controls. The treated group survived significantly longer than the untreated group; treatment increased the mean lifespan from 15.5 days in the untreated group to 21.7 days in the sodium butyrate treated group (range: 13-20 days for untreated, 14-30 days for treated). Although sodium butyrate may not be effective enough to be considered a 'cure' for SMA, it does demonstrate that inhibition of HDACs can ameliorate the severity of SMA symptoms and prolong the lifespan of SMA model mice. This initiated a large series of studies assessing the efficacy of HDAC inhibitors on the SMA phenotype, several of which have already progressed into clinical trials. Several of these, and their results, will be further discussed in this section.

Valproic acid in SMA therapy

As the HDAC inhibitor sodium butyrate had been identified as an upregulator of *smn2* mRNA and SMN protein levels, researchers hypothesized that other known HDAC inhibitors would have similar effects. Valproic acid (VPA) is a FDA approved drug and has been effectively utilized in the clinic for long-term treatment of epilepsy²¹², and therefore would be an attractive therapeutic candidate for the treatment of SMA. In 2003, two groups independently confirmed that the HDAC inhibitor valproic acid, an aliphatic

acid, increases the levels of full-length *smn2* mRNA as well as SMN protein levels^{213,214}. In SMA patient fibroblast cell lines, Sumner *et al.* demonstrated an approximate 1.8-fold increase in the ratio of full-length to exon 7-deleted *SMN* mRNAs, as well as an approximate 1.6-fold increase in SMN protein levels when treating with 10mM VPA for 24 hours. Brichta, *et al.* demonstrated a 1.5-fold increase in the ratio of full-length to exon 7-deleted *SMN* transcripts, with an additional augmentation in total full length *SMN* mRNA via transcriptional upregulation, for a maximal increase of 5.2-fold in full-length *SMN* mRNA compared to untreated controls. In their system, Brichta, *et al.*, also saw a 1.8-4.2 fold increase in SMN protein levels, with activity varying significantly between different SMA patient fibroblast cell lines, indicating a significant amount of variation between the two systems.

As SMA is a motor neuron disease, the next step in determining the efficacy of a potential therapeutic is to test the effect of the compound on the tissue of interest: neurons. Brichta *et al.* tested the effect of VPA in rat organotypic hippocampal slice cultures (OHSC), as a model for VPA efficacy in neuronal tissues. When treated with 2mM VPA for 12-48 hours, OHSCs demonstrated a 1.6 fold increase in rat *smn* mRNA, as well as a 1.8 fold increase in rat SMN protein levels. The authors hypothesized that since the splicing factors Htra2- β 1 and SF2/ASF⁴⁷ have been shown to affect the splicing of *smn* transcripts, it could be the upregulation of these proteins which results in the alteration in *smn* splice isoforms seen upon treatment with VPA. Western blots indicated an approximate 1.4-fold and 3-fold increase in Htra2- β 1 and SF2/ASF, respectively, lending some support to their hypothesis.

Tsai and colleagues reported their investigations into the therapeutic effect of VPA in Type III SMA model mice in 2008²¹⁵. SMA mice were treated from age 6 months to 12 months with 0.2mg/ml VPA supplied in the drinking water, corresponding to 40-75mg/kg VPA consumed per day. VPA-treated mice showed some prevention of SMA-induced morphology changes, including lengthened tails, larger ears and larger gastrocnemius muscle (back of the calf). However, no other muscles showed an increase in size, nor was there a change in overall body mass. A greater degree of choline acetyltransferase (ChAT) staining, a motor neuron marker, in spinal cord slices of VPA-treated versus untreated mice suggested that VPA treatment prevented some of the neuronal death seen in SMA, indicating that VPA may be a potential treatment for the amelioration of the effects of SMA.

However, when Rak *et al.* investigated the effect of VPA on motor neurons isolated from SMA model mice in 2009, their findings were somewhat more negative²¹⁶. Although VPA treatment increased SMN levels in the motor neurons, it was concomitantly detrimental to several disease relevant parameters, such as axon outgrowth. VPA treatment decreased viability of the motor neurons after four days in culture and reduced the axonal outgrowth and growth cone size of the neurons. The authors determined that these effects were due to decreased excitability of the neurons upon VPA treatment, with the detrimental phenotype being similar to blockers of voltage gated sodium channels¹⁴⁶, suggesting that VPA may evoke undesirable side effects in SMA patients.

However, the positive effects of valproic acid treatment on motor function in a mild SMA mouse model²¹⁵, generated significant interest within the SMA community.

As VPA is an FDA-approved drug with well-understood dosing regimen, Phase I clinical testing (which is generally used to assess drug safety) could be bypassed. Instead, testing began with a small Phase II clinical trial which was performed to test the efficacy of VPA treatment on seven adult patients with the milder Type III and Type IV forms of SMA²¹⁷. As it was an open-label trial, all patients enrolled in the study were treated, and there were no untreated controls. Four of the six patients showed statistically significant ($p=0.002$) improvement in strength, measured via handheld dynamometry. Dynamometers are routinely used in kinesiology to quantify the force a specific muscle or group of muscles is capable of exerting. This method is considered a reliable method for determining alterations in strength over time in patients demonstrating neuromuscular weakness. Additionally, all six patients reported subjective improvements, such as improved ease of breathing and increased walking endurance. Based on this small study, VPA seemed to be beneficial for adult patients with milder forms of SMA.

In 2009, a larger open label Phase II study of VPA was published by Swoboda *et al.*²¹⁸. This study enrolled a total of 42 patients: two Type I, 29 Type II and 11 Type III patients. All patients were 2 years old or older, to avoid the teratogenicity associated with VPA treatment. Dosages were in the range of 15-50mg/kg/day, similar to dosages utilized for anti-epileptic purposes²¹². Carnitine levels were monitored, as the serum carnitine levels of the first 13 patients in the study decreased within the first three months of treatment. Two subjects demonstrated a decrease in motor function, which was reversed upon carnitine supplementation. Carnitine is utilized in cells for the transport of long chain fatty acids, for example arachidonic or linoleic acids, into the mitochondria for

catalysis and generation of ATP^{219,220}. Therefore, loss of carnitine upon VPA treatment resulted in decreased motor function likely due to “starved” muscle tissue.

In this study, treatment with VPA was determined to be beneficial for non-ambulatory Type II children, while older subjects showed no response or slight decrease in motility. This was due in a few subjects to a moderate amount of weight gain, which was gained as fat mass rather than lean mass, resulting in deterioration of motor function. The levels of *SMN* transcripts in blood samples were also monitored in the patients, as previous studies demonstrated increased levels of *SMN* transcripts in patient-derived cells^{213,214}. However, *SMN* transcript levels in blood samples fluctuated greatly over the course of treatment, and overall seemed to decrease in the population. Previous reports utilizing testing VPA in patients and carriers indicated varying responses to the drug, therefore determination of biomarkers that can distinguish VPA-responders from non-responders may assist in selection of the appropriate SMA population to test²²¹.

Phenylbutyrate in SMA therapy

Since several HDAC inhibitors had shown efficacy in increasing the levels of *smn* transcripts and proteins in patient cells, in 2004 Andreassi and colleagues tested the HDAC inhibitor 4-phenylbutyrate (PBA)²²². Although the highly similar HDAC inhibitor sodium butyrate has also been tested in SMA²¹¹, PBA is more attractive as a therapeutic candidate, due to improved pharmacological properties, such as longer serum half-life²²³. Fibroblasts derived from 16 SMA patients, ranging from Type I to Type III in severity, were tested using 2mM PBA. All cell lines increased *SMN-FL* transcript

levels, with maximal responses ranging from approximately 1.2 to 4-fold increase. However, these increases dropped back to baseline within a few hours of treatment, unless PBA was re-administered to the cells every four hours. SMN protein levels were also quantified in three of these cell lines, and each showed a small, but not statistically significant increase in SMN protein levels, indicating that PBA may not be the most effective of the HDAC inhibitor tested to date.

Brahe and colleagues performed a small, six patient and three carrier, clinical study assessing the efficacy of PBA at increasing the levels of *SMN* transcripts in leukocytes of SMA patients and carriers²²². Patients ranged in age from 2.5 to 38 years old, and were either Type II or Type III. All patients had three copies of *SMN2*. Carriers were recruited from the parents of the patients. Patients were treated for seven days with 500mg/kg/day, divided evenly into 4 hour doses. Leukocytes were harvested from blood samples taken 1-3.5 hours after PBA administration. The levels of *SMN* transcripts changed between 0.4 to 2.4-fold in patients and 0.9 to 1.7 in carriers. Myometry was performed to determine whether muscle strength was altered, and found a statistically significant improvement across the population. However, again it was found that individual responses were greatly varied, with some patients showing no improvement. Altogether, this study indicated that PBA was safe for SMA patients and that it could increase the levels of *SMN* transcripts in peripheral blood leukocytes, in some cases. However, it did not show improved potency or efficacy compared to trial of another HDAC inhibitor valproic acid²¹⁷.

Hydroxyurea in SMA therapy

Another study conducted by Grzeschik and colleagues reported that hydroxyurea (HU), also an HDAC inhibitor, was a potential therapeutic agent for SMA ²²⁴. Their studies demonstrated that HU treatment of patient-derived lymphocytes was effective at increasing the ratio of full-length to exon 7-deleted *SMN* transcripts (FL:Δ7), as well as *SMN* protein production. The ratio of FL:Δ7 *SMN* transcripts increased a maximal 2 to 3-fold with 0.5mM HU treatment. Total levels of *SMN* mRNA did not change upon HU treatment, indicating the effect was due to alteration of splicing rather than activation of the promoter. *SMN* protein production however, showed maximal effect at 5μg/ml with protein levels decreasing below baseline at concentrations greater than 50μg/ml. The variability of response between the cell lines derived from patients was too great to determine statistical significance, although there was a trend with an average 1.3-fold increase across cell lines.

However, these results spurred the testing of HU in SMA patients, and in 2008 Liang and colleagues reported a small trial enrolling 33 SMA patients ²²⁵. The patients selected for study were the milder Type II and Type III individuals, and were treated with 20-40mg/kg/day for 8 weeks. Although HU was demonstrated to be safe for SMA patients at these dosages, the effects were not statistically significant. However, there was a trend towards slight increases in muscle strength and elevation of blood *SMN* mRNA levels. The authors suggest that the lack of statistical significance may be due to the small sample size. Therefore, the authors initiated a larger, placebo-controlled clinical trial to determine whether a larger group may allow for determination of statistically significant

efficacy of hydroxyurea in SMA patients ²²⁶, however this study also showed no improvement in the clinical markers of SMA.

Second-generation HDAC inhibitors in SMA therapy

HDAC inhibitors have been studied as anti-cancer agents, due to their ability to initiate growth arrest and apoptosis of neoplastic cells ²²⁷. Due to the intense interest of many academic laboratories as well as pharmaceutical companies in this area, second generation HDAC inhibitors have been developed, with improved potencies and efficacies against HDACs ²²⁸. Hahnen *et al.* investigated the efficacy of these second generation HDAC inhibitors in enhancing the levels of *smn* transcripts and SMN protein levels in human and rat organotypic hippocampal brain slices (OHSCs) and rat motor neuron-enriched cell fractions ²²⁹. The second generation HDAC inhibitors tested included the hydroxamic acids as well as the benzamides. The hydroxamic acids were: suberoylanilide hydroxamic acid (SAHA, Vorinostat), *m*-carboxycinnimic acid bis-hydroamide (CBHA) and suberoyl bishydroxamic acid (SBHA) ²²⁸. The benzamides were: N-(2-Aminophenyl)-4-[N-(pyridine-3-ylmethoxycarbonyl)aminomethyl]benzamide (MS-275) and 4-Dimethylamino-N-(6-hydroxycarbamoylhexyl)benzamide N-Hydroxy-7-(4-dimethylaminobenzoyl) amino-heptanamide (M344) ^{230,231}. The authors selected these tissues for testing in order to determine whether these compounds were active in a CNS-derived cellular context. The compounds SAHA, SBHA, CBHA and M344 and the positive control VPA increased SMN protein levels in F98 rat glioma cells approximately 1.5 to 1.9 fold, while MS-275 had no activity. SAHA, M344, and MS-275 were active at

low micromolar concentrations, while SBHA and CBHA were active in the 50-250 μ M range. VPA was used at 2mM. SAHA, M344 and VPA also increased wild-type murine *smn* transcript levels approximately 1.8 to 2.5 fold, at their respective relevant concentrations. Additionally, higher concentrations of SAHA (32-64 μ M) demonstrated approximately 1.8-fold increase in SMN protein levels in human OHSCs after 48 hours of treatment, demonstrating SAHA's efficacy in human CNS tissues.

Due to the success of SAHA's efficacy in the tissue explants, Riessland and colleagues tested the compound's effects on two severe mouse models of SMA²³². Treatment of pregnant heterozygote mothers with 200mg/kg/day of SAHA, a dosage which has been demonstrated to decrease histone acetylation levels in the brain²³³, indicating that an effective concentration is passing the blood-brain barrier. SAHA treatment rescued the embryonic lethality evident in the homozygous pups, as the treated mothers birthed five SMA pups, while the solvent-treated mothers only birthed one. However, all homozygote pups developed an SMA-like phenotype, indicating that SAHA is not able to prevent the onset of disease.

To determine if SAHA could ameliorate the symptoms of disease, it was further tested in the newborn SMA pups. However, the high dosage of SAHA utilized in the adult mothers demonstrated significant toxicity in the SMA pups, and the dosage had to be reduced to 25mg/kg/day. At this dosage, mouse survival was increased 30% ($P < 0.001$), extending survival from 9.9 to 12.9 days, demonstrating a significant improvement in the SMA phenotype. SAHA-treated animals also demonstrated improved motor performance and decreased motor neuron loss, two hallmarks of a compound which has potential for

treatment of SMA. As SAHA is an FDA-approved drug, clinical trials may soon be forthcoming.

Indoprofen in SMA therapy

HDAC inhibition is not the only mechanism by which small molecule can upregulate SMN protein levels. Indoprofen, an analog of ibuprofen, was discovered as a modulator of SMN protein levels in 2004 by Lunn and colleagues²³⁴. Indoprofen was discovered in a small molecule screen of approximately 47,000 compounds using a *SMN* minigene-luciferase reporter system²³⁵. In this system, exons 6-8 and intervening introns of either the *SMN1* or *SMN2* gene are fused with the luciferase gene. The luciferase gene, however, is in frame only when exon 7 is spliced properly. Therefore, this cell line can be used to identify small molecules that increase the inclusion of exon 7 in the *SMN2* background by assaying for increased luciferase expression. The *SMN1-luciferase* construct served as a control for small molecules that may cause increases in luciferase signal non-specifically, e.g. through global enhancement of translation. Indoprofen was identified as a compound that significantly increased *SMN2-luciferase* signal relative to *SMN1-luciferase*. Indoprofen is a non-steroidal anti-inflammatory drug (NSAID). NSAIDs act as analgesics by inhibiting the cyclooxygenases COX-1 and COX-2, which are important in the inflammatory pathway, as well as potentially regulating other pain-regulation pathways²³⁶. Inhibition of COX-1 can lead to irritation of the gastrointestinal tract²³⁷. Although indoprofen was initially FDA-approved, it was pulled from shelves in the 1980s due to a significant number of cases reporting gastrointestinal bleeding.

Through a structure-activity relationship study testing other NSAIDs, including the closely related analog ibuprofen, indoprofen was determined to be the only NSAID tested with activity in the luciferase assay, suggesting the mechanism of action was not through inhibition of the COX enzymes. Human SMA patient Type I fibroblast cells treated with $\sim 10\mu\text{M}$ indoprofen showed a reproducible average 1.13-fold increase in SMN protein levels, which was moderate but statistically significant ($p < 0.014$). Indoprofen's effect on a severe mouse model of SMA was tested in the *Smn*^{-/-}, *TgSMN2*^{+/-} model, in which the murine *smn* gene is replaced by the human *smn2* transgene⁵⁶. The homozygous embryos from this mouse model die on average at embryonic day 11. Heterozygous mice were crossed and the pregnant mothers were treated with IP injections of 5mg/kg indoprofen twice daily for the initial 14 days of pregnancy, resulting in an average $3.0\mu\text{M}$ indoprofen concentration in the embryos of the treated mothers by embryonic day 13. At day 14, the embryos were genotyped to determine the number of surviving homozygotes. In the untreated mothers (n=7), none of the litters contained any *Smn*^{-/-}, *TgSMN2*^{+/-} embryos, however three of the seven indoprofen-treated mothers retained *Smn*^{-/-}, *TgSMN2*^{+/-} embryos. Although this result was not statistically significant due to the small sample size ($p = 0.096$), the increases in litter size and number of SMA embryos suggested a trend of increased viability upon indoprofen treatment.

Due to the potential therapeutic effect of indoprofen, the Spinal Muscular Atrophy Project selected this structure for additional medicinal chemistry efforts (<http://www.smaproject.org/>). The SMA Project was established by the National Institute of Neurological Disorders and Stroke (NINDS) to focus on pre-clinical drug development for SMA, facilitating translation of potential SMA therapeutics from basic research into

clinical trials. Medicinal chemistry efforts by the SMA Project, reported at the 2007 SMA Summit on Drug Development ²³⁸, were shown to be successful in creating analogs of indoprofen that retain SMN upregulation but do not inhibit COX-1, thereby removing the risk of negative gastrointestinal effects. Additionally, the indoprofen analogs generated have greatly improved blood-brain barrier penetration, a necessary property for a CNS-active drug. Mouse trials will hopefully be forthcoming for these promising analogs.

Looking towards the future for SMA therapeutics

Although a great degree of progress has been made toward identifying small molecule therapeutics for Spinal Muscular Atrophy, the limited efficacies of the compounds tested in clinical trials to date demonstrate how much further we need to go in order to develop a cure for this fatal disease. Interest in alternative therapeutics such as gene therapy and cell replacement have burgeoned in the SMA field, and several attempts have been made to rescue the SMA phenotype in mouse models of SMA utilizing viral vectors. The first study utilized intramuscular injections of a self-inactivating lentiviral vector expressing *SMN* into young SMA pups ²³, which increased survival of the SMA mice 20-38% (3 and 5 days, respectively). While these results appear somewhat milder than expected, it has been argued that this type of viral injection may not be an efficient method of transducing neurons ²³⁹.

Another method, utilizing high-titer systemic injections of the self-complementary (sc) AAV serotype 9 vector (scAAV9) have demonstrated transduction of approximately 60% of motor neurons ²⁴⁰. Foust and colleagues utilized this system to

transduce a SMN expression vector into the motor neurons of postnatal (PN) day 2 and day 10 SMA model mice²⁴¹. Transgene expression of SMN starting at PN2 significantly improved motor function and demonstrated strong rescue of survival, as scAAV9-GFP all died before PN25 but all scAAV9-SMN transduced mice lived past PN60. However, another study by Valori and colleagues using similar methodology reported a lower degree of rescue. In their study, approximately 80% of the injected mice demonstrated increased survival, extending life span from 11.2 days in the scAAV9-GFP injected mice to 69.1 days in the scAAV9-SMN injected mice²⁴².

An unfortunate discovery from a therapeutics perspective was that transduction of PN10 mice in the Foust study showed no demonstrable rescue of the motor function or survival²⁴¹. This suggests that there may be a finite window of opportunity for viral-mediated rescue of the SMA phenotype.

Although advances in gene therapy are ongoing, it is unclear how long they will take to get into the clinic, and therefore there is still a need for identification of new, effective small molecule therapeutics. Additionally, novel small molecules which modulate SMN protein levels are needed in order to probe the cellular mechanisms involved in SMN regulation. Identifying new cellular pathways capable of altering SMN protein levels provides new therapeutic targets, opening up new avenues for research.

References

1. Hyman, S.E. The role of molecular biology in psychiatry. *Psychosomatics* **29**, 328-332 (1988).
2. Nance, M.A., Mathias-Hagen, V., Breningstall, G., Wick, M.J. & McGlennen, R.C. Analysis of a very large trinucleotide repeat in a patient with juvenile Huntington's disease. *Neurology* **52**, 392-394 (1999).
3. Walker, F.O. Huntington's disease. *Lancet* **369**, 218-228 (2007).
4. Shao, J., Welch, W.J. & Diamond, M.I. ROCK and PRK-2 mediate the inhibitory effect of Y-27632 on polyglutamine aggregation. *FEBS Lett* **582**, 1637-1642 (2008).
5. Bauer, P.O., *et al.* Harnessing chaperone-mediated autophagy for the selective degradation of mutant huntingtin protein. *Nat Biotechnol* **28**, 256-263 (2010).
6. Ravikumar, B., *et al.* Inhibition of mTOR induces autophagy and reduces toxicity of polyglutamine expansions in fly and mouse models of Huntington disease. *Nat Genet* **36**, 585-595 (2004).
7. Katsuno, M., *et al.* Clinical features and molecular mechanisms of spinal and bulbar muscular atrophy (SBMA). *Adv Exp Med Biol* **685**, 64-74 (2010).
8. Katsuno, M., *et al.* Efficacy and safety of leuprorelin in patients with spinal and bulbar muscular atrophy (JASMITT study): a multicentre, randomised, double-blind, placebo-controlled trial. *Lancet Neurol* **9**, 875-884 (2010).
9. Banno, H., *et al.* Phase 2 trial of leuprorelin in patients with spinal and bulbar muscular atrophy. *Ann Neurol* **65**, 140-150 (2009).
10. Yang, Z., *et al.* ASC-J9 ameliorates spinal and bulbar muscular atrophy phenotype via degradation of androgen receptor. *Nat Med* **13**, 348-353 (2007).
11. Till, S.M. The developmental roles of FMRP. *Biochem Soc Trans* **38**, 507-510 (2010).
12. Lagerbauer, B., Ostareck, D., Keidel, E.M., Ostareck-Lederer, A. & Fischer, U. Evidence that fragile X mental retardation protein is a negative regulator of translation. *Hum Mol Genet* **10**, 329-338 (2001).
13. Silverman, J.L., Tolu, S.S., Barkan, C.L. & Crawley, J.N. Repetitive self-grooming behavior in the BTBR mouse model of autism is blocked by the mGluR5 antagonist MPEP. *Neuropsychopharmacology* **35**, 976-989 (2010).
14. Campuzano, V., *et al.* Friedreich's ataxia: autosomal recessive disease caused by an intronic GAA triplet repeat expansion. *Science* **271**, 1423-1427 (1996).
15. Stemmler, T.L., Lesuisse, E., Pain, D. & Dancis, A. Frataxin and mitochondrial FeS cluster biogenesis. *J Biol Chem* **285**, 26737-26743 (2010).
16. Pandolfo, M. Molecular genetics and pathogenesis of Friedreich ataxia. *Neuromuscul Disord* **8**, 409-415 (1998).
17. Mancuso, M., Orsucci, D., Choub, A. & Siciliano, G. Current and emerging treatment options in the management of Friedreich ataxia. *Neuropsychiatr Dis Treat* **6**, 491-499 (2010).
18. Rosen, D.R., *et al.* Mutations in Cu/Zn superoxide dismutase gene are associated with familial amyotrophic lateral sclerosis. *Nature* **362**, 59-62 (1993).

19. Jung, C., *et al.* Synthetic superoxide dismutase/catalase mimetics reduce oxidative stress and prolong survival in a mouse amyotrophic lateral sclerosis model. *Neurosci Lett* **304**, 157-160 (2001).
20. Surtees, R. & Blau, N. The neurochemistry of phenylketonuria. *Eur J Pediatr* **159 Suppl 2**, S109-113 (2000).
21. Pindolia, K., Jordan, M. & Wolf, B. Analysis of mutations causing biotinidase deficiency. *Hum Mutat* **31**, 983-991 (2010).
22. Blake, D.J., Weir, A., Newey, S.E. & Davies, K.E. Function and genetics of dystrophin and dystrophin-related proteins in muscle. *Physiol Rev* **82**, 291-329 (2002).
23. Azzouz, M., *et al.* Lentivector-mediated SMN replacement in a mouse model of spinal muscular atrophy. *J Clin Invest* **114**, 1726-1731 (2004).
24. Lefebvre, S., *et al.* Identification and characterization of a spinal muscular atrophy-determining gene. *Cell* **80**, 155-165 (1995).
25. Hahnen, E., *et al.* Molecular analysis of candidate genes on chromosome 5q13 in autosomal recessive spinal muscular atrophy: evidence of homozygous deletions of the SMN gene in unaffected individuals. *Hum Mol Genet* **4**, 1927-1933 (1995).
26. Kostova, F.V., *et al.* Spinal muscular atrophy: classification, diagnosis, management, pathogenesis, and future research directions. *J Child Neurol* **22**, 926-945 (2007).
27. Melki, J., *et al.* De novo and inherited deletions of the 5q13 region in spinal muscular atrophies. *Science* **264**, 1474-1477 (1994).
28. Dooley, J., Gordon, K.E., Dodds, L. & MacSween, J. Duchenne muscular dystrophy: a 30-year population-based incidence study. *Clin Pediatr (Phila)* **49**, 177-179 (2010).
29. Su, Y.N., *et al.* Carrier Screening for Spinal Muscular Atrophy (SMA) in 107,611 Pregnant Women during the Period 2005-2009: A Prospective Population-Based Cohort Study. *PLoS One* **6**, e17067 (2011).
30. Hendrickson, B.C., *et al.* Differences in SMN1 allele frequencies among ethnic groups within North America. *J Med Genet* **46**, 641-644 (2009).
31. Cuppini, R., *et al.* The role of sensory input in motor neuron sprouting control. *Somatosens Mot Res* **19**, 279-285 (2002).
32. Yu, Z., *et al.* Androgen-dependent pathology demonstrates myopathic contribution to the Kennedy disease phenotype in a mouse knock-in model. *J Clin Invest* **116**, 2663-2672 (2006).
33. Dubowitz, V. Very severe spinal muscular atrophy (SMA type 0): an expanding clinical phenotype. *Eur J Paediatr Neurol* **3**, 49-51 (1999).
34. Pearn, J.H., Hudgson, P. & Walton, J.N. A clinical and genetic study of spinal muscular atrophy of adult onset: the autosomal recessive form as a discrete disease entity. *Brain* **101**, 591-606 (1978).
35. Brzustowicz, L.M., *et al.* Genetic mapping of chronic childhood-onset spinal muscular atrophy to chromosome 5q11.2-13.3. *Nature* **344**, 540-541 (1990).
36. Melki, J., *et al.* Gene for chronic proximal spinal muscular atrophies maps to chromosome 5q. *Nature* **344**, 767-768 (1990).
37. Brzustowicz, L.M., *et al.* Fine-mapping of the spinal muscular atrophy locus to a region flanked by MAP1B and D5S6. *Genomics* **13**, 991-998 (1992).

38. Burglen, L., *et al.* Structure and organization of the human survival motor neurone (SMN) gene. *Genomics* **32**, 479-482 (1996).
39. Monani, U.R., McPherson, J.D. & Burghes, A.H. Promoter analysis of the human centromeric and telomeric survival motor neuron genes (SMNC and SMNT). *Biochim Biophys Acta* **1445**, 330-336 (1999).
40. Echaniz-Laguna, A., Miniou, P., Bartholdi, D. & Melki, J. The promoters of the survival motor neuron gene (SMN) and its copy (SMNc) share common regulatory elements. *Am J Hum Genet* **64**, 1365-1370 (1999).
41. Monani, U.R., *et al.* A single nucleotide difference that alters splicing patterns distinguishes the SMA gene SMN1 from the copy gene SMN2. *Hum Mol Genet* **8**, 1177-1183 (1999).
42. Coover, D.D., *et al.* The survival motor neuron protein in spinal muscular atrophy. *Hum Mol Genet* **6**, 1205-1214 (1997).
43. Lorson, C.L., Hahnen, E., Androphy, E.J. & Wirth, B. A single nucleotide in the SMN gene regulates splicing and is responsible for spinal muscular atrophy. *Proc Natl Acad Sci U S A* **96**, 6307-6311 (1999).
44. Burnett, B.G., *et al.* Regulation of SMN protein stability. *Mol Cell Biol* **29**, 1107-1115 (2009).
45. Cho, S. & Dreyfuss, G. A degron created by SMN2 exon 7 skipping is a principal contributor to spinal muscular atrophy severity. *Genes Dev* **24**, 438-442 (2010).
46. Vitte, J., *et al.* Refined characterization of the expression and stability of the SMN gene products. *Am J Pathol* **171**, 1269-1280 (2007).
47. Cartegni, L. & Krainer, A.R. Disruption of an SF2/ASF-dependent exonic splicing enhancer in SMN2 causes spinal muscular atrophy in the absence of SMN1. *Nat Genet* **30**, 377-384 (2002).
48. Chang, H.C., *et al.* Modeling spinal muscular atrophy in *Drosophila*. *PLoS One* **3**, e3209 (2008).
49. Kashima, T. & Manley, J.L. A negative element in SMN2 exon 7 inhibits splicing in spinal muscular atrophy. *Nat Genet* **34**, 460-463 (2003).
50. Cartegni, L., Hastings, M.L., Calarco, J.A., de Stanchina, E. & Krainer, A.R. Determinants of exon 7 splicing in the spinal muscular atrophy genes, SMN1 and SMN2. *Am J Hum Genet* **78**, 63-77 (2006).
51. Taylor, J.E., *et al.* Correlation of SMNt and SMNc gene copy number with age of onset and survival in spinal muscular atrophy. *Eur J Hum Genet* **6**, 467-474 (1998).
52. Mailman, M.D., *et al.* Molecular analysis of spinal muscular atrophy and modification of the phenotype by SMN2. *Genet Med* **4**, 20-26 (2002).
53. Wathayati, M.S., *et al.* Combination of SMN2 copy number and NAIP deletion predicts disease severity in spinal muscular atrophy. *Brain Dev* **31**, 42-45 (2009).
54. Paushkin, S., *et al.* The survival motor neuron protein of *Schizosaccharomyces pombe*. Conservation of survival motor neuron interaction domains in divergent organisms. *J Biol Chem* **275**, 23841-23846 (2000).
55. Burt, E.C., Towers, P.R. & Sattelle, D.B. *Caenorhabditis elegans* in the study of SMN-interacting proteins: a role for SMI-1, an orthologue of human Gemin2 and the identification of novel components of the SMN complex. *Invert Neurosci* **6**, 145-159 (2006).

56. Monani, U.R., *et al.* The human centromeric survival motor neuron gene (SMN2) rescues embryonic lethality in *Smn*(^{-/-}) mice and results in a mouse with spinal muscular atrophy. *Hum Mol Genet* **9**, 333-339 (2000).
57. Schrank, B., *et al.* Inactivation of the survival motor neuron gene, a candidate gene for human spinal muscular atrophy, leads to massive cell death in early mouse embryos. *Proc Natl Acad Sci U S A* **94**, 9920-9925 (1997).
58. Wirth, B., *et al.* Allelic association and deletions in autosomal recessive proximal spinal muscular atrophy: association of marker genotype with disease severity and candidate cDNAs. *Hum Mol Genet* **4**, 1273-1284 (1995).
59. Litteljohn, D., *et al.* Inflammatory mechanisms of neurodegeneration in toxin-based models of Parkinson's disease. *Parkinsons Dis* **2011**, 713517 (2010).
60. Chio, A., Benzi, G., Dossena, M., Mutani, R. & Mora, G. Severely increased risk of amyotrophic lateral sclerosis among Italian professional football players. *Brain* **128**, 472-476 (2005).
61. Rochette, C.F., Gilbert, N. & Simard, L.R. SMN gene duplication and the emergence of the SMN2 gene occurred in distinct hominids: SMN2 is unique to *Homo sapiens*. *Hum Genet* **108**, 255-266 (2001).
62. Stone, A.C., *et al.* More reliable estimates of divergence times in Pan using complete mtDNA sequences and accounting for population structure. *Philos Trans R Soc Lond B Biol Sci* **365**, 3277-3288 (2010).
63. Armitage, S.J., *et al.* The southern route "out of Africa": evidence for an early expansion of modern humans into Arabia. *Science* **331**, 453-456 (2011).
64. Golembe, T.J., *et al.* Lymphotropic Herpesvirus saimiri uses the SMN complex to assemble Sm cores on its small RNAs. *Mol Cell Biol* **25**, 602-611 (2005).
65. Voss, M.D., *et al.* Functional cooperation of Epstein-Barr virus nuclear antigen 2 and the survival motor neuron protein in transactivation of the viral LMP1 promoter. *J Virol* **75**, 11781-11790 (2001).
66. Hamamoto, S., Nishitsuji, H., Amagasa, T., Kannagi, M. & Masuda, T. Identification of a novel human immunodeficiency virus type 1 integrase interactor, Gemin2, that facilitates efficient viral cDNA synthesis in vivo. *J Virol* **80**, 5670-5677 (2006).
67. Miguel-Aliaga, I., *et al.* The *Caenorhabditis elegans* orthologue of the human gene responsible for spinal muscular atrophy is a maternal product critical for germline maturation and embryonic viability. *Hum Mol Genet* **8**, 2133-2143 (1999).
68. Talbot, K., *et al.* Missense mutation clustering in the survival motor neuron gene: a role for a conserved tyrosine and glycine rich region of the protein in RNA metabolism? *Hum Mol Genet* **6**, 497-500 (1997).
69. Buhler, D., Raker, V., Luhrmann, R. & Fischer, U. Essential role for the tudor domain of SMN in spliceosomal U snRNP assembly: implications for spinal muscular atrophy. *Hum Mol Genet* **8**, 2351-2357 (1999).
70. Sun, Y., *et al.* Molecular and functional analysis of intragenic SMN1 mutations in patients with spinal muscular atrophy. *Hum Mutat* **25**, 64-71 (2005).
71. Hannus, S., Buhler, D., Romano, M., Seraphin, B. & Fischer, U. The *Schizosaccharomyces pombe* protein Yab8p and a novel factor, Yip1p, share

- structural and functional similarity with the spinal muscular atrophy-associated proteins SMN and SIP1. *Hum Mol Genet* **9**, 663-674 (2000).
72. Liu, Q., Fischer, U., Wang, F. & Dreyfuss, G. The spinal muscular atrophy disease gene product, SMN, and its associated protein SIP1 are in a complex with spliceosomal snRNP proteins. *Cell* **90**, 1013-1021 (1997).
 73. Kelly, W.G., Xu, S., Montgomery, M.K. & Fire, A. Distinct requirements for somatic and germline expression of a generally expressed *Caenorhabditis elegans* gene. *Genetics* **146**, 227-238 (1997).
 74. Chan, Y.B., *et al.* Neuromuscular defects in a *Drosophila* survival motor neuron gene mutant. *Hum Mol Genet* **12**, 1367-1376 (2003).
 75. McWhorter, M.L., Monani, U.R., Burghes, A.H. & Beattie, C.E. Knockdown of the survival motor neuron (Smn) protein in zebrafish causes defects in motor axon outgrowth and pathfinding. *J Cell Biol* **162**, 919-931 (2003).
 76. Nasevicius, A. & Ekker, S.C. Effective targeted gene 'knockdown' in zebrafish. *Nat Genet* **26**, 216-220 (2000).
 77. Le, T.T., *et al.* SMN Δ 7, the major product of the centromeric survival motor neuron (SMN2) gene, extends survival in mice with spinal muscular atrophy and associates with full-length SMN. *Hum Mol Genet* **14**, 845-857 (2005).
 78. Kariya, S., *et al.* Reduced SMN protein impairs maturation of the neuromuscular junctions in mouse models of spinal muscular atrophy. *Hum Mol Genet* **17**, 2552-2569 (2008).
 79. McGovern, V.L., Gavrulina, T.O., Beattie, C.E. & Burghes, A.H. Embryonic motor axon development in the severe SMA mouse. *Hum Mol Genet* **17**, 2900-2909 (2008).
 80. Kong, L., *et al.* Impaired synaptic vesicle release and immaturity of neuromuscular junctions in spinal muscular atrophy mice. *J Neurosci* **29**, 842-851 (2009).
 81. Gavrulina, T.O., *et al.* Neuronal SMN expression corrects spinal muscular atrophy in severe SMA mice while muscle-specific SMN expression has no phenotypic effect. *Hum Mol Genet* **17**, 1063-1075 (2008).
 82. Hammond, S.M., *et al.* Mouse survival motor neuron alleles that mimic SMN2 splicing and are inducible rescue embryonic lethality early in development but not late. *PLoS One* **5**, e15887 (2010).
 83. Novelli, G., *et al.* Expression study of survival motor neuron gene in human fetal tissues. *Biochem Mol Med* **61**, 102-106 (1997).
 84. Burlet, P., *et al.* The distribution of SMN protein complex in human fetal tissues and its alteration in spinal muscular atrophy. *Hum Mol Genet* **7**, 1927-1933 (1998).
 85. La Bella, V., Cisterni, C., Salaun, D. & Pettmann, B. Survival motor neuron (SMN) protein in rat is expressed as different molecular forms and is developmentally regulated. *Eur J Neurosci* **10**, 2913-2923 (1998).
 86. Battaglia, G., Princivalle, A., Forti, F., Lizier, C. & Zeviani, M. Expression of the SMN gene, the spinal muscular atrophy determining gene, in the mammalian central nervous system. *Hum Mol Genet* **6**, 1961-1971 (1997).
 87. Jablonka, S., Schrank, B., Kralewski, M., Rossoll, W. & Sendtner, M. Reduced survival motor neuron (Smn) gene dose in mice leads to motor neuron

- degeneration: an animal model for spinal muscular atrophy type III. *Hum Mol Genet* **9**, 341-346 (2000).
88. Liu, Q. & Dreyfuss, G. A novel nuclear structure containing the survival of motor neurons protein. *EMBO J* **15**, 3555-3565 (1996).
 89. Young, P.J., Le, T.T., thi Man, N., Burghes, A.H. & Morris, G.E. The relationship between SMN, the spinal muscular atrophy protein, and nuclear coiled bodies in differentiated tissues and cultured cells. *Exp Cell Res* **256**, 365-374 (2000).
 90. Morris, G.E. The Cajal body. *Biochim Biophys Acta* **1783**, 2108-2115 (2008).
 91. Young, P.J., *et al.* Nuclear gems and Cajal (coiled) bodies in fetal tissues: nucleolar distribution of the spinal muscular atrophy protein, SMN. *Exp Cell Res* **265**, 252-261 (2001).
 92. Gubitz, A.K., Feng, W. & Dreyfuss, G. The SMN complex. *Exp Cell Res* **296**, 51-56 (2004).
 93. Sprangers, R., Selenko, P., Sattler, M., Sinning, I. & Groves, M.R. Definition of domain boundaries and crystallization of the SMN Tudor domain. *Acta Crystallogr D Biol Crystallogr* **59**, 366-368 (2003).
 94. Sprangers, R., Groves, M.R., Sinning, I. & Sattler, M. High-resolution X-ray and NMR structures of the SMN Tudor domain: conformational variation in the binding site for symmetrically dimethylated arginine residues. *J Mol Biol* **327**, 507-520 (2003).
 95. Kotani, T., *et al.* A novel mutation at the N-terminal of SMN Tudor domain inhibits its interaction with target proteins. *J Neurol* **254**, 624-630 (2007).
 96. Shpargel, K.B. & Matera, A.G. Gemin proteins are required for efficient assembly of Sm-class ribonucleoproteins. *Proc Natl Acad Sci U S A* **102**, 17372-17377 (2005).
 97. Cusco, I., Barcelo, M.J., del Rio, E., Baiget, M. & Tizzano, E.F. Detection of novel mutations in the SMN Tudor domain in type I SMA patients. *Neurology* **63**, 146-149 (2004).
 98. Workman, E., *et al.* A SMN missense mutation complements SMN2 restoring snRNPs and rescuing SMA mice. *Hum Mol Genet* **18**, 2215-2229 (2009).
 99. Gabanella, F., *et al.* Ribonucleoprotein assembly defects correlate with spinal muscular atrophy severity and preferentially affect a subset of spliceosomal snRNPs. *PLoS One* **2**, e921 (2007).
 100. Winkler, C., *et al.* Reduced U snRNP assembly causes motor axon degeneration in an animal model for spinal muscular atrophy. *Genes Dev* **19**, 2320-2330 (2005).
 101. Fischer, U., Liu, Q. & Dreyfuss, G. The SMN-SIP1 complex has an essential role in spliceosomal snRNP biogenesis. *Cell* **90**, 1023-1029 (1997).
 102. Monani, U.R., *et al.* A transgene carrying an A2G missense mutation in the SMN gene modulates phenotypic severity in mice with severe (type I) spinal muscular atrophy. *J Cell Biol* **160**, 41-52 (2003).
 103. Lorson, C.L., *et al.* SMN oligomerization defect correlates with spinal muscular atrophy severity. *Nat Genet* **19**, 63-66 (1998).
 104. Pellizzoni, L., Charroux, B. & Dreyfuss, G. SMN mutants of spinal muscular atrophy patients are defective in binding to snRNP proteins. *Proc Natl Acad Sci U S A* **96**, 11167-11172 (1999).

105. Nguyen thi, M., *et al.* A two-site ELISA can quantify upregulation of SMN protein by drugs for spinal muscular atrophy. *Neurology* **71**, 1757-1763 (2008).
106. Hahnen, E., *et al.* Missense mutations in exon 6 of the survival motor neuron gene in patients with spinal muscular atrophy (SMA). *Hum Mol Genet* **6**, 821-825 (1997).
107. Carrel, T.L., *et al.* Survival motor neuron function in motor axons is independent of functions required for small nuclear ribonucleoprotein biogenesis. *J Neurosci* **26**, 11014-11022 (2006).
108. Young, P.J., *et al.* A direct interaction between the survival motor neuron protein and p53 and its relationship to spinal muscular atrophy. *J Biol Chem* **277**, 2852-2859 (2002).
109. Iwahashi, H., *et al.* Synergistic anti-apoptotic activity between Bcl-2 and SMN implicated in spinal muscular atrophy. *Nature* **390**, 413-417 (1997).
110. Sato, K., Eguchi, Y., Kodama, T.S. & Tsujimoto, Y. Regions essential for the interaction between Bcl-2 and SMN, the spinal muscular atrophy disease gene product. *Cell Death Differ* **7**, 374-383 (2000).
111. Glinka, M., *et al.* The heterogeneous nuclear ribonucleoprotein-R is necessary for axonal beta-actin mRNA translocation in spinal motor neurons. *Hum Mol Genet* **19**, 1951-1966 (2010).
112. Todd, A.G., *et al.* SMN, Gemin2 and Gemin3 associate with beta-actin mRNA in the cytoplasm of neuronal cells in vitro. *J Mol Biol* **401**, 681-689 (2010).
113. Paushkin, S., Gubitz, A.K., Massenet, S. & Dreyfuss, G. The SMN complex, an assemblysome of ribonucleoproteins. *Curr Opin Cell Biol* **14**, 305-312 (2002).
114. Battle, D.J., *et al.* The SMN complex: an assembly machine for RNPs. *Cold Spring Harb Symp Quant Biol* **71**, 313-320 (2006).
115. Pellizzoni, L., Yong, J. & Dreyfuss, G. Essential role for the SMN complex in the specificity of snRNP assembly. *Science* **298**, 1775-1779 (2002).
116. Eggert, C., Chari, A., Laggerbauer, B. & Fischer, U. Spinal muscular atrophy: the RNP connection. *Trends Mol Med* **12**, 113-121 (2006).
117. Lerner, M.R. & Steitz, J.A. Antibodies to small nuclear RNAs complexed with proteins are produced by patients with systemic lupus erythematosus. *Proc Natl Acad Sci U S A* **76**, 5495-5499 (1979).
118. Lerner, M.R., Boyle, J.A., Mount, S.M., Wolin, S.L. & Steitz, J.A. Are snRNPs involved in splicing? *Nature* **283**, 220-224 (1980).
119. Raker, V.A., Hartmuth, K., Kastner, B. & Luhrmann, R. Spliceosomal U snRNP core assembly: Sm proteins assemble onto an Sm site RNA nonanucleotide in a specific and thermodynamically stable manner. *Mol Cell Biol* **19**, 6554-6565 (1999).
120. Charroux, B., *et al.* Gemin3: A novel DEAD box protein that interacts with SMN, the spinal muscular atrophy gene product, and is a component of gems. *J Cell Biol* **147**, 1181-1194 (1999).
121. Charroux, B., *et al.* Gemin4. A novel component of the SMN complex that is found in both gems and nucleoli. *J Cell Biol* **148**, 1177-1186 (2000).
122. Gubitz, A.K., *et al.* Gemin5, a novel WD repeat protein component of the SMN complex that binds Sm proteins. *J Biol Chem* **277**, 5631-5636 (2002).

123. Pellizzoni, L., Baccon, J., Rappsilber, J., Mann, M. & Dreyfuss, G. Purification of native survival of motor neurons complexes and identification of Gemin6 as a novel component. *J Biol Chem* **277**, 7540-7545 (2002).
124. Baccon, J., Pellizzoni, L., Rappsilber, J., Mann, M. & Dreyfuss, G. Identification and characterization of Gemin7, a novel component of the survival of motor neuron complex. *J Biol Chem* **277**, 31957-31962 (2002).
125. Carissimi, C., *et al.* Gemin8 is a novel component of the survival motor neuron complex and functions in small nuclear ribonucleoprotein assembly. *J Biol Chem* **281**, 8126-8134 (2006).
126. Carissimi, C., *et al.* Unrip is a component of SMN complexes active in snRNP assembly. *FEBS Lett* **579**, 2348-2354 (2005).
127. Yan, X., Mouillet, J.F., Ou, Q. & Sadovsky, Y. A novel domain within the DEAD-box protein DP103 is essential for transcriptional repression and helicase activity. *Mol Cell Biol* **23**, 414-423 (2003).
128. Chari, A., *et al.* An assembly chaperone collaborates with the SMN complex to generate spliceosomal SnRNPs. *Cell* **135**, 497-509 (2008).
129. Brahm, H., Meheus, L., de Brabandere, V., Fischer, U. & Luhrmann, R. Symmetrical dimethylation of arginine residues in spliceosomal Sm protein B/B' and the Sm-like protein LSm4, and their interaction with the SMN protein. *RNA* **7**, 1531-1542 (2001).
130. Meister, G., *et al.* Methylation of Sm proteins by a complex containing PRMT5 and the putative U snRNP assembly factor pICln. *Curr Biol* **11**, 1990-1994 (2001).
131. Meister, G. & Fischer, U. Assisted RNP assembly: SMN and PRMT5 complexes cooperate in the formation of spliceosomal UsnRNPs. *EMBO J* **21**, 5853-5863 (2002).
132. Friesen, W.J., *et al.* The methylosome, a 20S complex containing JBP1 and pICln, produces dimethylarginine-modified Sm proteins. *Mol Cell Biol* **21**, 8289-8300 (2001).
133. Meister, G., Buhler, D., Pillai, R., Lottspeich, F. & Fischer, U. A multiprotein complex mediates the ATP-dependent assembly of spliceosomal U snRNPs. *Nat Cell Biol* **3**, 945-949 (2001).
134. Battle, D.J., *et al.* The Gemin5 protein of the SMN complex identifies snRNAs. *Mol Cell* **23**, 273-279 (2006).
135. Mouaikel, J., *et al.* Interaction between the small-nuclear-RNA cap hypermethylase and the spinal muscular atrophy protein, survival of motor neuron. *EMBO Rep* **4**, 616-622 (2003).
136. Kamboj, V.P., Singh, M.M. & Chowdhury, S.R. Effect of a post-caesarian insertion of intrauterine contraceptive device on the involution of rat uterus. *Indian J Exp Biol* **14**, 314-316 (1976).
137. Huber, J., Dickmanns, A. & Luhrmann, R. The importin-beta binding domain of snurportin1 is responsible for the Ran- and energy-independent nuclear import of spliceosomal U snRNPs in vitro. *J Cell Biol* **156**, 467-479 (2002).
138. Narayanan, U., Achsel, T., Luhrmann, R. & Matera, A.G. Coupled in vitro import of U snRNPs and SMN, the spinal muscular atrophy protein. *Mol Cell* **16**, 223-234 (2004).

139. Carvalho, T., *et al.* The spinal muscular atrophy disease gene product, SMN: A link between snRNP biogenesis and the Cajal (coiled) body. *J Cell Biol* **147**, 715-728 (1999).
140. Matera, A.G., Terns, R.M. & Terns, M.P. Non-coding RNAs: lessons from the small nuclear and small nucleolar RNAs. *Nat Rev Mol Cell Biol* **8**, 209-220 (2007).
141. McWhorter, M.L., Boon, K.L., Horan, E.S., Burghes, A.H. & Beattie, C.E. The SMN binding protein Gemin2 is not involved in motor axon outgrowth. *Dev Neurobiol* **68**, 182-194 (2008).
142. Rossoll, W., *et al.* Specific interaction of Smn, the spinal muscular atrophy determining gene product, with hnRNP-R and gry-rbp/hnRNP-Q: a role for Smn in RNA processing in motor axons? *Hum Mol Genet* **11**, 93-105 (2002).
143. Friesen, W.J. & Dreyfuss, G. Specific sequences of the Sm and Sm-like (Lsm) proteins mediate their interaction with the spinal muscular atrophy disease gene product (SMN). *J Biol Chem* **275**, 26370-26375 (2000).
144. Rossoll, W., *et al.* Smn, the spinal muscular atrophy-determining gene product, modulates axon growth and localization of beta-actin mRNA in growth cones of motoneurons. *J Cell Biol* **163**, 801-812 (2003).
145. Kislauskis, E.H., Zhu, X. & Singer, R.H. Sequences responsible for intracellular localization of beta-actin messenger RNA also affect cell phenotype. *J Cell Biol* **127**, 441-451 (1994).
146. Jablonka, S., Beck, M., Lechner, B.D., Mayer, C. & Sendtner, M. Defective Ca²⁺ channel clustering in axon terminals disturbs excitability in motoneurons in spinal muscular atrophy. *J Cell Biol* **179**, 139-149 (2007).
147. Giesemann, T., *et al.* A role for polyproline motifs in the spinal muscular atrophy protein SMN. Profilins bind to and colocalize with smn in nuclear gems. *J Biol Chem* **274**, 37908-37914 (1999).
148. Sharma, A., *et al.* A role for complexes of survival of motor neurons (SMN) protein with gemins and profilin in neurite-like cytoplasmic extensions of cultured nerve cells. *Exp Cell Res* **309**, 185-197 (2005).
149. Pantaloni, D. & Carlier, M.F. How profilin promotes actin filament assembly in the presence of thymosin beta 4. *Cell* **75**, 1007-1014 (1993).
150. Lambrechts, A., *et al.* Profilin II is alternatively spliced, resulting in profilin isoforms that are differentially expressed and have distinct biochemical properties. *Mol Cell Biol* **20**, 8209-8219 (2000).
151. Bowerman, M., Shafey, D. & Kothary, R. Smn depletion alters profilin II expression and leads to upregulation of the RhoA/ROCK pathway and defects in neuronal integrity. *J Mol Neurosci* **32**, 120-131 (2007).
152. Braiteh, F., *et al.* Phase I study of epigenetic modulation with 5-azacytidine and valproic acid in patients with advanced cancers. *Clin Cancer Res* **14**, 6296-6301 (2008).
153. Amano, M., Nakayama, M. & Kaibuchi, K. Rho-kinase/ROCK: A key regulator of the cytoskeleton and cell polarity. *Cytoskeleton (Hoboken)* **67**, 545-554 (2010).
154. Amano, M., *et al.* Phosphorylation and activation of myosin by Rho-associated kinase (Rho-kinase). *J Biol Chem* **271**, 20246-20249 (1996).

155. Da Silva, J.S., *et al.* RhoA/ROCK regulation of neuritogenesis via profilin IIA-mediated control of actin stability. *J Cell Biol* **162**, 1267-1279 (2003).
156. Oprea, G.E., *et al.* Plastin 3 is a protective modifier of autosomal recessive spinal muscular atrophy. *Science* **320**, 524-527 (2008).
157. Dent, E.W. & Gertler, F.B. Cytoskeletal dynamics and transport in growth cone motility and axon guidance. *Neuron* **40**, 209-227 (2003).
158. Bowerman, M., *et al.* SMN, profilin IIA and plastin 3: a link between the deregulation of actin dynamics and SMA pathogenesis. *Mol Cell Neurosci* **42**, 66-74 (2009).
159. Bowerman, M., Beauvais, A., Anderson, C.L. & Kothary, R. Rho-kinase inactivation prolongs survival of an intermediate SMA mouse model. *Hum Mol Genet* **19**, 1468-1478 (2010).
160. Bechade, C., *et al.* Subcellular distribution of survival motor neuron (SMN) protein: possible involvement in nucleocytoplasmic and dendritic transport. *Eur J Neurosci* **11**, 293-304 (1999).
161. Wishart, T.M., *et al.* SMN deficiency disrupts brain development in a mouse model of severe spinal muscular atrophy. *Hum Mol Genet* **19**, 4216-4228 (2010).
162. Hsieh-Li, H.M., *et al.* A mouse model for spinal muscular atrophy. *Nat Genet* **24**, 66-70 (2000).
163. Murray, L.M., *et al.* Selective vulnerability of motor neurons and dissociation of pre- and post-synaptic pathology at the neuromuscular junction in mouse models of spinal muscular atrophy. *Hum Mol Genet* **17**, 949-962 (2008).
164. Cifuentes-Diaz, C., *et al.* Neurofilament accumulation at the motor endplate and lack of axonal sprouting in a spinal muscular atrophy mouse model. *Hum Mol Genet* **11**, 1439-1447 (2002).
165. Murray, L.M., *et al.* Pre-symptomatic development of lower motor neuron connectivity in a mouse model of severe spinal muscular atrophy. *Hum Mol Genet* **19**, 420-433 (2010).
166. Voigt, T., Meyer, K., Baum, O. & Schumperli, D. Ultrastructural changes in diaphragm neuromuscular junctions in a severe mouse model for Spinal Muscular Atrophy and their prevention by bifunctional U7 snRNA correcting SMN2 splicing. *Neuromuscul Disord* **20**, 744-752 (2010).
167. Ling, K.K., Lin, M.Y., Zingg, B., Feng, Z. & Ko, C.P. Synaptic defects in the spinal and neuromuscular circuitry in a mouse model of spinal muscular atrophy. *PLoS One* **5**, e15457 (2010).
168. Salinas, S., Carazo-Salas, R.E., Proukakis, C., Schiavo, G. & Warner, T.T. Spastin and microtubules: Functions in health and disease. *J Neurosci Res* **85**, 2778-2782 (2007).
169. Penny, E.B. & McCabe, B.D. All neuropathies great and small. *J Clin Invest* **115**, 2968-2971 (2005).
170. Park, S.G., Schimmel, P. & Kim, S. Aminoacyl tRNA synthetases and their connections to disease. *Proc Natl Acad Sci U S A* **105**, 11043-11049 (2008).
171. Thomas, B. & Beal, M.F. Parkinson's disease. *Hum Mol Genet* **16 Spec No. 2**, R183-194 (2007).

172. Setola, V., *et al.* Axonal-SMN (a-SMN), a protein isoform of the survival motor neuron gene, is specifically involved in axonogenesis. *Proc Natl Acad Sci U S A* **104**, 1959-1964 (2007).
173. Conti-Fine, B.M., Milani, M. & Kaminski, H.J. Myasthenia gravis: past, present, and future. *J Clin Invest* **116**, 2843-2854 (2006).
174. Takamori, M. Lambert-Eaton myasthenic syndrome: search for alternative autoimmune targets and possible compensatory mechanisms based on presynaptic calcium homeostasis. *J Neuroimmunol* **201-202**, 145-152 (2008).
175. Titulaer, M.J., *et al.* Screening for tumours in paraneoplastic syndromes: report of an EFNS task force. *Eur J Neurol* **18**, 19-e13 (2011).
176. Geppert, M., *et al.* Synaptotagmin I: a major Ca²⁺ sensor for transmitter release at a central synapse. *Cell* **79**, 717-727 (1994).
177. Mizutani, A., Fukuda, M., Ibata, K., Shiraishi, Y. & Mikoshiba, K. SYNCRIP, a cytoplasmic counterpart of heterogeneous nuclear ribonucleoprotein R, interacts with ubiquitous synaptotagmin isoforms. *J Biol Chem* **275**, 9823-9831 (2000).
178. Rizo, J. & Rosenmund, C. Synaptic vesicle fusion. *Nat Struct Mol Biol* **15**, 665-674 (2008).
179. Lee, H.K., *et al.* Dynamic Ca²⁺-dependent stimulation of vesicle fusion by membrane-anchored synaptotagmin I. *Science* **328**, 760-763 (2010).
180. Fernandez-Chacon, R., *et al.* Synaptotagmin I functions as a calcium regulator of release probability. *Nature* **410**, 41-49 (2001).
181. Jorgensen, E.M., *et al.* Defective recycling of synaptic vesicles in synaptotagmin mutants of *Caenorhabditis elegans*. *Nature* **378**, 196-199 (1995).
182. Fergestad, T. & Broadie, K. Interaction of stoned and synaptotagmin in synaptic vesicle endocytosis. *J Neurosci* **21**, 1218-1227 (2001).
183. Boon, K.L., *et al.* Zebrafish survival motor neuron mutants exhibit presynaptic neuromuscular junction defects. *Hum Mol Genet* **18**, 3615-3625 (2009).
184. Ruiz, R., Casanas, J.J., Torres-Benito, L., Cano, R. & Tabares, L. Altered intracellular Ca²⁺ homeostasis in nerve terminals of severe spinal muscular atrophy mice. *J Neurosci* **30**, 849-857 (2010).
185. Zhang, H., Robinson, N., Wu, C., Wang, W. & Harrington, M.A. Electrophysiological properties of motor neurons in a mouse model of severe spinal muscular atrophy: in vitro versus in vivo development. *PLoS One* **5**, e11696 (2010).
186. Jablonka, S., *et al.* Gene targeting of Gemin2 in mice reveals a correlation between defects in the biogenesis of U snRNPs and motoneuron cell death. *Proc Natl Acad Sci U S A* **99**, 10126-10131 (2002).
187. Alioto, T.S. U12DB: a database of orthologous U12-type spliceosomal introns. *Nucleic Acids Res* **35**, D110-115 (2007).
188. Levine, A. & Durbin, R. A computational scan for U12-dependent introns in the human genome sequence. *Nucleic Acids Res* **29**, 4006-4013 (2001).
189. Baumer, D., *et al.* Alternative splicing events are a late feature of pathology in a mouse model of spinal muscular atrophy. *PLoS Genet* **5**, e1000773 (2009).
190. Briese, M., Esmaeili, B. & Sattelle, D.B. Is spinal muscular atrophy the result of defects in motor neuron processes? *Bioessays* **27**, 946-957 (2005).

191. Broder, S. The development of antiretroviral therapy and its impact on the HIV-1/AIDS pandemic. *Antiviral Res* **85**, 1-18 (2010).
192. Morris, E.J. & Geller, H.M. Induction of neuronal apoptosis by camptothecin, an inhibitor of DNA topoisomerase-I: evidence for cell cycle-independent toxicity. *J Cell Biol* **134**, 757-770 (1996).
193. Tang, D., Lahti, J.M. & Kidd, V.J. Caspase-8 activation and bid cleavage contribute to MCF7 cellular execution in a caspase-3-dependent manner during staurosporine-mediated apoptosis. *J Biol Chem* **275**, 9303-9307 (2000).
194. Alessenko, A.V., *et al.* Mechanisms of cycloheximide-induced apoptosis in liver cells. *FEBS Lett* **416**, 113-116 (1997).
195. Lupardus, P.J., Shen, A., Bogyo, M. & Garcia, K.C. Small molecule-induced allosteric activation of the *Vibrio cholerae* RTX cysteine protease domain. *Science* **322**, 265-268 (2008).
196. Wolan, D.W., Zorn, J.A., Gray, D.C. & Wells, J.A. Small-molecule activators of a proenzyme. *Science* **326**, 853-858 (2009).
197. Jarecki, J., *et al.* Diverse small-molecule modulators of SMN expression found by high-throughput compound screening: early leads towards a therapeutic for spinal muscular atrophy. *Hum Mol Genet* **14**, 2003-2018 (2005).
198. Singh, J., *et al.* DcpS as a therapeutic target for spinal muscular atrophy. *ACS Chem Biol* **3**, 711-722 (2008).
199. Andreassi, C., *et al.* Aclarubicin treatment restores SMN levels to cells derived from type I spinal muscular atrophy patients. *Hum Mol Genet* **10**, 2841-2849 (2001).
200. Marks, P.A. Histone deacetylase inhibitors: a chemical genetics approach to understanding cellular functions. *Biochim Biophys Acta* **1799**, 717-725 (2010).
201. Struhl, K. Histone acetylation and transcriptional regulatory mechanisms. *Genes Dev* **12**, 599-606 (1998).
202. Riggs, M.G., Whittaker, R.G., Neumann, J.R. & Ingram, V.M. n-Butyrate causes histone modification in HeLa and Friend erythroleukaemia cells. *Nature* **268**, 462-464 (1977).
203. Van Lint, C., Emiliani, S. & Verdin, E. The expression of a small fraction of cellular genes is changed in response to histone hyperacetylation. *Gene Expr* **5**, 245-253 (1996).
204. Yang, X.J. & Seto, E. HATs and HDACs: from structure, function and regulation to novel strategies for therapy and prevention. *Oncogene* **26**, 5310-5318 (2007).
205. L'Hernault, S.W. & Rosenbaum, J.L. Chlamydomonas alpha-tubulin is posttranslationally modified by acetylation on the epsilon-amino group of a lysine. *Biochemistry* **24**, 473-478 (1985).
206. Piperno, G. & Fuller, M.T. Monoclonal antibodies specific for an acetylated form of alpha-tubulin recognize the antigen in cilia and flagella from a variety of organisms. *J Cell Biol* **101**, 2085-2094 (1985).
207. Yang, X.J. & Gregoire, S. Metabolism, cytoskeleton and cellular signalling in the grip of protein Nepsilon - and O-acetylation. *EMBO Rep* **8**, 556-562 (2007).
208. Wheless, J.W., Clarke, D.F. & Carpenter, D. Treatment of pediatric epilepsy: expert opinion, 2005. *J Child Neurol* **20 Suppl 1**, S1-S6; quiz S59-60 (2005).

209. Loscher, W. Basic pharmacology of valproate: a review after 35 years of clinical use for the treatment of epilepsy. *CNS Drugs* **16**, 669-694 (2002).
210. Kuendgen, A., *et al.* The histone deacetylase (HDAC) inhibitor valproic acid as monotherapy or in combination with all-trans retinoic acid in patients with acute myeloid leukemia. *Cancer* **106**, 112-119 (2006).
211. Chang, J.G., *et al.* Treatment of spinal muscular atrophy by sodium butyrate. *Proc Natl Acad Sci U S A* **98**, 9808-9813 (2001).
212. Calleja, S., Salas-Puig, J., Ribacoba, R. & Lahoz, C.H. Evolution of juvenile myoclonic epilepsy treated from the outset with sodium valproate. *Seizure* **10**, 424-427 (2001).
213. Sumner, C.J., *et al.* Valproic acid increases SMN levels in spinal muscular atrophy patient cells. *Ann Neurol* **54**, 647-654 (2003).
214. Brichta, L., *et al.* Valproic acid increases the SMN2 protein level: a well-known drug as a potential therapy for spinal muscular atrophy. *Hum Mol Genet* **12**, 2481-2489 (2003).
215. Tsai, L.K., Tsai, M.S., Ting, C.H. & Li, H. Multiple therapeutic effects of valproic acid in spinal muscular atrophy model mice. *J Mol Med* **86**, 1243-1254 (2008).
216. Rak, K., *et al.* Valproic acid blocks excitability in SMA type I mouse motor neurons. *Neurobiol Dis* **36**, 477-487 (2009).
217. Swoboda, K.J., *et al.* Phase II open label study of valproic acid in spinal muscular atrophy. *PLoS One* **4**, e5268 (2009).
218. Swoboda, K.J., *et al.* SMA CARNI-VAL trial part I: double-blind, randomized, placebo-controlled trial of L-carnitine and valproic acid in spinal muscular atrophy. *PLoS One* **5**, e12140 (2010).
219. Noland, R.C., *et al.* Carnitine insufficiency caused by aging and overnutrition compromises mitochondrial performance and metabolic control. *J Biol Chem* **284**, 22840-22852 (2009).
220. Littarru, G.P. & Tiano, L. Clinical aspects of coenzyme Q10: an update. *Curr Opin Clin Nutr Metab Care* **8**, 641-646 (2005).
221. Brichta, L., Holker, I., Haug, K., Klockgether, T. & Wirth, B. In vivo activation of SMN in spinal muscular atrophy carriers and patients treated with valproate. *Ann Neurol* **59**, 970-975 (2006).
222. Andreassi, C., *et al.* Phenylbutyrate increases SMN expression in vitro: relevance for treatment of spinal muscular atrophy. *Eur J Hum Genet* **12**, 59-65 (2004).
223. Gilbert, J., *et al.* A phase I dose escalation and bioavailability study of oral sodium phenylbutyrate in patients with refractory solid tumor malignancies. *Clin Cancer Res* **7**, 2292-2300 (2001).
224. Grzeschik, S.M., Ganta, M., Prior, T.W., Heavlin, W.D. & Wang, C.H. Hydroxyurea enhances SMN2 gene expression in spinal muscular atrophy cells. *Ann Neurol* **58**, 194-202 (2005).
225. Liang, W.C., *et al.* The effect of hydroxyurea in spinal muscular atrophy cells and patients. *J Neurol Sci* **268**, 87-94 (2008).
226. Chen, T.H., *et al.* Randomized, double-blind, placebo-controlled trial of hydroxyurea in spinal muscular atrophy. *Neurology* **75**, 2190-2197 (2010).

227. Marks, P.A., Richon, V.M., Miller, T. & Kelly, W.K. Histone deacetylase inhibitors. *Adv Cancer Res* **91**, 137-168 (2004).
228. Richon, V.M., *et al.* Second generation hybrid polar compounds are potent inducers of transformed cell differentiation. *Proc Natl Acad Sci U S A* **93**, 5705-5708 (1996).
229. Hahnen, E., *et al.* In vitro and ex vivo evaluation of second-generation histone deacetylase inhibitors for the treatment of spinal muscular atrophy. *J Neurochem* **98**, 193-202 (2006).
230. Jung, M., *et al.* Amide analogues of trichostatin A as inhibitors of histone deacetylase and inducers of terminal cell differentiation. *J Med Chem* **42**, 4669-4679 (1999).
231. Saito, A., *et al.* A synthetic inhibitor of histone deacetylase, MS-27-275, with marked in vivo antitumor activity against human tumors. *Proc Natl Acad Sci U S A* **96**, 4592-4597 (1999).
232. Riessland, M., *et al.* SAHA ameliorates the SMA phenotype in two mouse models for spinal muscular atrophy. *Hum Mol Genet* **19**, 1492-1506 (2010).
233. Hockly, E., *et al.* Suberoylanilide hydroxamic acid, a histone deacetylase inhibitor, ameliorates motor deficits in a mouse model of Huntington's disease. *Proc Natl Acad Sci U S A* **100**, 2041-2046 (2003).
234. Lunn, M.R., *et al.* Indoprofen upregulates the survival motor neuron protein through a cyclooxygenase-independent mechanism. *Chem Biol* **11**, 1489-1493 (2004).
235. Zhang, M.L., Lorson, C.L., Androphy, E.J. & Zhou, J. An in vivo reporter system for measuring increased inclusion of exon 7 in SMN2 mRNA: potential therapy of SMA. *Gene Ther* **8**, 1532-1538 (2001).
236. Cashman, J.N. The mechanisms of action of NSAIDs in analgesia. *Drugs* **52 Suppl 5**, 13-23 (1996).
237. Higuchi, K., *et al.* Present status and strategy of NSAIDs-induced small bowel injury. *J Gastroenterol* **44**, 879-888 (2009).
238. Samson, K. SMA Drug Development Gains Momentum Under NINDS Model for Neuro-Research Partnerships. *Neurology Today* **7**, 11-20 (2007).
239. Passini, M.A. & Cheng, S.H. Prospects for the gene therapy of spinal muscular atrophy. *Trends Mol Med* (2011).
240. Foust, K.D., *et al.* Intravascular AAV9 preferentially targets neonatal neurons and adult astrocytes. *Nat Biotechnol* **27**, 59-65 (2009).
241. Foust, K.D., *et al.* Rescue of the spinal muscular atrophy phenotype in a mouse model by early postnatal delivery of SMN. *Nat Biotechnol* **28**, 271-274 (2010).
242. Valori, C.F., *et al.* Systemic delivery of scAAV9 expressing SMN prolongs survival in a model of spinal muscular atrophy. *Sci Transl Med* **2**, 35ra42 (2010).

Chapter 2. Small molecule upregulator reveals regulation of SMN protein levels by Ras

High-throughput screen for small molecule upregulators of SMN protein levels

Bioactive small molecules have enabled major advances in biological research and drug development. Although many efforts have focused on the identification of small molecule inhibitors of protein function, the ability to upregulate protein abundance or otherwise increase protein activity can provide complementary insights that cannot be obtained through loss of function studies alone ¹. Although the number of compounds known to function as protein upregulators is quite small, they have important research and therapeutic applications. Examples include histone deacetylase inhibitors, used in the treatment of psychiatric conditions, neurologic disorders and cutaneous T cell lymphoma ²⁻⁴, and proteasome inhibitors, used in the treatment of multiple myeloma ⁵ and for the study of the ubiquitin-proteasome system ⁶.

Unfortunately, these known upregulating compounds lack specificity, altering the levels of hundreds to thousands of gene products ⁷. Such broad spectrum effects, in addition to potentially being therapeutically undesirable, make these compounds unsuitable for investigations of mechanisms regulating the abundance of an individual or limited number of proteins. Small molecules that can upregulate specific protein targets are needed in order to expand the small molecule toolkit, and would be especially advantageous for the study of loss of function diseases. However, we lack systematic methods for identifying such compounds.

In order to address this need, we developed a high-throughput screening approach to identify small molecule upregulators of a specific protein. This assay detects increases in the abundance of a target protein after treatment with small molecule libraries. We selected the Survival of Motor Neuron (SMN) protein as a target for modulation. Decreased SMN protein levels result in the loss of function neurodegenerative disease Spinal Muscular Atrophy⁸. In patients, SMN protein levels are severely decreased to 10% of carrier levels, due to homozygous deletion of the *survival of motor neuron 1* (*smn1*) gene, but retention of the *smn2* gene⁹. The *smn2* gene is nearly identical to *smn1*, but contains a translationally silent C to T transition which causes the *smn2* pre-mRNA to be aberrantly spliced, generating only ~10% of the full-length, functional protein produced by the *smn1* gene¹⁰. This small amount of SMN protein prevents the embryonic lethality seen in an SMN null background¹¹, but cannot prevent the motor neuron degeneration observed in SMA. Small molecule upregulators of SMN could provide novel insights into the regulation of SMN protein levels, leading the way to new therapeutic targets.

We screened 69,189 small molecules and discovered three SMN-upregulating compounds. Mechanistic investigations of the most effective compound, Chemical Upregulator of SMN Protein-1 (cuspin-1), revealed that increasing Ras signaling upregulates SMN protein levels by enhancing the rate of SMN translation.

Screen development and optimization

In order to identify compounds upregulating SMN protein levels, we developed a high-throughput screen for monitoring the levels of endogenous SMN protein in SMA patient fibroblast cells. Previous screens searching for SMN-upregulating compounds focused on altering either the transcription or splicing of *smn2*^{12,13}. Our screen focuses on the desired final product, SMN protein abundance, in order to be inclusive of all aspects of SMN protein regulation, from transcription through degradation. This method permits identification of small molecule upregulators of SMN protein without bias towards their mechanism of action.

To quantify SMN protein levels in a 384-well format, the cyto blot assay¹⁴, a modified enzyme-linked immunosorbent assay (ELISA), was optimized for microtiter-based screening using SMA patient fibroblasts. A schematic of the primary screening workflow is shown in Figure 1. The assay protocol involved the seeding of cells and subsequent treatment with small molecules for 48 hours. This incubation period was selected to allow sufficient time for the compounds to increase SMN protein levels, while limiting the depletion of nutrients and accumulation of toxins in the microtiter format during prolonged incubation¹⁵. After incubation, cells were fixed, permeabilized and incubated with primary and secondary antibodies in-plate. Horseradish peroxidase-derived chemiluminescence was detected using an automated platereader. The optimized SMN cyto blot is a suitably robust format for detecting SMN levels in cells, as indicated by a *Z'* factor¹⁶ of 0.5 in the optimized assay, using the #3814 SMA carrier cell line as a positive control.

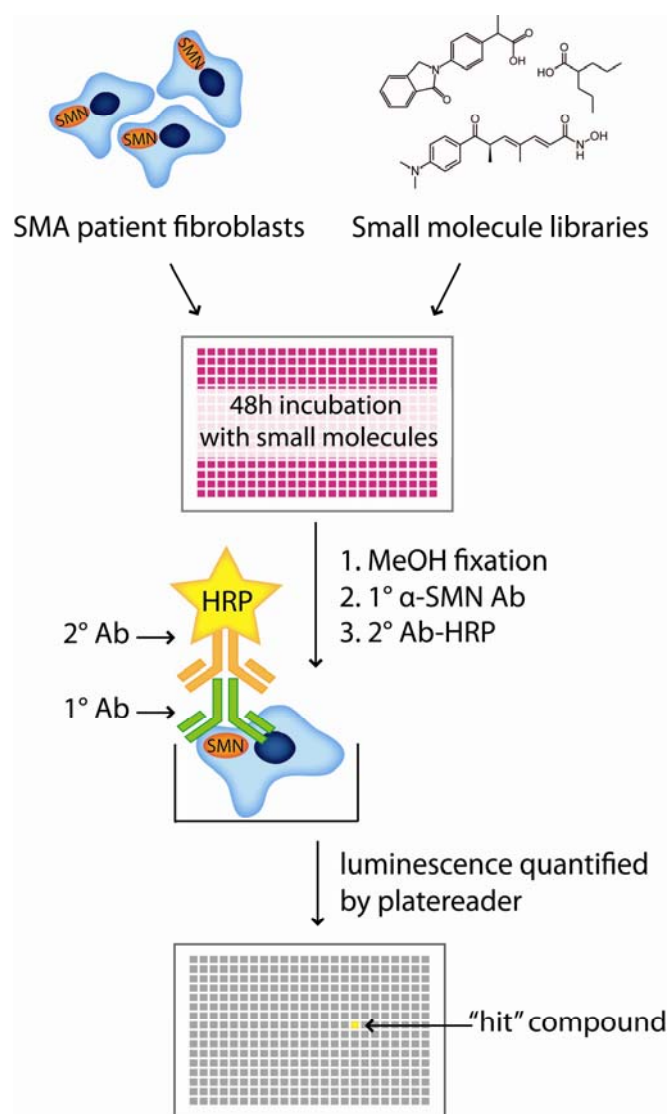


Figure 1. Schematic of the primary screening workflow. SMA patient fibroblast cells are seeded into 384-well plates and incubated for 48 h with a single compound per well. After 48 h, cells are fixed, permeabilized and SMN protein levels are quantified by incubation with a primary anti-SMN antibody, and a secondary antibody conjugated to horseradish peroxidase (HRP). Incubation of HRP with a luminal solution produces photons in correlation with the amount of bound HRP; the amount of light produced per well is quantified on a plate reader.

Screening and hit validation

Compounds screened in this assay were from two libraries assembled from commercial vendors. The first was our previously reported small molecule library¹⁷, described in Materials and Methods. The second library was composed of compounds specifically chosen for their predicted ability to cross the blood-brain barrier (BBB), an important first step in small molecule selection, as the development of CNS-active compounds is impeded by the inability of a large portion of compounds to penetrate the BBB. Small molecules for the second library were selected by *in silico* filtering for compounds likely to be BBB-penetrant and filtering out known toxic and reactive species. This work was performed by Dr. Andras Bauer, a Stockwell Lab member. The resultant set of compounds was dubbed the “BBB library”.

Primary screening was performed in triplicate in 9677 SMA patient fibroblast cells in 384-well format. A total of 69,189 small molecules were evaluated in the SMN cytoblot assay. To remain inclusive of compounds with moderate efficacy, a ‘hit’ was defined as having a median signal greater than two standard deviation from the median of the untreated wells. The 1,106 compounds passing hit criteria in the primary screen were retested in dose-response series in three SMA patient fibroblast lines (232, 3813 and 9677). The 105 candidates showing dose-response activity in at least two cell lines were tested by Western blot. Three structurally distinct compounds were found to significantly increase endogenous SMN protein levels (Figure 2 and 3). The EC₅₀ values for the three

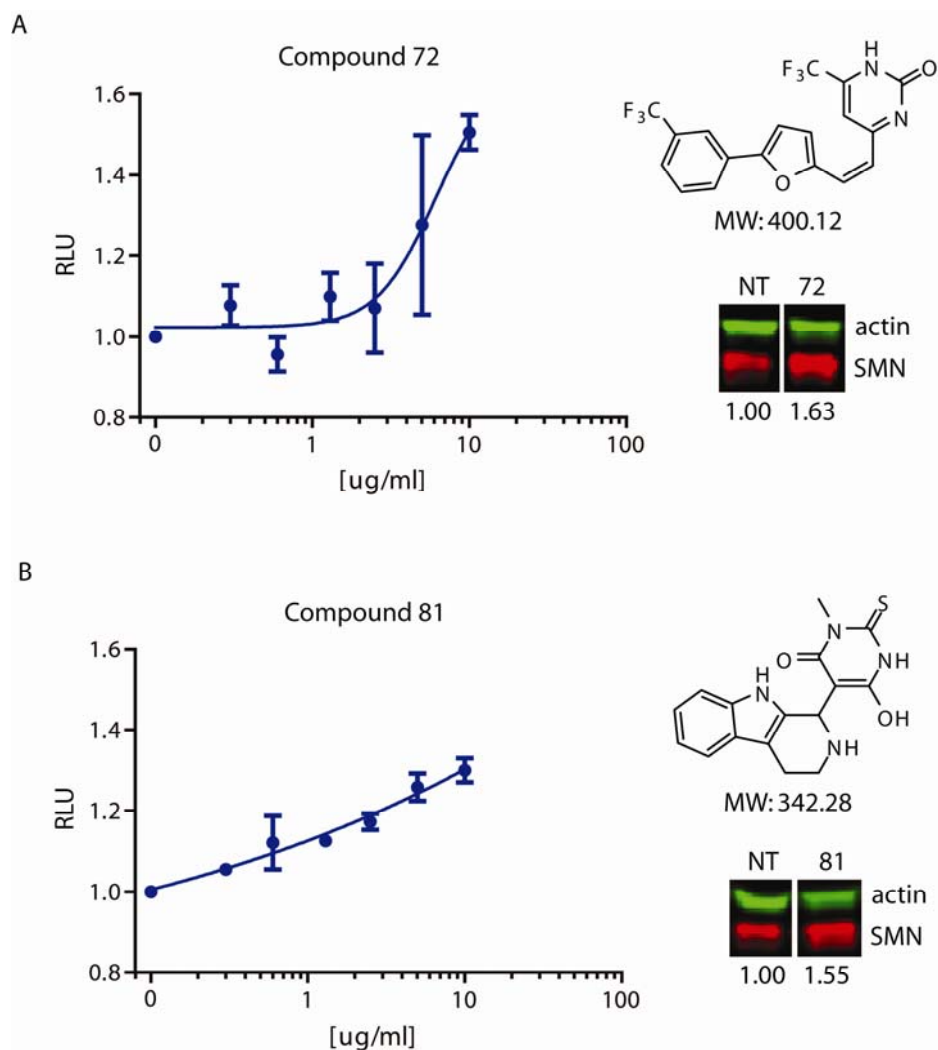


Figure 2. Dose-response of the SMN-upregulating compounds 72 and 81.

9677 SMA patient fibroblast cells were incubated with (A) compound 72, or (B) compound 81 for 48 h prior to SMN protein quantification in plate-based assay. The data represent the average of triplicates \pm SEM. RLU: relative luminescence units. Small molecule structures and Western blot quantification of SMN-upregulating activity are shown to the right of each dose-curve. Values below Western blots represent quantification of SMN protein bands normalized to actin as loading control, compared to DMSO-control.

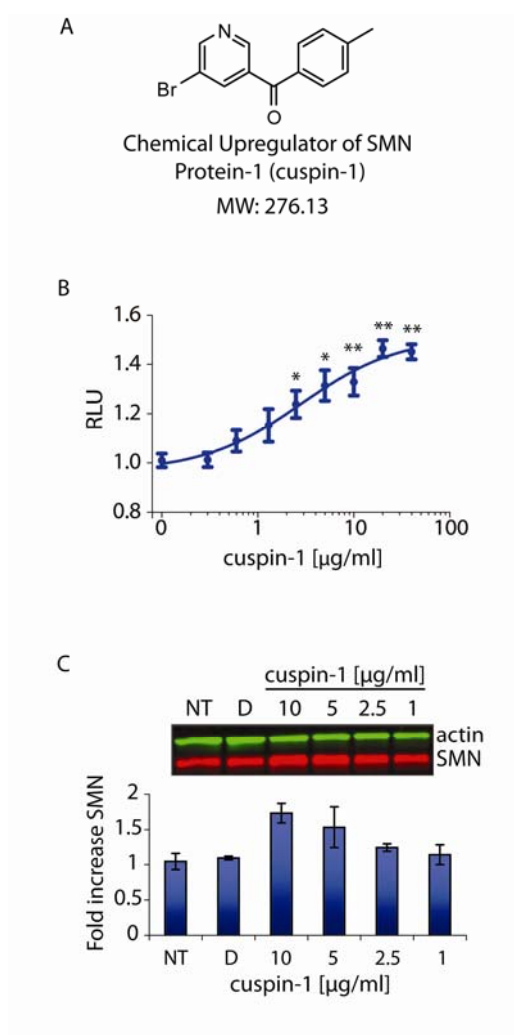


Figure 3. Cuspin-1 upregulates SMN protein levels in SMA patient fibroblast cells.

(A) Structure and molecule weight of the optimal hit compound identified in our screen, Chemical Upregulator of SMN-1 (cuspin-1). (B) Dose-response curve of 9677 SMA patient fibroblast cells treated with cuspin-1 for 48 h. The data represent the average of triplicates \pm SEM. RLU: relative luminescence units. P-values were calculated using two-tailed t-test. (* = $p < 0.01$, ** = $p < 0.001$) (C) Western blot and graph quantification of 9677 cells treated with a dose-curve of cuspin-1 for 48 h. SMN protein levels are normalized to actin as loading control. Data represents average of duplicates \pm standard deviation.

scaffolds were in the range of 10-20 μM , typical for hits from high-throughput, cell-based screens. A summary of the screen can be found in Table 1.

We focused on the most robust of these three hits, a bromobenzophenone analog we designated cuspin-1 (Chemical Upregulator of SMN Protein-1, Figure 1B). Cuspin-1 showed strong activity in the plate-based dose response assay (Figure 3B) and increased SMN levels by 50% compared to DMSO-treated controls at 5 $\mu\text{g}/\text{mL}$ (18 μM) in SMA patient fibroblast cells (Figure 3C). Toxicity was observed at concentrations at or above 80 $\mu\text{g}/\text{mL}$ (720 μM), providing a robust effective concentration (EC) to lethal concentration (LC) ratio for cell culture studies. It has proven challenging to find small molecules that significantly upregulate endogenous SMN protein levels¹⁸. Thus, cuspin-1, despite its modest overall effect, was selected as a suitable probe for further characterization as it showed moderate activity and low cellular toxicity.

The ability of cuspin-1 to upregulate SMN protein levels in diverse genetic backgrounds was tested in a panel of cell lines, including wild-type and SMA human and rodent cells (Table 2). Although cuspin-1 was active in the majority of human cell lines, it was inactive in the rodent lines tested, suggesting that its target or mechanism may not be conserved across species.

Structure-activity relationship of cuspin-1

To evaluate the features necessary for the activity of cuspin-1, a structure-activity relationship (SAR) analysis was undertaken through analog synthesis and testing. Although few structural analogs were commercially available (Figure 4A), one highly

Library	No. of cmpds	Hitpicked	Tested by WB	Confirmed by WB
TIC	23,686	595	82	2
ACL	2,337	5	1	0
NINDS	1,040	36	2	0
CGX	20,000	296	0	0
BBC	4,621	49	3	0
BBL	5,240	31	7	0
BBA	12,265	94	10	1
Total	69,189	1,106	105	3

Table 1. Summary of small molecule screen. Listed are number of compounds in each library screened. Additionally listed are the number of small molecules which passed primary hit criteria ('Hitpicked'), passing secondary hit criteria ('Tested by WB'), and confirmed in tertiary assay by quantification of SMN protein levels by Western blot.

Cell Line	Cell Line Origin and Cell Type	Rel. SMN Change (%) <i>by Western blot</i>	SD <i>n ≥ 2</i>
<i>Human</i>			
232	Fibroblast, SMA patient type I	129%	15%
3813	Fibroblast, SMA patient type I	171%	18%
9677	Fibroblast, SMA patient type I	193%	24%
3814	Fibroblast, SMA carrier	173%	38%
10684	Lymphoblast, SMA patient type I	118%	11%
ESC-MN	ESC-derived MN, WT	99%	8%
HT1080	Fibrosarcoma	132%	14%
293T	Embryonic kidney	110%	6%
A549	Lung carcinoma	121%	7%
<i>Rodent</i>			
WT MEF	Embryonic fibroblast, mouse	112%	18%
PC12	Pheochromocytoma, rat	92%	2%
ST14A	Striatal cells, rat	100%	15%
mESC-MN	ESC-derived MN, WT mouse	79%	13%

Table 2. Genotype-specificity testing of cusp1n-1. Table lists designations and origins of each cell line, as well as the mean percent increase of SMN normalized to actin upon treatment with 5µg/ml (18µM) cusp1n-1 for 48 h. Standard deviation is shown in the right-most column.

similar analog (5-bromo-3-pyridinyl)(4-ethylphenyl)-methanone, designated cuspin-2, increased SMN protein abundance to comparable levels as cuspin-1. Although cuspin-2 was active, it did not improve upon the potency or efficacy of cuspin-1. All other cuspin-1 analogs that we synthesized, using the synthetic scheme in Figure 4B, including analogs lacking either the bromine, nitrogen or methyl group, were inactive (Figure 4C). Additionally, while cuspin-2 demonstrated that extension of the methyl to an ethyl group retained activity, extension to a propyl group rendered the compound inactive, indicating a possible steric clash with cuspin-1's target. As modifications to the cuspin-1 scaffold generally resulted in loss of activity, further work is required to identify modifications that would improve the potency and efficacy of the compound. However, the current cuspin-1 scaffold represents a valuable tool for the study of SMN regulation.

Cuspin-1 reveals link between Ras signaling and SMN protein levels

In exploring the mechanism of action of cuspin-1 we observed that treatment with cuspin-1 increased phosphorylation of extracellular signal-related kinase (Erk) (Figure 5A). Proteins involved in other signaling pathways, such as Akt, were not activated (Figure 5A). The canonical pathway resulting in phosphorylation of Erk (p-Erk) is the Ras-Raf-MEK signaling cascade¹⁹. To test whether Ras could be responsible for the cuspin-1 mediated upregulation of SMN protein, Ras signaling was increased in #3813 SMA patient fibroblast cells by expression of a constitutively active form of Ras (*NRas^{G12D}*). *NRas^{G12D}* expression resulted in a 2.7-fold increase in SMN protein level

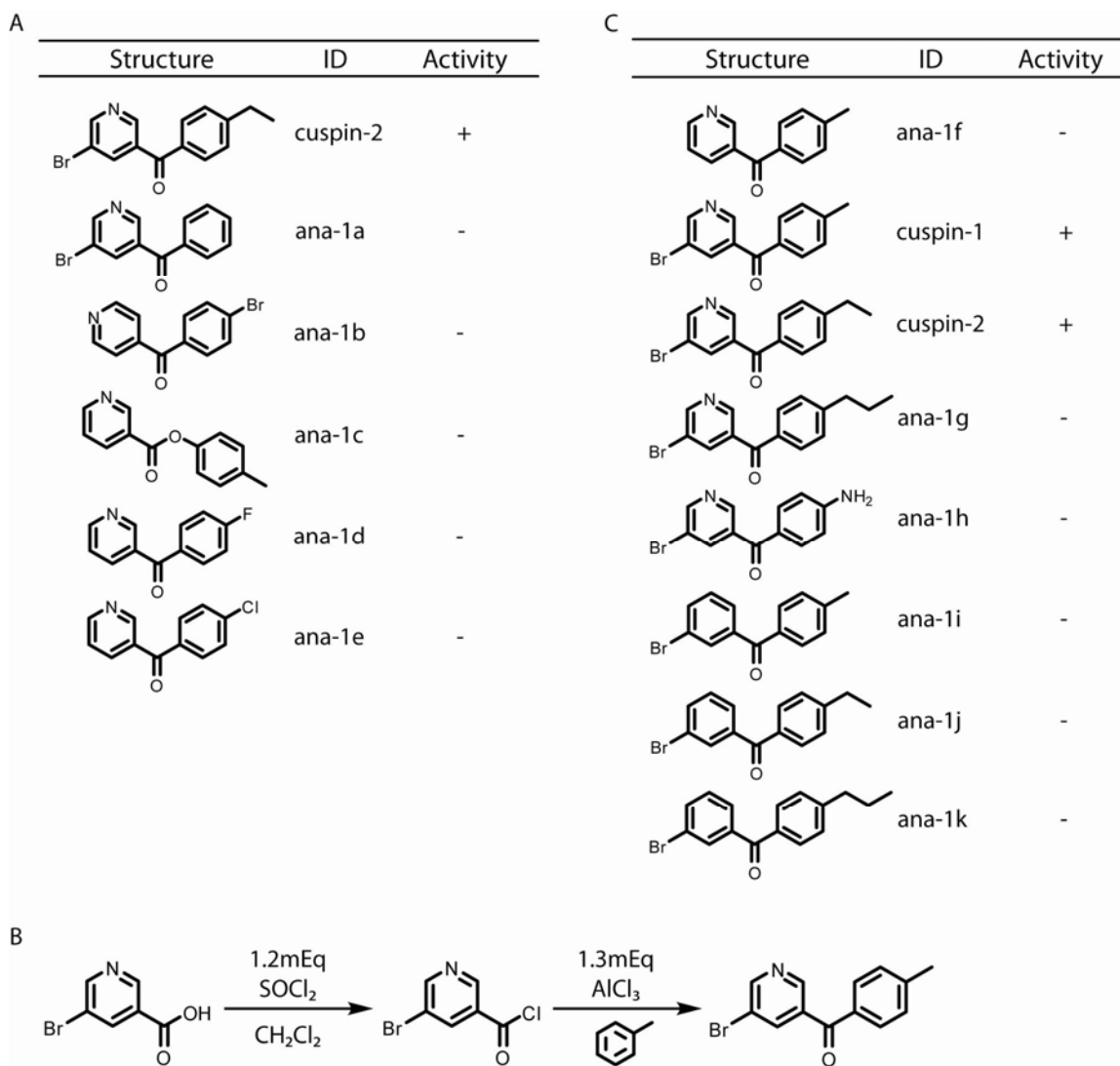


Figure 4. Structure-activity relationship of cuspin-1.

(A) Structures and activities of the highest similarity commercially-sourced cuspin-1 analogs. (B) Friedel-Crafts acylation scheme for analogs synthesized in-house. (C) Structures and activities of analogs synthesized in-house.

compared to vector alone (Figure 5B). The 5-fold increase in p-Erk in the *NRas*^{G12D} expressing cells confirmed a strong increase in Ras signaling in these cells. Similar increases in SMN and p-Erk levels were observed in #9677 and #232 SMA patient fibroblasts, indicating this effect of *NRas*^{G12D} is not unique to one SMA patient cell line.

Further experiments investigating the effect of activated Ras on SMN protein levels, could not be performed in the SMA patient cell lines, as non-transformed cells senesce shortly after introduction of oncogenic Ras²⁰. Therefore, we utilized the tumorigenic *HRas*^{V12}-expressing BJeLR cell line for subsequent experiments. The G12V mutation in the *HRas*^{V12} protein is functionally equivalent to the G12D mutation used previously, as they both inactivate GTPase activity, rendering the proteins constitutively active. BJeLR cells are an engineered cell line created by sequential introduction of viral and mammalian genetic elements into parental BJeH human foreskin fibroblasts²⁰. The BJeHLT cell line contains all genetic elements found in the BJeLR cell line, with the exception of *HRas*^{V12}. Comparison of SMN protein levels in the BJ cell lines demonstrated a 3-fold increase in SMN protein in the BJeLR cell line compared to the parental cell line, BJeH (Figure 5C). The lack of increase in SMN in the BJeHLT cell line indicates that activated Ras is the sole genetic element responsible for upregulation of SMN protein abundance in this cell line (Figure 5C). Interestingly, a literature review revealed that this phenotype had been noted before, in a comparison of the SMN protein levels in the oncogenic cell line HeLa compared to normal fibroblasts⁹, however the authors did not discuss or follow up on this observation.

This upregulation in SMN protein could be the result of either global upregulation of protein translation or via a more specific mechanism. To exclude the possibility that

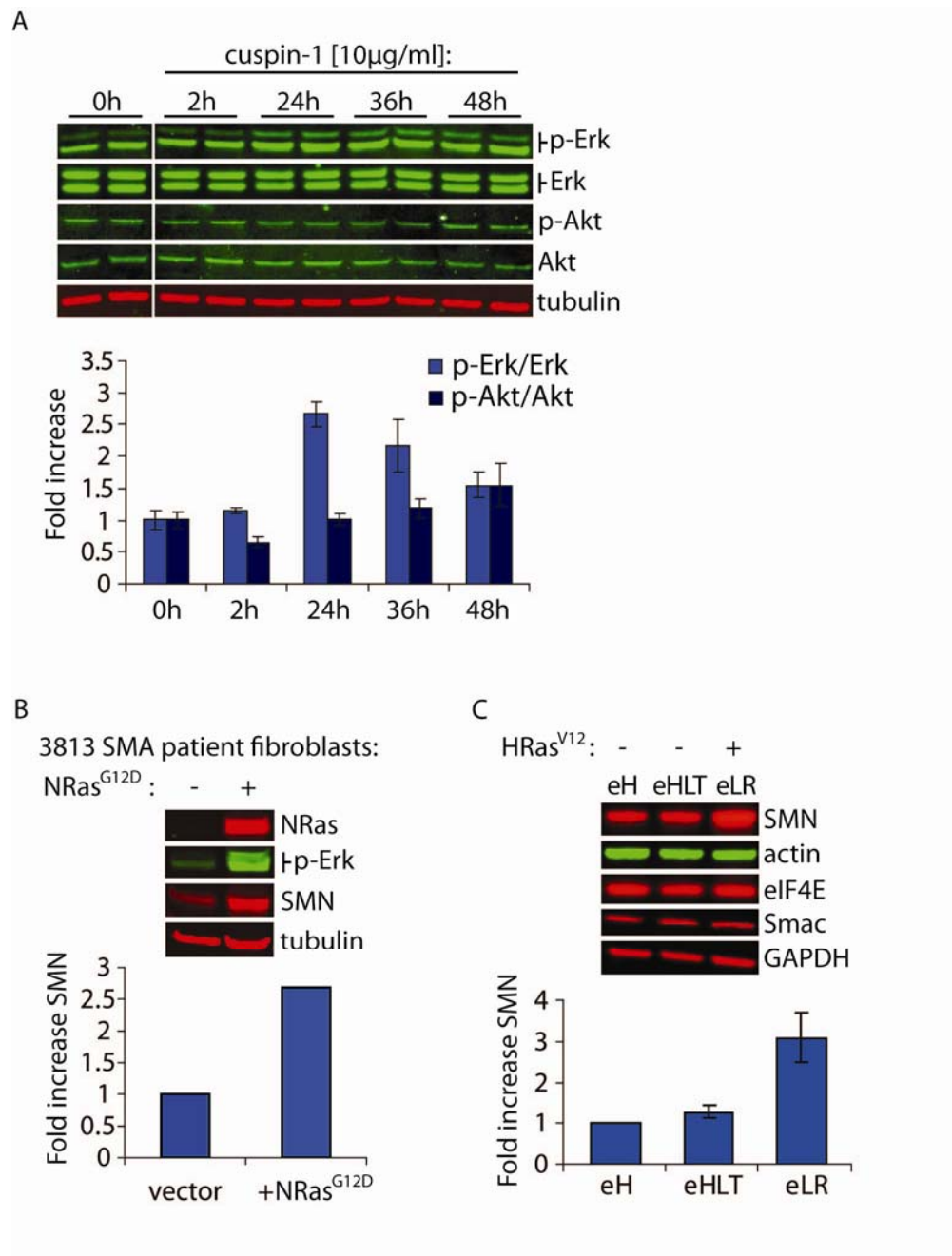


Figure 5. Increased Ras signaling upregulates SMN protein abundance.

(A) Western blot analysis of 9677 cells treated with 10 μ g/ml cuspin-1, harvested at indicated time points and blotted for p-Erk, total Erk, p-Akt, total Akt and tubulin. Graph shows quantification of phospho-protein to respective total protein ratios, normalized to tubulin as loading control. (B) Western blot analysis for NRas, p-Erk, SMN and tubulin

the observed effect on SMN protein levels was due to global upregulation of translation, the levels of several control proteins were examined by Western blot. These proteins are in 3813 SMA patient fibroblast cells transduced with either vector alone or constitutively active *NRas*^{G12D} viral plasmid. Graph shows fold increase of SMN compared to vector-only control, normalized to tubulin as loading control. (C) Comparison of the engineered tumor cell line BJeLR (eLR), expressing *HRas*^{V12}, versus the parental line (eH) and the isogenic line BJeHLT (eHLT) which contains all genes ectopically expressed in BJeLR with the exception of *HRas*^{V12}. Samples were blotted for SMN and several control proteins. Graph shows the fold increase of SMN in BJeHLT and BJeLR compared to BJeH, normalized to actin as loading control. In (A) and (C) the data represents the average of two independent samples \pm standard deviation.

involved in diverse cellular processes, including glucose metabolism (GAPDH), the cytoskeleton (actin), translation (eIF4E), and cell death (Smac). The abundance of these proteins remained unaltered by oncogenic Ras expression (Figure 5C), suggesting a level of specificity to Ras-mediated SMN upregulation. We have shown that multiple isoforms of Ras can upregulate SMN protein levels in diverse cell lines.

Mechanistic studies of Ras-mediated upregulation of SMN protein levels

To investigate the mechanism underlying SMN protein upregulation by activated Ras, we utilized the BJ cell lines to determine the cellular process through which Ras exerts its effect on SMN protein levels. First, we tested whether alterations in transcription or splicing of *smn* mRNA were responsible for the increase in SMN protein abundance. The BJeLR (+*HRas*^{V12}) cell line did not show increased levels of either full-length or $\Delta 7$ *smn* mRNA, nor did it have an altered ratio of the spliced isoforms, as compared to the parental line BJeH (-*HRas*^{V12}) (Figure 6A). This lack of increase in *smn* mRNA levels suggests that the upregulation of SMN protein levels was not due to activation of p38 mitogen-activated kinase, a Ras effector protein, which was recently shown to upregulate SMN protein levels via stabilization of *smn* mRNA²¹. Unexpectedly, the BJeLR line showed consistently lower levels of *smn* mRNAs than the BJeH parental line. This could be due to a feedback mechanism downregulating *smn* transcripts in response to strongly elevated SMN protein levels.

Next, we examined the effect of increased Ras signaling on SMN turnover. Cycloheximide (CHX), a protein synthesis inhibitor, was used to inhibit the translation of

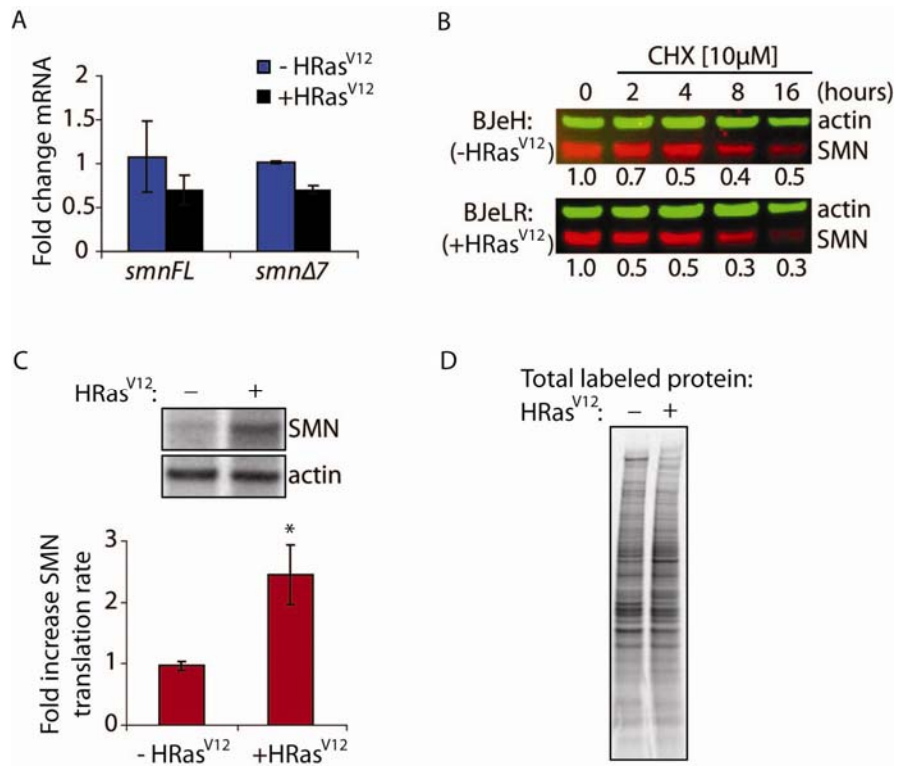


Figure 6. Increased Ras signaling enhances SMN translation rate

(A) Quantification of RT-PCR of full-length (*smnFL*) and exon 7-deleted (*smnΔ7*) *smn* mRNA levels from BJeH (-HRas^{V12}) and BJeLR (+HRas^{V12}) cells. Transcript cycle times were normalized to *hprt* to control for total mRNA. Data represents the average of three independent samples ± standard deviation. (B) Representative Western blot analysis of SMN and actin in BJeH (-HRas^{V12}) and BJeLR (+HRas^{V12}) cells treated with the protein synthesis inhibitor cycloheximide (CHX [10μM]) for indicated times. Quantification of SMN to actin ratio normalized to respective untreated control (0h) is shown below each lane. (C) Phosphorimager bands and quantification of translation rate analysis of SMN and actin in BJeH (-HRas^{V12}) versus BJeLR (+HRas^{V12}) cells. Data represent mean ± standard deviation, n=2. P-values were calculated using two-tailed t-test. (* = p<0.01) (D) Phosphorimager lanes demonstrating equivalent levels metabolic labeling in BJeH (-HRas^{V12}) versus BJeLR (+HRas^{V12}) cells.

nascent SMN peptides in order to quantify the half-life of SMN. The half-life of SMN in the BJ cell lines was ~3 hours, similar to previous reports^{22,23}. The degradation rate of SMN protein remained unchanged in the *HRas*^{V12}-expressing cells, indicating that increased Ras signaling does not affect the rate of SMN degradation (Figure 6B).

Having ruled out alterations in transcription, splicing and turnover, we tested whether *HRas*^{V12} affected the translation rate of SMN. A translation rate assay, using radioactive ³⁵S-methionine and cysteine to label newly synthesized protein with subsequent immunoprecipitation of proteins of interest, was performed to quantify the translation rate of SMN. *HRas*^{V12}-expressing cells showed a significant 2.5-fold increase (p<0.01) in the rate of SMN translation compared to parental cells (Figure 6C). No differences were observed in the total amount of label incorporated in each cell line (Figure 6D), suggesting the increased translation rate of SMN protein is unlikely to be due to a global increase in translation. We have determined that activated Ras signaling upregulates SMN protein abundance via translational regulation, however further investigation will be required to determine the exact nature of the connection between Ras signaling and SMN translation rate.

We developed a high-throughput screen for identification of small molecule upregulators of the SMN protein and identified three novel SMN-upregulating compounds. Mechanistic studies of cuspin-1 led to the discovery that Ras signaling regulates SMN protein abundance at the level of translational regulation. In addition to the novel SMN regulatory pathway identified, this study provides a proof of principle that mechanistically unbiased screens can uncover unexpected connections between cellular pathways and provide novel small molecule tools for the study of biological processes.

The Raf-MEK-Erk pathway is not responsible for Ras-mediated upregulation of SMN

Although the connection between Ras signaling and SMN protein level increase was discovered due to an observed increase in p-Erk staining upon cuspin-1 treatment, further experiments indicated that while Ras activation is necessary for SMN upregulation, activation of the Raf-MEK-Erk pathway is not. The importance of the Raf-MEK-Erk pathway was tested by transducing 3813 SMA patient fibroblast cells with retroviral plasmids expressing the constitutive active proteins NRas^{G12D}, B Raf^{V600E} or MEK^{S218D,S222D} (from hereon referred to as NRas^{G12D}, Raf and MEK). Although Raf and MEK both increased p-Erk levels, to a higher degree even than NRas^{G12D}, they did not increase SMN protein levels (Figure 7A). Only NRas^{G12D} expression was able to upregulate SMN protein levels. This data suggested that the Raf-MEK-Erk pathway is not the effector pathway of Ras responsible for mediating SMN upregulation.

To confirm that the Raf-MEK-Erk pathway was not involved in upregulation of SMN protein levels, the MEK inhibitor U0126²⁴ was tested to determine if it could inhibit the upregulation of SMN protein levels observed upon treatment with cuspin-1. Since MEK is the kinase responsible for phosphorylation of Erk, U0126 activity in these cells was demonstrated by blotting for p-Erk levels, which were decreased to approximately 5% of untreated cells. Interestingly, treatment with cuspin-1 increased phosphorylation of Erk 2-fold, regardless of the whether the cells were also treated with U0126 (Figure 7B). Additionally, U0126 co-treatment did not reduce the upregulation of SMN protein levels due to cuspin-1 treatment. However, U0126 treatment did decrease basal SMN protein levels 15-30%, though this decrease may be due to the moderate

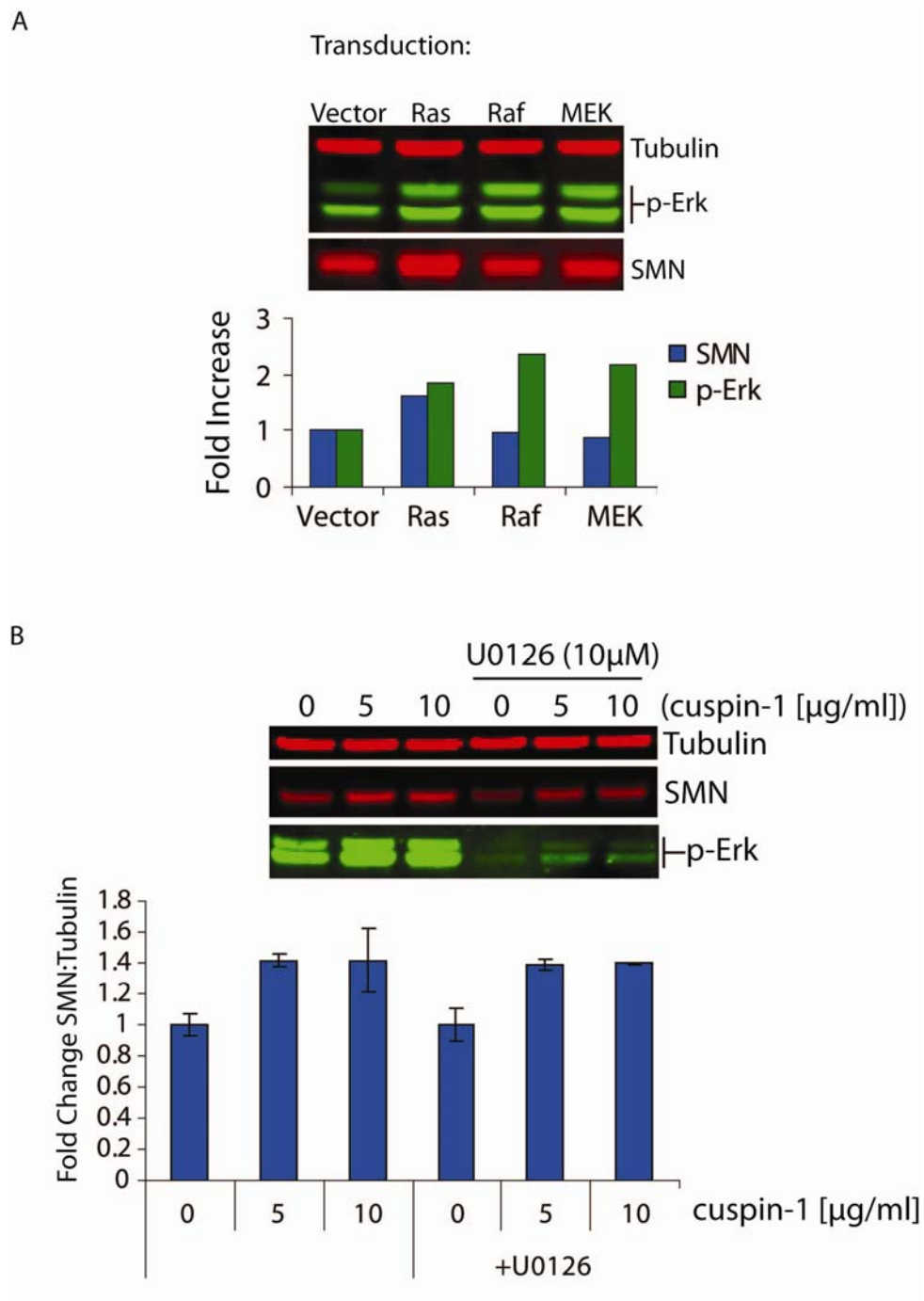


Figure 7. SMN upregulation due to increased Ras signaling is not mediated by the Raf-MEK-Erk effector pathway. (A) Western blot analysis of SMN protein levels in 3813 SMA patient fibroblast cells transduced with either empty viral vector (vector), or vector containing oncogenic NRas^{G12D}, BRAf^{V600E} or MEK^{S218D,S222D} 5 d post-

transduction. Increased phosphorylation of Erk is observed upon expression of any of the three oncogenic proteins, indicating activation of the Erk-mediated signaling pathway, however only expression of NRas^{G12D} upregulates SMN protein levels. Graph shows fold increase of SMN and phosphorylated Erk (p-Erk) compared to vector-only control, normalized to tubulin as loading control. **(B)** Western blot analysis of SMN, tubulin and p-Erk in 9677 SMA patient fibroblast cells treated with 5 μ g/mL or 10 μ g/mL with or without 10 μ M of the MEK inhibitor U0126 for 48 h. Graph shows fold increase of SMN compared to DMSO-treated control, normalized to tubulin as loading control. Data represent mean \pm standard deviation, n=2. Inhibition of MEK is evident from the 95% decrease in basal p-Erk levels, however cuspin-1 treatment results in ~140% increase in SMN protein levels irrespective of MEK inhibition.

toxicity inherent to U0126 treatment. Together with the lack of SMN-upregulating activity of Raf and MEK overexpression, these results strongly suggest that the Raf-MEK-Erk pathway is not involved in Ras-mediated increase of SMN protein levels.

A wider range of small molecule inhibitors of Ras effector kinases were also tested in the *HRas*^{V12}-expressing BJeLR cell lines, to determine whether inhibition of any of these downstream pathways of Ras could reduce the upregulated SMN levels observed in these oncogenic Ras-expressing cells. BJeLR cells were treated for 24 hours with either 5 μ M or 10 μ M U0126 (MEK inhibitor), 7 μ M SP600125 (Jnk inhibitor), 1 μ M Wortmannin (PI3K inhibitor-1), 25 μ M LY294002 (PI3K inhibitor-2), 2 μ M Akt 1 and 2 inhibitor (Akt inhibitor), 5mM 3-methyladenine (PI3K inhibitor-3) and 1 μ M Raf-1 inhibitor. These concentrations were previously determined by Dr. Adam Wolpaw, another member of the Stockwell Laboratory, as maximizing efficacy while limiting toxicity in the BJeLR cell line (personal communication). None of these treatments demonstrated an effect on SMN protein levels, indicating that these pathways are likely not involved in Ras-mediated upregulation of SMN protein levels (Figure 8). However, overexpression studies are still required in order to conclusively eliminate these pathways as modulators of SMN protein levels.

Although surprising, the discovery that the Raf-MEK-Erk pathway does not mediate activated Ras-induced upregulation of SMN protein levels does not invalidate the results observed upon cuspin-1 treatment. The elevation of phosphorylated Erk in cuspin-1 treated cells remains indicative of increased Ras signaling. Although it is not

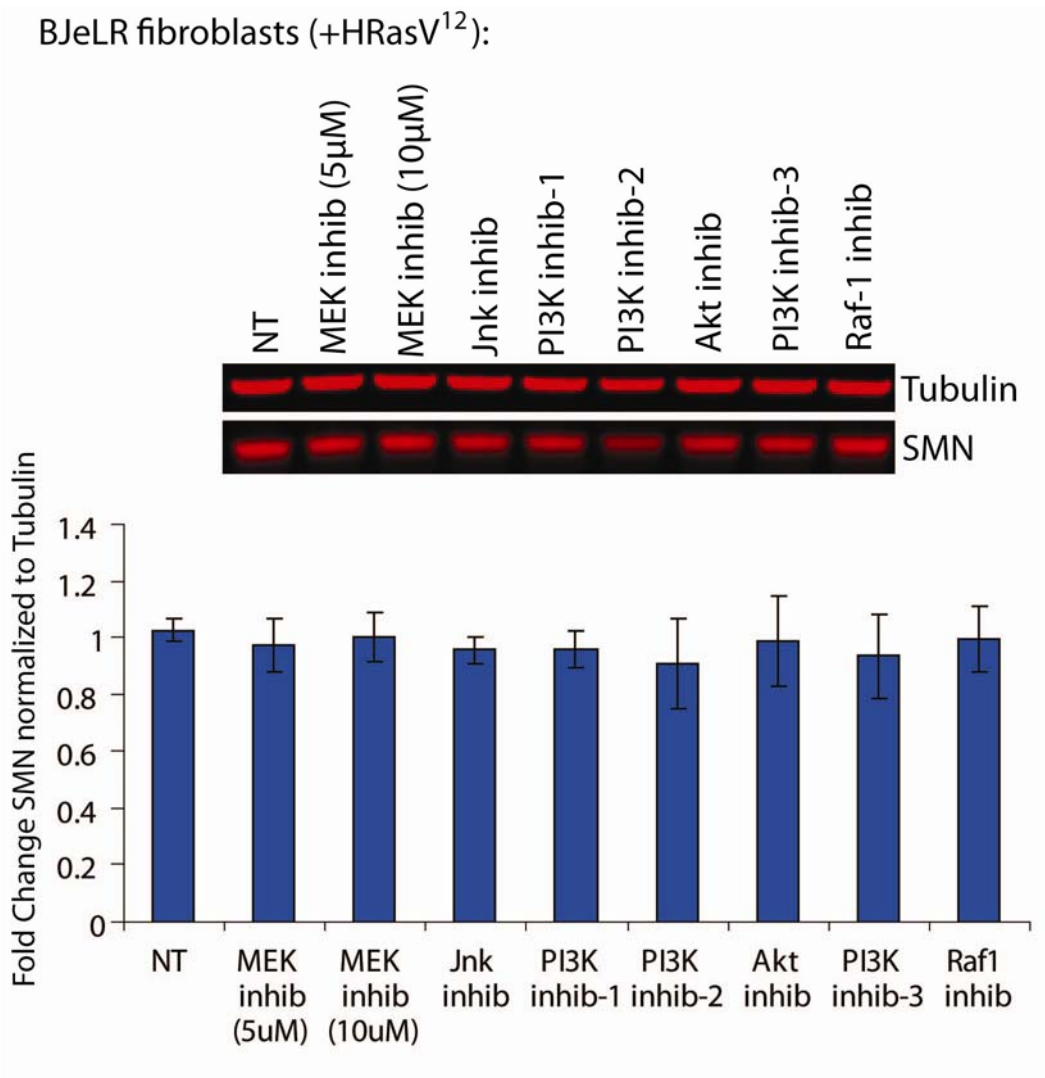


Figure 8. Small molecule inhibition of downstream Ras effector kinases does not inhibit oncogenic Ras-mediated upregulation of SMN protein levels. Western blot analysis of SMN and tubulin levels in BJeLR fibroblast cells expressing an oncogenic isoform of HRas (*HRas*^{V12}) treated with various kinase inhibitors for 24 h. Graph quantification of SMN normalized to tubulin as loading control compared to DMSO-treated control. Data represents the average of two independent samples ± standard deviation.

directly responsible for the upregulation of SMN, it still serves as a biomarker for Ras activation. Preliminary investigations aimed at determining the downstream Ras effector pathways regulating SMN protein levels have been negative to date, therefore further work is required to identify the relevant effector pathway. Due to the extensive number of targets downstream of Ras activation, it is possible that a pathway we have yet to explore will prove to be the one responsible for the Ras-mediated upregulation of SMN protein levels.

Mammalian target of rapamycin modulates SMN protein levels

As the Ras-mediated upregulation of SMN protein was determined to be at the level of translational regulation, it was investigated whether this effect could be mediated via the translational regulator mammalian target of rapamycin (mTOR) ²⁵. Several important cellular signaling pathways converge on mTOR, including those responsible for sensing the intracellular levels of amino acids and growth factors ²⁶. Sufficient levels of both of these factors result in activation of mTOR signaling, resulting in pro-growth downstream effects. Activated mTOR inhibits the translational repressor eukaryotic initiation factor 4E-binding protein (4E-BP1), via hyperphosphorylation ²⁷. Additionally, activated mTOR phosphorylates ribosomal protein S6 kinase 1 (S6K1), resulting in enhanced translation ^{27,28}. Inactivation of mTOR signaling, via starvation or treatment with the potent small molecule inhibitor rapamycin ²⁹, conversely downregulates protein synthesis and activates autophagy ^{30,31}, demonstrating its crucial role in nutrient-mediated regulation of cell growth.

The starvation response downregulates SMN protein levels

The mammalian target of rapamycin (mTOR) protein is a key regulator of the starvation response, integrating signals from several homeostatic pathways, including amino acid and growth factor sensing pathways. As the signaling output from mTOR is pro-growth, lack of stimulatory input, such as starvation, inhibits mTOR signaling. To determine whether inhibition of mTOR signaling could modulate SMN protein levels, SMA patient fibroblasts were placed under starvation conditions by incubation in Earle's Balanced Salt Solution (EBSS). EBSS contains the inorganic salts potassium chloride, sodium bicarbonate, sodium chloride and sodium phosphate monobasic as well as D-glucose, but no amino acids or serum components. Starvation of SMA patient fibroblasts in EBSS for 24 hours decreased SMN protein 50-60%, indicating that SMN protein levels were responsive to starvation conditions (Figure 9, first four lanes).

SMN downregulation is stimulated by serum deprivation

To determine whether introduction of amino acids or serum could rescue the decrease in SMN, either amino acids or dialyzed serum were added to the EBSS. The FBS was dialyzed in PBS overnight in dialysis membrane with a 6-8,000 molecular weight cutoff (Spectra/Por 132 655) in order to remove amino acids naturally found in serum. Adding amino acids to the EBSS did not rescue the starvation-induced decrease in SMN protein levels. However, addition of the dialyzed serum resulted in rescue of SMN

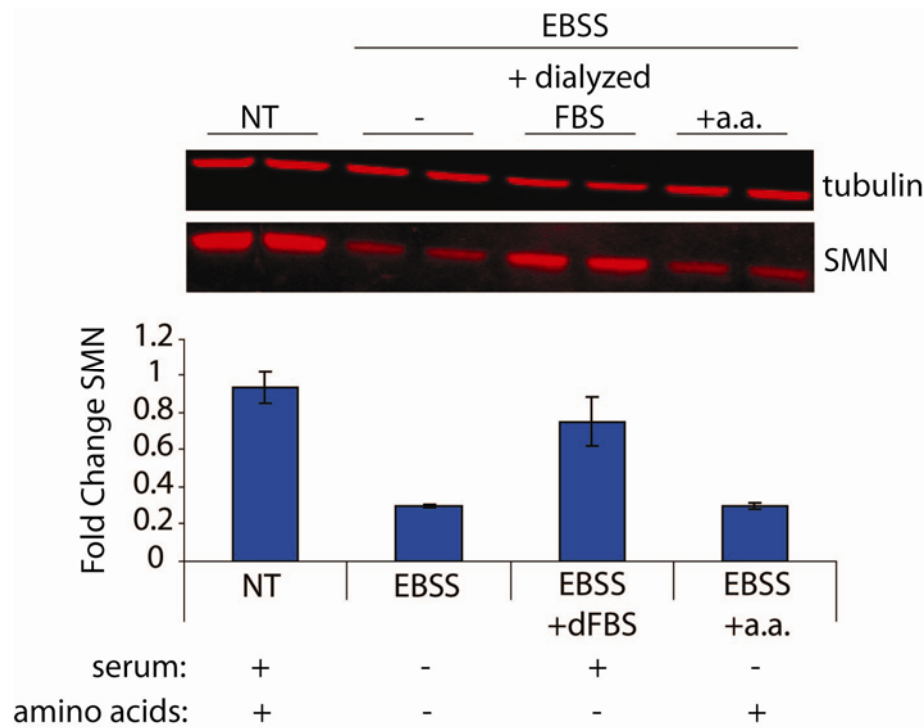


Figure 9. Serum starvation downregulates SMN protein levels.

9677 SMA patient fibroblast cells were cultured either in normal 15% serum cell culture media, or starved of both serum and amino acids in Earle's Balanced Salt Solution (EBSS). Western blot analysis of SMN and tubulin demonstrate a ~70% decrease in SMN protein levels, normalized to tubulin as loading control, upon starvation in EBSS for 24 h. Data represents the mean \pm standard deviation, n=2. The addition of serum (dialyzed to remove amino acids) rescues starvation-mediated downregulation of SMN protein levels to 80% of unstarved cells, while addition of amino acids has no effect.

protein levels up to 80% of the unstarved control (Figure 9). It is unclear why addition of serum did not completely rescue. However as serum factors smaller than 8kDa would have been dialyzed out along with the amino acids, it is possible that one or more of these smaller factors are important for mediating this effect. Examples of serum factors under 8kDa include hormones or small growth factors, such as insulin-like growth factor 1, which has a molecular weight of 7.6kDa³². Although the rescue was not complete, these results indicate that lack of serum factors, but not amino acids, can significantly decrease SMN protein levels.

Of interest, serum starvation had no effect on SMN levels in the BJeLR cell line, which overexpresses HRas^{V12}, or the oncogenic HT1080 cells. This suggests that increased Ras signaling can functionally interact with mTOR in such a way as to prevent the downregulation of SMN protein levels due to starvation-mediated inhibition of mTOR signaling.

Inhibition of mTOR by the small molecule rapamycin reduces SMN protein levels

As mTOR signaling is generally considered to be dependent on both amino acid and serum signaling pathways, to conclusively determine whether inhibition of mTOR signaling was responsible for the decrease in SMN protein levels SMA patient fibroblast cells were treated with rapamycin, a potent small molecule inhibitor of mTOR signaling

29

To determine the optimal concentration of rapamycin, SMA patient fibroblast cells were treated for 24 hours with rapamycin at 1nM, 10nM, 0.1 μ M or 1 μ M. All

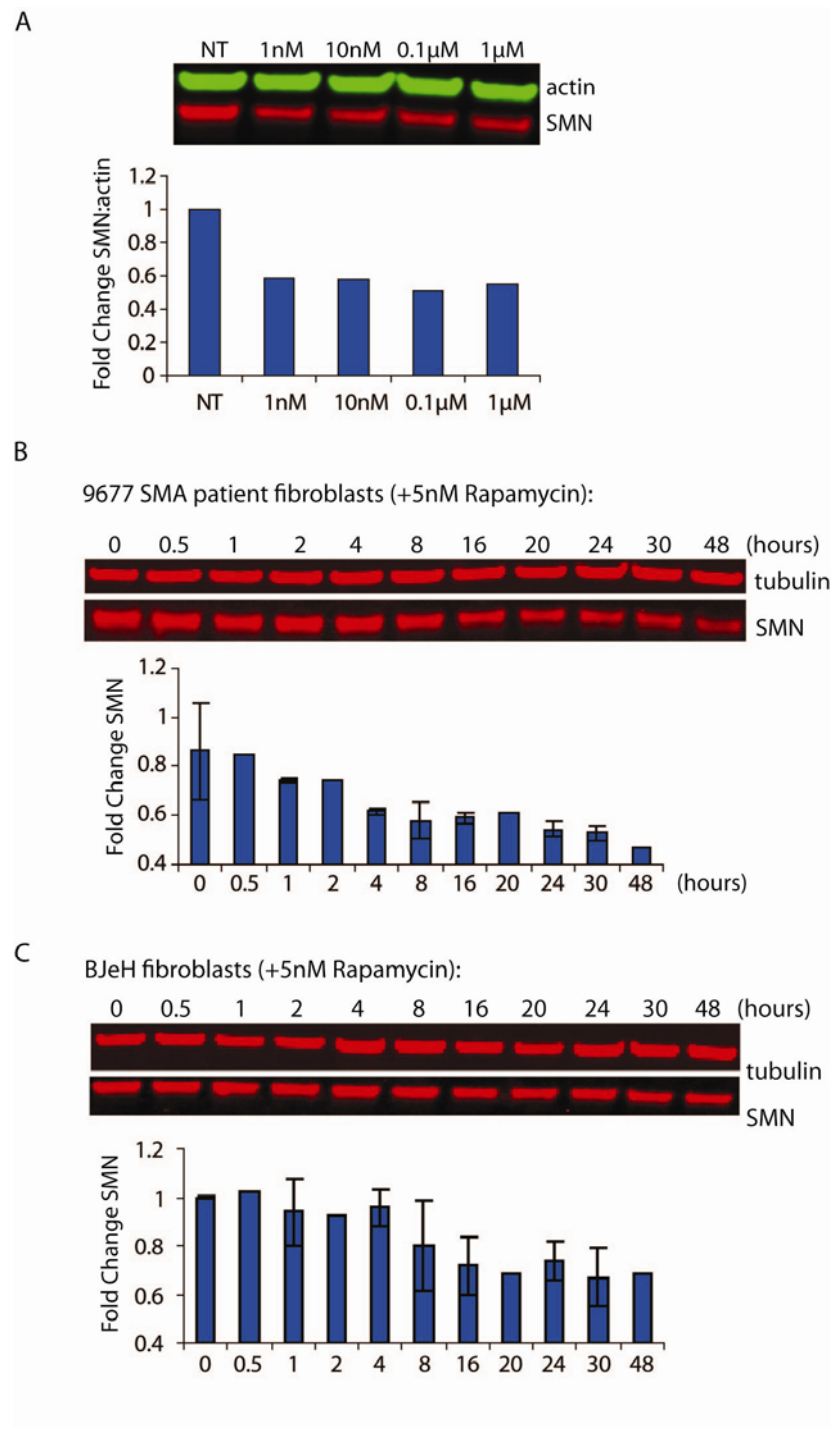


Figure 10. Treatment with the mTOR inhibitor rapamycin decreases SMN protein levels. (A) Western blot analysis of SMN and tubulin in 9677 SMA patient fibroblast cells treated with 1nM, 10nM, 0.1µM or 1 µM of the mTOR inhibitor rapamycin for 24 h. Graph shows quantification of SMN normalized to tubulin, compared to DMSO-treated

control. Rapamycin demonstrated high potency, showing maximal efficacy of SMN decrease (40% decrease) at 1nM. **(B)** Time course of rapamycin treatment (5nM) in 9677 SMA patient fibroblast cells, or **(C)** BJeH wild-type human fibroblast cells. Graphs quantify SMN levels normalized to tubulin, compared to DMSO-treated controls. For **(B)** and **(C)**, data represents the average of two independent samples \pm standard deviation.

concentrations resulted in a ~40% decrease in SMN protein levels (Figure 10A), indicating rapamycin's activity on SMN protein levels was maximal at low nanomolar concentrations. I selected 5nM as the optimal rapamycin concentration for inhibition of mTOR signaling for future studies. To determine the time course of SMN protein reduction, cells were treated with 5nM rapamycin in a time course lasting 48 hours. Rapamycin treatment resulted in a ~30% reduction in SMN protein levels within 20 hours, which remained consistent through the 48 hour time point (Figure 10B). After 48 hours treatment with rapamycin, cells were significantly reduced in viability. BJeH, a wild-type fibroblast cell line, showed a similar response to the SMA fibroblast cell line (Figure 10C), indicating this effect of rapamycin is independent of basal SMN protein levels.

Interestingly, just as serum starvation of BJeLR cells showed no demonstrable effect on SMN protein levels, the same held true for rapamycin treatment. BJeLR cells were treated with 5nM or 50nM rapamycin for 24 hours, however this did not result in decreased SMN protein levels (Figure 11). Rapamycin's inhibition of mTOR signaling was confirmed by blotting for the conversion of myosin light chain 3B (LC3BI) to LC3BII. This conversion occurs at the onset of autophagy³³, and indicates mTOR is being inhibited. Treatment with either concentration of rapamycin increased LC3BII levels approximately 3-fold, indicating inhibition of mTOR signaling and consequent upregulation of autophagy (Figure 11). However, as neither starvation nor rapamycin-induced inhibition of mTOR signaling affected SMN protein levels in this cell line, it is likely that some consequence of Ras activation is preventing the mTOR

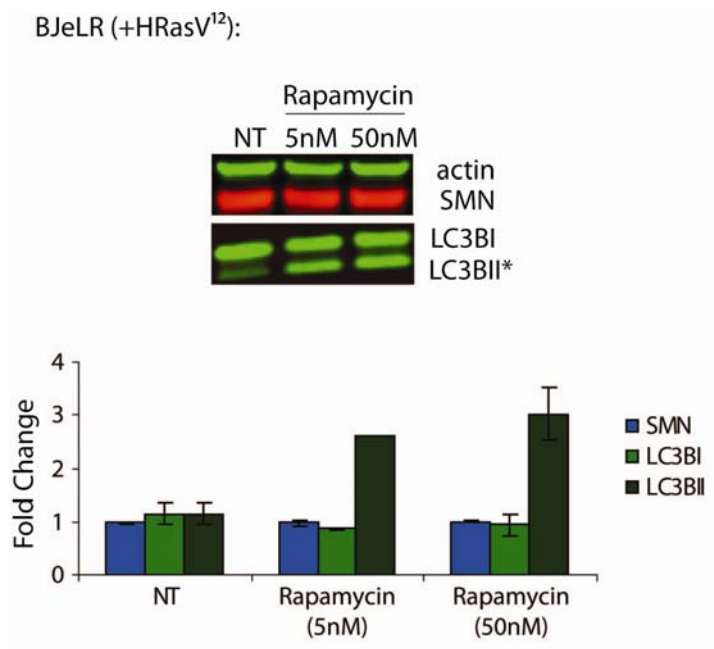


Figure 11. Ras activation inhibits rapamycin-mediated downregulation of SMN protein levels. Western blot analysis of SMN, tubulin and LC3BI/II in BJeLR cells (human fibroblasts expressing the oncogenic *HRas*^{V12} isoform) treated with 5nM or 50nM of the mTOR inhibitor rapamycin. Graph quantification of SMN, LC3BI and LC3BII levels normalized to actin is shown below. Data represents the average of two independent samples ± standard deviation. *Increased levels of LC3BII, a post-translational conversion product of LC3BI used as a marker of activation of autophagy, demonstrates activity of the mTOR pathway in this cell line, and the ability of rapamycin to inhibit mTOR signaling in these cells. However, activation of Ras signaling prevents the downregulation of SMN protein levels observed in non-oncogenic cell lines.

inhibition-mediated decrease in SMN protein level. This modulation of the SMN-downregulating effect is likely at a point downstream of mTOR, as rapamycin treatment demonstrates that the signaling from the mTOR complex is still functional and able to be inhibited in the BJeLR cells.

SMN downregulation is mediated by the proteasome

Although SMN has been identified to be a substrate of the proteasome^{22,34}, serum starvation-mediated inhibition of mTOR signaling is generally considered an inducer of autophagy³⁰. As other proteins have been demonstrated to be substrates of both the proteasome and autophagic degradative pathways³⁵, inhibitors of each process were tested to determine which could rescue the decrease in SMN upon serum starvation. SMA patient fibroblast cells were serum starved for 24 hours and simultaneously treated with either 25 μ M chloroquine (CHQ), an inhibitor of autophagy³⁶, or 2.5 μ M MG-132, a proteasome inhibitor³⁷. I additionally tested cuspin-1 (10 μ g/ml) in this assay as well, to determine whether cuspin-1 treatment would modulate this phenotype. Treatment with CHQ or cuspin-1 did not rescue the decrease in SMN protein levels upon serum starvation. Only the proteasome inhibitor MG-132 was able to rescue the levels of SMN, and it was able to do so completely (Figure 12A).

As chloroquine is not an extremely potent inhibitor of autophagy, to confirm that inhibition of autophagy did not rescue SMN protein levels in serum starved cells, two additional autophagy inhibitors, Bafilomycin A1³⁸ and ammonium chloride (NH₄Cl)³⁹, were also tested. Bafilomycin A1, an inhibitor of the vacuolar H⁺ ATPase

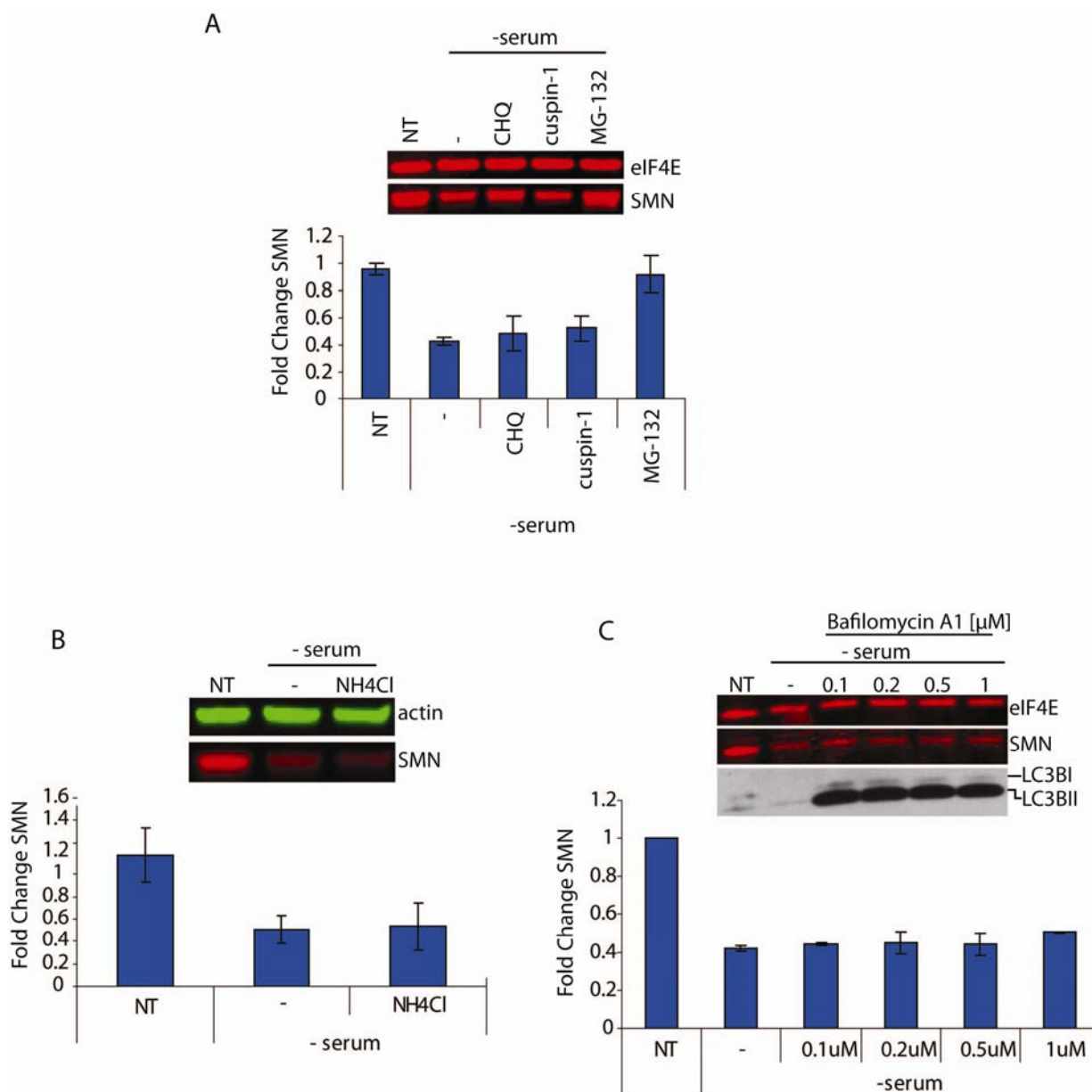


Figure 12. Inhibitors of autophagy cannot rescue starvation-mediated downregulation of SMN protein levels. (A) Western blot analysis of 9677 SMA patient fibroblast cells serum-starved for 24 h and treated with either 25 μM chloroquine (CHQ) (autophagy inhibitor), 10 μg/ml cuspin-1 or 2.5 μM MG-132 (proteasome inhibitor). Graph quantification of SMN protein levels normalized to tubulin. Serum starvation leads to a ~60% decrease in SMN protein levels, which cannot be rescued by co-treatment with

chloroquine or cuspin-1, however treatment with MG-132 results in complete rescue, indicating the decrease in SMN protein levels is mediated by the proteasome. Testing of the autophagy inhibitors **(B)** ammonium chloride (NH₄Cl) or **(C)** Bafilomycin A1 demonstrated the same inability of autophagy inhibitors to rescue starvation-mediated downregulation of SMN protein levels. Graphs quantify fold change in SMN normalized to loading controls. Western blot in **(C)** additionally shows LC3B staining; the significant upregulation of LC3BII indicates inhibition of autophagy. For all figures, data represents the average of two independent samples \pm standard deviation.

prevents acidification of the lysosomal vacuole. Ammonium chloride, a weak base, neutralizes the acidity of the lysosomal compartment. These autophagy inhibitors also failed to rescue the decrease in SMN protein levels upon serum starvation (Figure 12B and C).

To confirm that the decrease in SMN protein levels upon serum starvation is mediated by the proteasome, serum-starved SMA patient fibroblast cells were treated with several different proteasome inhibitors: MG132, lactacystin and MG262³⁷. All three proteasome inhibitors rescued SMN levels to the same degree, although in this experiment the rescue was not complete, as cells were starved for 9 hours prior to addition of the proteasome inhibitors (Figure 13). These experiments demonstrate that serum starvation strongly downregulates SMN protein levels, and this decrease can be rescued by inhibition of the proteasome. However, the mechanism resulting in this downregulation is still unclear. The decrease in SMN protein levels could be the result of either translational inhibition with normal degradation rates, or due to stimulation of degradation. Further studies will be required to determine the mechanism relevant to starvation-induced decrease of SMN protein levels.

These data demonstrate that SMN protein levels are strongly downregulated upon inhibition of mTOR signaling via either serum deprivation or by treatment with the small molecule rapamycin. This decrease could be inhibited by the co-treatment of various proteasome inhibitors, indicating that the downregulation of SMN protein levels is mediated by the proteasome. Interestingly, neither serum starvation nor rapamycin treatment had an effect on SMN protein levels in cells expressing an oncogenic isoform of Ras, indicating that increased Ras signaling is able to override the negative signaling

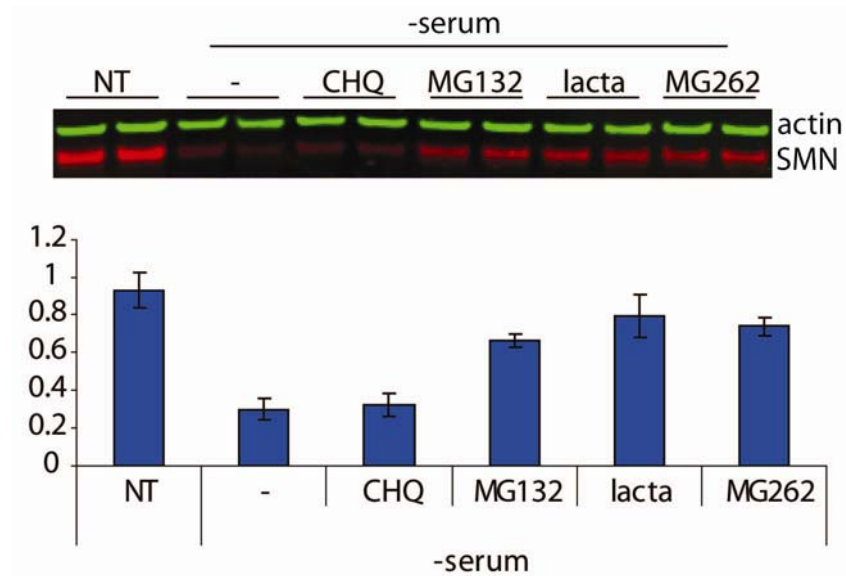


Figure 13. Starvation-mediated downregulation of SMN protein levels is prevented by proteasome inhibitors. Western blot analysis of 9677 SMA patient fibroblast cells serum starved for 24 h and treated with either DMSO (-), 25 μ M chloroquine (CHQ)(autophagy inhibitor), or the proteasome inhibitors MG132 (2.5 μ M), lactacystin (lacta)(10 μ M) or MG262 (2 μ M). Graph shows quantification of SMN normalized to actin as loading control, data represents the mean \pm standard deviation, n=2. The autophagy inhibitor chloroquine shows no effect, however treatment with any of the proteasome inhibitors rescues SMN protein levels.

from mTOR which results in decreased levels of SMN protein in non-oncogenic cells. Identification of the mechanism by which mTOR signaling modulates SMN levels, as well as the Ras effector pathway inhibiting mTOR modulation, may reveal novel insights into the cellular mechanisms regulating SMN protein levels.

Discussion

Small molecule upregulators of protein abundance are an under-utilized class of bioactive compounds, with the potential to elucidate protein regulation and function. The work presented here defines a straightforward method for identifying small molecule upregulators of a target protein's abundance. These compounds have two important uses. First, based on the premise that upregulating the abundance of a target protein will increase its level of cellular activity, such compounds could act as protein function activators, allowing dose-dependent and reversible studies on the effects of increasing protein function. Discovery of small molecule activators has mainly focused on identifying compounds that increase the intrinsic activity of the steady-state levels of proteins. Small molecule activators have been identified for a handful of targets, such as caspases⁴⁰, the proteasome⁴¹ and several cell surface receptors^{8,42,43}. However, the number and classes of protein targets for these direct activators are likely as limited as those for inhibitors of protein functions. In comparison to inhibitors, upregulators are not restricted to specific protein families, as they do not rely on the protein of interest being directly "druggable", generally defined as the presence of a catalytic region that interacts with small molecules or an endogenous ligand binding site⁴⁴. Upregulators have the

advantage of targeting members of the regulatory pathways of the protein of interest, greatly increasing the range of protein families that can be modulated in this manner.

The second advantage of small molecule upregulators is their utility as probes to investigate the pathways involved in regulating the levels of a target protein. As many currently intractable conditions fall into the category of loss of function diseases, such as Spinal Muscular Atrophy, cystic fibrosis and Duchenne muscular dystrophy⁴⁵, elucidation of the pathways governing the abundance of the disease gene products may identify new therapeutic candidates. Additionally, small molecule upregulators of sufficient potency and efficacy have the potential to be developed into lead therapeutics.

Using a high-throughput screening approach for identification of small molecule upregulators of protein abundance, we discovered three small molecule upregulators of the Survival of Motor Neuron (SMN) protein. SMN has been shown to be involved in many cellular processes, such as pre-mRNA splicing⁴⁶ and β -actin mRNA localization to neuronal growth cones⁴⁷. SMN protein levels are decreased in the loss of function neurodegenerative disease Spinal Muscular Atrophy⁴⁸, making it a target of interest for both research and biomedical applications. The most active scaffold identified in our screen, a bromobenzophenone analog designated cuspin-1 (Chemical Upregulator of SMN Protein -1), was utilized as a probe to reveal a novel regulatory pathway governing SMN protein abundance. Treatment of Type I SMA fibroblast cells with cuspin-1 resulted in a 50-100% increase in endogenous SMN protein levels, as well as a concomitant increase in the phosphorylation of Erk. Since the major pathway responsible for phosphorylation of Erk is the Ras-Raf-MEK cascade¹⁹, we expressed constitutively active isoforms of Ras, and determined that increasing Ras signaling resulted in a robust

~270-300% increase in SMN protein abundance. Mechanistic studies revealed that this upregulation was due to Ras-mediated enhancement of SMN translation rate.

Increasing the translation rate of a target protein is an unusual mechanism of action, though recent studies suggest that translation regulation may have a role in diverse cellular process such as cancer, aging and mitochondrial function ⁴⁹. As the mammalian target of rapamycin (mTOR) protein is a highly conserved regulator of translation ⁵⁰⁻⁵², we investigated whether mTOR signaling could be involved in Ras-mediated regulation of SMN protein levels. Inhibition of mTOR signaling via starvation or small molecule inhibition resulted in a robust 40-60% decrease in SMN protein levels, indicating that mTOR is capable of modulating SMN protein levels. Of note, the downregulation of SMN mediated by mTOR could be completely rescued by increasing Ras signaling via expression of an oncogenic isoform of Ras. Cusp1's inability to rescue may be due to its inability to activate the Ras signaling pathway as strongly as constitutively active Ras, or due to the shorter time frame of Ras activation with compound treatment versus a cell line stably expressing constitutively active Ras. These results indicate that mTOR signaling is involved in regulation of SMN protein levels, and that this pathway may be involved in the robust upregulation of SMN protein levels due to increased Ras signaling.

The findings of SMN protein regulation by the mTOR and Ras pathways may be relevant to each other, as the mTOR and Ras pathways have shown to be linked via feedback loops. Inhibition of mTOR by rapamycin has been demonstrated to result in increased phosphorylation of Erk via Ras ⁵³. Additionally, mTOR inhibition has also been shown to increase receptor tyrosine kinase signaling upstream of Ras activation, resulting in increased activation of Akt, a downstream Ras effector ⁵⁴. However, since Ras

activation increases SMN protein levels while mTOR inhibition decreases SMN protein levels, this specific feedback loop may not be relevant to SMN protein regulation.

Future studies defining the mechanism by which increased Ras signaling affects translation of SMN protein could identify pathways of interest for SMA and perhaps other loss of function diseases. Although Ras is best known for its oncogenic properties, its ability to upregulate non-oncogenic proteins, such as SMN, demonstrate potential therapeutically beneficial downstream consequences of Ras activation. There is also significant evidence for a pro-survival effect of Ras activation, especially in neurons, where Ras has been shown to be activated by pro-survival neurotrophic factors ⁵⁵. Expression of constitutively active isoforms of Ras (CA-Ras) has shown beneficial effects on the survival and outgrowth of cultured chick embryonic neurons ⁵⁶. Additionally, in a mouse model of motor neuron degeneration, neuron-selective expression of CA-Ras resulted in complete rescue from lesion-induced degeneration ⁵⁷). The identification of the mechanisms downstream of Ras activation resulting in cell survival could lead to novel therapeutic targets for diseases resulting from pathological cell death.

Methods

Cell Culture

Type I spinal muscular atrophy (SMA)-affected human primary fibroblasts were obtained live with low passage number (Coriell Cell Repositories/#GM03813, #GM09677, #GM00232). The cells were cultured in Minimum Essential Medium

(MEM) with Earle's salts and non-essential amino acids (Invitrogen/#10370-021) supplemented with 15% (v/v) fetal bovine serum (FBS) (Invitrogen/#26140-079), 2 mM L-glutamine (Invitrogen/#25030-081), and antibiotics (100,000 units penicillin/L MEM, 100 mg streptomycin/L MEM) (Invitrogen/#15140-122). Cells were allowed to grow in 50 mL of the aforementioned medium at 37°C with 5% carbon dioxide in 175 cm² tissue culture treated flasks (Corning/#431080). The foreskin fibroblast-derived BJ cell lines were cultured in DMEM (Invitrogen/#11995-040) supplemented with 10% (v/v) FBS, 2mM L-glutamine and antibiotics. Cells were grown under the same conditions as SMA cell lines.

Small Molecule Libraries Selected for Screening

The commercially available small molecule libraries selected for screening consisted of the National Institute of Neurological Disorders and Stroke (NINDS) Custom Collection of Known Bioactives (1,040 compounds), the Annotated Compound Library (ACL) (2,337 compounds), the TIC library (a select composite from TimTech, InterBioScreen and Chembridge totaling 23,685 compounds) (15), and the Comgenex library (20,000 compounds).

A second unique set of small molecules, designated the Blood-Brain Barrier (BBB) libraries, were selected from five commercially available compound libraries. These libraries contain a total of 1,322,183 unique structures which were subjected to *in silico* filtering using MOE 2004.03. All compounds were pre-processed by assigning polar hydrogen atoms and charges according to the MMFFx forcefield. Salts were converted to free-base or free-acid form. These pre-processed libraries were first screened

for reactive functional groups and unsuitable scaffolds, as defined by Hann et al. (38) using a SMILES-string-based search method. We then proceeded to assess the BBB-penetrating potential of the compounds that passed the first two filtering steps by constructing a set of filters to predict logBB (logarithm of brain to blood partitioning ratio). The molecules' logBB values were predicted using a model trained on 73 compounds with experimentally determined logBB values and validated on a set of 36 CNS positive and negative drugs. The obtained model gave an $R^2 = 0.8225$ for the training and $R^2 = 0.6989$ for the validating set. Of note, the predictions gave no false negatives in this data set.

From this screen, 126,877 compounds with predicted logBB values greater than zero (on a log scale from -3 to +6) were selected. A value of zero indicates equal partitioning between the blood and brain, while a positive value indicates that the compound would partition preferentially into CNS tissues compared to plasma. Of these compounds, we discarded those with molecular weights less than 250 or containing three or more aromatic rings. These filters were designed to eliminate very simple compounds or planar compounds that might intercalate into DNA.

The final 79,691 compounds passing these filters were submitted to clustering to assess their diversity and to remove close structural analogs, which are frequently created during syntheses used by commercial vendors. This clustering was achieved by annotating the compounds with MACCS (Molecular Design Limited) structural keys; the clustering itself was performed using the Jarvis-Patrick method. Molecular similarity was determined by the Tanimoto coefficient, the threshold for which was set at 0.7. The

procedure yielded 27,577 structurally distinct clusters from four vendors. Three vendors (Asinex, Chembridge and Life Chemicals) were chosen based on pricing, and one compound from each cluster was purchased, yielding a library of 22,795 compounds likely to cross the blood-brain barrier and to be drug-like.

Preparation of Compound Libraries for Primary Screening

Compound libraries were either obtained at a concentration of 4 mg/mL in dimethyl sulfoxide (DMSO) or were solubilized in DMSO and plated at this concentration in 384-well, clear, polypropylene, 13mm deep "mother" plates (Greiner/#781280). These stocks were diluted into media to create "daughter" plates as follows: 148 μ L of Dulbecco's Modified Eagle's Medium (Invitrogen/#11995-040) were dispensed using a Biomek FX into each well of a 384-well, clear, polypropylene, 22mm deep daughter plate (Greiner/#781270). Two μ L from the mother plate were transferred to the daughter plates and thoroughly mixed using a Beckman Biomek FX workstation. This resulted in a compound concentration of 53.33 μ g/mL in each well of the daughter plates.

Primary Screen

GM03813 cells (herein referred to as "#3813"), GM09677 cells ("#9677"), and GM00232 cells ("#232") were trypsinized, centrifuged at 214g (1000rpm with 19.2cm rotor radius) for five minutes and resuspended in culture media at a concentration of 420,000 cells/mL. Thirty-six μ L of cell suspension were dispensed into each well of a 384-well, opaque bottom, white, tissue culture-treated, 13mm deep assay plate (Perkin

Elmer/#6007680) using a Biomek FX, for a concentration of 15,000 cells/well. Four μL from the daughter plate was transferred to each assay plate using a Biomek FX, resulting in a final compound concentration of 5.33 $\mu\text{g}/\text{mL}$ per well. The plate was covered with the supplied lid and incubated at 37°C and 5% carbon dioxide for 48 hours. All compounds were tested in triplicate.

Cytoblot Fixation, Permeabilization and Antibody Staining

After 48 hours incubation with small molecules, the growth medium was aspirated out of each assay plate, and 30 μL of ice cold (-20°C) methanol was added to each well for fixation and permeabilization using a Biomek FX. The plates were incubated for 5 minutes on ice, after which the methanol was aspirated and the primary antibody solution was immediately added. Twenty μL of 10% (v/v) goat serum (Invitrogen/#16210-072) in PBS with 0.1% Tween® 20 (Aldrich/#274348) containing primary antibody (see below for dilutions) was dispensed to each well using a Biomek FX. Plates were sealed using a Velocity11 PlateLoc and incubated overnight at 4°C. The following day, the seals were removed and the primary antibody solution was aspirated out of each assay plate. Twenty μL of secondary antibody in the same blocking buffer was dispensed into each well using a Biomek FX. Plates were incubated for one hour at room temperature prior to signal detection. HRP SMN cyto blot: mouse anti-SMN (BD Transduction Laboratories/#610647) (1:3,000 dilution) and goat anti-mouse-HRP (Santa Cruz Biotechnology/#sc-2031) (1:9,000 dilution)

Cytoblot Signal Detection

After the one hour incubation period, the secondary antibody solution was aspirated out of each assay plate. Fifty μL of 10% (v/v) goat serum in PBS with 0.1% Tween® 20 were added to each well using a Biomek FX, to rinse out unbound secondary antibody. After 10 minute incubation on ice, the solution was aspirated. Twenty μL of enhanced chemiluminescence (ECL) reagent were added to each well using a Biomek FX. ECL reagent is composed of two solutions mixed together immediately prior to use – Solution A: 5 mL Tris (pH 8.5) (Roche/#0604205) and 4 μL H_2O_2 (Sigma/#H1009); Solution B: 5 mL Tris (pH 8.5) (Roche/#0604205), 22 μL 90 mM coumaric acid (Sigma/#C9008), and 50 μL 250 mM luminol (Fluka/#09253). Luminescence was read using a Perkin Elmer Victor 3 microtiter platereader (#1420-041) equipped with an infrared filter, using a 0.8 s integration time per well. Data was exported and evaluated in Excel.

Dose-response experiments

Compounds showing activity in the primary screen were retested in dilution series, daughter plates of the hit-containing mother plates were recreated (as described above). For the “step-daughter” plates, fifty-eight μL of DMEM (as diluent) were dispensed using a Biomek FX into every well (except for columns 8 and 15) of an empty, 384-well, clear, polypropylene, 22mm deep plate (Greiner/#781270). One hundred and sixteen (116) μL of hit compound in media (53.33 $\mu\text{g}/\text{ml}$) were transferred using the Span-8 head of a Biomek FX from the daughter plate to the step-daughter plate. Picked hits were dispensed in columns 8 and 15 using rows C through N (one well per compound), allowing 24 hits per step-daughter plate. A two-fold, six-point serial dilution

was performed by the Biomek FX Span-8 head: compounds in column 8 were diluted through column 13, and compounds in column 15 were diluted through column 20. All compounds were tested in triplicate.

Robotic Scripts and Settings

BioMek FX (software version 2.5e) method files are available upon request.

Analog Synthesis

Solvents and starting materials were purchased from Sigma-Aldrich and used without further purification. Analogs were synthesized using chlorination and Friedel-Crafts acylation. Briefly, 50-100mg of 5-bromonicotinic acid, or desired nicotinic acid, was dissolved in ~10mL of anhydrous dimethyl chloride. Thionyl chloride (1.2 mEq) was added to solution. Reaction progress was monitored using pH paper. Once complete, solvent was removed under high vacuum. Acyl chlorides were coupled to desired benzene derivative in anhydrous dimethyl chloride with aluminum trichloride (1.3 mEq), overnight. Unreacted starting materials were removed by aqueous extraction and products were purified by chromatography in hexanes/ethyl acetate. Identity and purity was confirmed by mass spectrometry. Yields ranged between 20-75%, providing sufficient material for testing. Synthetically prepared cuspin-1 and cuspin-2 showed similar activity to that of the commercially sourced compounds, verifying the identity of the compounds.

Western blot analysis

SMA patient fibroblast lines were plated at 30,000 cells per well in a 6-well plate ~24 hours prior to compound treatment. Cells were treated with desired concentration of compound for 48 hours. Cells were harvested at <75% confluence, confluence may be lower due to compound toxicity. Cells were washed twice in ice-cold PBS and lysed by scraping in 100 μ L ice-cold lysis buffer (50mM HEPES, 40mM NaCl, 2mM EDTA, 0.5% Triton-X, 1.5mM Na_3VO_4 , 50mM NaF, 10mM Na-pyrophosphate, 10mM Na β -glycerophosphate, Roche protease inhibitor tablet). Insoluble materials were spun out by centrifugation at 10,621g for 10 minutes at 4°C. Supernatants were boiled with SDS-PAGE sample buffer prior to being separated on a 4-12% Bis-Tris NuPage gel in 1X NuPage MES running buffer. Proteins were transferred to a PVDF membrane using Invitrogen iBlot blotting system, setting P3 for 6 minutes and 40 seconds. Membranes were blocked in Odyssey blocking buffer (LI-COR/#927-40010) for 20 minutes at room temperature, then incubated overnight at 4°C with primary antibodies (see below for dilutions). Membranes were washed three times in TBS with 0.1% Tween-20, then incubated for 45-60 minutes with 680nm-conjugated anti-mouse IgG secondary antibody at 1:3,000 (Invitrogen/#A21058) and 800nm-conjugated anti-rabbit IgG secondary antibody at 1:3,000 (LI-COR/#926-322110). Signals were detected and quantified using the LiCor Odyssey system and software (LI-COR Biosciences).

Antibodies: mouse anti-SMN (BD Biosciences/#610647) (1:1,000), rabbit anti-actin (Santa Cruz Biotechnologies/#sc-1616-R) (1:3,000), mouse anti-alpha tubulin (Santa Cruz Biotechnologies/#sc-32293) (1:5,000), rabbit anti-phospho-Erk1/2 (Cell Signaling/#9101S) (1:1,000), rabbit anti-Erk1/2 (Cell Signaling/#9102)(1:3,000), rabbit anti-phospho-Akt (Cell Signaling/#9271)(1:2,000), rabbit anti-Akt (Cell

Signaling/#9272)(1:2,000), mouse anti-NRas (EMD Biosciences/#OP25) (1:2,000), mouse anti-eIF4E (BD Biosciences/#610269)(1:2,000), mouse anti-Smac/DIABLO (BD Biosciences/#612244)(1:1,000), mouse anti-GAPDH (Santa Cruz Biotechnologies/#sc-47724)(1:5,000) and rabbit anti-LC3B (Cell Signalling/#2775S)(1:1,000).

Retroviral preparation and transduction

To prepare the retroviral supernatants, 2×10^6 Plat-GP cells (Cell Biolabs/#RV-103) were seeded per 10cm culture dish in DMEM supplemented with 10% (v/v) fetal bovine serum (FBS), 2 mM L-glutamine, and antibiotics (100,000 units penicillin/L MEM, 100 mg streptomycin/L MEM) and $5 \mu\text{g/ml}$ G418 (Invitrogen/#11811-031). Cells were allowed to attach overnight. The following morning pVSV-G helper plasmids with the MigR1 vector either empty or containing *NRas*^{G12D} were co-transfected into the Plat-GP cells using FuGENE 6 Transfection Reagent (Roche/#11-814-443-001). Thirty hours post-transfection, culture media was replaced by Viral Collection Media (VCM, normal culture media with 30% (v/v) FBS). VCM was collected and replaced twice at 12 hour intervals to collect viral particles released into the supernatant. Viral supernatant was filtered through 0.45 micron filters prior to use or storage at -80°C . For transduction, #3813 SMA patient fibroblast cells were plated at 2×10^5 cells per well into a 6-well plate and allowed to attach overnight. The following day, the infection cocktail was prepared by mixing 0.75mL viral supernatant, 1.25mL growth media, and $2 \mu\text{L}$ of 8mg/mL polybrene (Sigma/#H9268). The culture media in each well was replaced with the infection cocktail, and then plates were spun at 1,089g (2,250 rpm with 19.2cm rotor

radius) for 90 minutes before incubation. Cells were cultured for two days prior to harvesting.

RT-qPCR of SMN transcripts

RNA was harvested from 5×10^6 cells using the Qiagen RNeasy Kit as per manufacturer's protocol. RNA from each sample (2 μ g) was reverse transcribed using Applied Biosystems Taqman® kit (N808-0234) as per manufacturer's protocol. Quantitative PCR was performed on 7300 Real-Time PCR System (Applied Biosystems) using 1X Power SYBR Green PCR Master Mix (Applied Biosystems/#4367659), 77ng cDNA and 0.15 μ M primers per well in a MicroAmp Optical 96-well plate (Applied Biosystems/#N801-0560). The cycle times of the *smn* transcripts were normalized to cycle times for hypoxanthine guanine phosphoribosyltransferase (*hprt*) as loading control. Amplification conditions: 50°C for 2 min, 95°C for 10 min, 40 cycles of 95°C for 15 sec and 60°C for 1 min. $\Delta\Delta$ CT was calculated after normalization to *hprt* expression. Primer sequences: *smnFL*-forward: 5'-CAAAAAGAAGGAAGGTGCTCA-3', *smnFL*-reverse: 5'-TGGTGTCATTTAGTGCTGCTC-3', *smn Δ 7*-forward: 5'-ATTCTCTTGATGATGCTGATGCT-3', *smn Δ 7*-reverse: 5'-TATGCCAGCCATTTCCATATAATAG-3', *hprt*-forward: 5'-TGACACTGGCAAAACAATGCA-3', *hprt*-reverse: 5'-GGTCCTTTTCACCAGCAAGCT-3'

³⁵S-methionine/cysteine translation rate assay

Cells were seeded at 5×10^6 cells per 10cm dish and allowed to attach overnight. For methionine/cysteine starvation, cells were rinsed twice in PBS and incubated for 30 minutes in starvation media: Met/Cys-free DMEM (Invitrogen/#21013-024), 10% dialyzed FBS (v/v) and 2mM L-glutamine. After the starvation period, cells were pulsed with 100 μ Ci TRAN35S-Label Metabolic Labeling Reagent (MP/#015100907) for one hour. Cells were lysed in 1 mL IP Buffer (50mM Tris [pH 7.75], 250mM NaCl, 200mM EDTA, 150mM MgCl₂, 0.3% NP-40, 1% Empigen BB and Roche protease inhibitor tablet), scraped and insoluble materials were spun out at 10,621g for 10min at 4°C. Lysates were pre-cleared with 20 μ L Protein A/G-agarose bead slurry (Pierce/#20421) for 30 minutes, supernatants were transferred to tubes containing 30 μ L Protein A/G-agarose pre-coupled to 2.5 μ g mouse anti-SMN antibody (BD Biosciences/#610647) and immunoprecipitated overnight at 4°C. After SMN IP, lysates were transferred to tubes containing 30 μ L Protein A/G-agarose pre-coupled to 2 μ g rabbit anti-actin antibody (Santa Cruz Biotechnologies/#sc-1616-R) and immunoprecipitated for 4 hours at 4°C. Beads were washed three times in IP buffer, and bound proteins were eluted by boiling in SDS-PAGE buffer. Samples were run on NuPAGE 4-12% Bis-Tris gels (Invitrogen/#WG1402BOX) in 1X NuPAGE MES running buffer, fixed in 50% methanol + 10% acetic acid, and dried before exposing overnight to phosphorimager screen. Bands were imaged using a Storm phosphorimager (Molecular Dynamics) and quantification was performed using ImageQuant software (Molecular Dynamics). Values are reported as SMN to actin ratio normalized to BJeH (-HRas^{V12}).

References

1. Sopko, R., *et al.* Mapping pathways and phenotypes by systematic gene overexpression. *Mol Cell* **21**, 319-330 (2006).
2. Atmaca, M. Valproate and neuroprotective effects for bipolar disorder. *Int Rev Psychiatry* **21**, 410-413 (2009).
3. Trinka, E. The use of valproate and new antiepileptic drugs in status epilepticus. *Epilepsia* **48 Suppl 8**, 49-51 (2007).
4. Marks, P.A. Discovery and development of SAHA as an anticancer agent. *Oncogene* **26**, 1351-1356 (2007).
5. Richardson, P.G., Hideshima, T. & Anderson, K.C. Bortezomib (PS-341): a novel, first-in-class proteasome inhibitor for the treatment of multiple myeloma and other cancers. *Cancer Control* **10**, 361-369 (2003).
6. Sun, L., Trausch-Azar, J.S., Ciechanover, A. & Schwartz, A.L. E2A protein degradation by the ubiquitin-proteasome system is stage-dependent during muscle differentiation. *Oncogene* **26**, 441-448 (2007).
7. Chateauvieux, S., Morceau, F., Dicato, M. & Diederich, M. Molecular and therapeutic potential and toxicity of valproic acid. *J Biomed Biotechnol* **2010**(2010).
8. Small, K.M., McGraw, D.W. & Liggett, S.B. Pharmacology and physiology of human adrenergic receptor polymorphisms. *Annu Rev Pharmacol Toxicol* **43**, 381-411 (2003).
9. Coovert, D.D., *et al.* The survival motor neuron protein in spinal muscular atrophy. *Hum Mol Genet* **6**, 1205-1214 (1997).
10. Monani, U.R., *et al.* A single nucleotide difference that alters splicing patterns distinguishes the SMA gene SMN1 from the copy gene SMN2. *Hum Mol Genet* **8**, 1177-1183 (1999).
11. Burghes, A.H. & Beattie, C.E. Spinal muscular atrophy: why do low levels of survival motor neuron protein make motor neurons sick? *Nat Rev Neurosci* **10**, 597-609 (2009).
12. Jarecki, J., *et al.* Diverse small-molecule modulators of SMN expression found by high-throughput compound screening: early leads towards a therapeutic for spinal muscular atrophy. *Hum Mol Genet* **14**, 2003-2018 (2005).

13. Andreassi, C., *et al.* Aclarubicin treatment restores SMN levels to cells derived from type I spinal muscular atrophy patients. *Hum Mol Genet* **10**, 2841-2849 (2001).
14. Stockwell, B.R., Haggarty, S.J. & Schreiber, S.L. High-throughput screening of small molecules in miniaturized mammalian cell-based assays involving post-translational modifications. *Chem Biol* **6**, 71-83 (1999).
15. Root, D.E., Flaherty, S.P., Kelley, B.P. & Stockwell, B.R. Biological mechanism profiling using an annotated compound library. *Chem Biol* **10**, 881-892 (2003).
16. Zhang, J.H., Chung, T.D. & Oldenburg, K.R. A Simple Statistical Parameter for Use in Evaluation and Validation of High Throughput Screening Assays. *J Biomol Screen* **4**, 67-73 (1999).
17. Kelley, B.P., *et al.* A flexible data analysis tool for chemical genetic screens. *Chem Biol* **11**, 1495-1503 (2004).
18. Lunn, M.R. & Wang, C.H. Spinal muscular atrophy. *Lancet* **371**, 2120-2133 (2008).
19. Vojtek, A.B. & Der, C.J. Increasing complexity of the Ras signaling pathway. *J Biol Chem* **273**, 19925-19928 (1998).
20. Hahn, W.C., *et al.* Creation of human tumour cells with defined genetic elements. *Nature* **400**, 464-468 (1999).
21. Farooq, F., Balabanian, S., Liu, X., Holcik, M. & MacKenzie, A. p38 Mitogen-activated protein kinase stabilizes SMN mRNA through RNA binding protein HuR. *Hum Mol Genet* **18**, 4035-4045 (2009).
22. Burnett, B.G., *et al.* Regulation of SMN protein stability. *Mol Cell Biol* **29**, 1107-1115 (2009).
23. Cho, S. & Dreyfuss, G. A degron created by SMN2 exon 7 skipping is a principal contributor to spinal muscular atrophy severity. *Genes Dev* **24**, 438-442 (2010).
24. Newton, R., *et al.* The MAP kinase inhibitors, PD098059, UO126 and SB203580, inhibit IL-1beta-dependent PGE(2) release via mechanistically distinct processes. *Br J Pharmacol* **130**, 1353-1361 (2000).
25. Hay, N. & Sonenberg, N. Upstream and downstream of mTOR. *Genes Dev* **18**, 1926-1945 (2004).
26. Tokunaga, C., Yoshino, K. & Yonezawa, K. mTOR integrates amino acid- and energy-sensing pathways. *Biochem Biophys Res Commun* **313**, 443-446 (2004).

27. Burnett, P.E., Barrow, R.K., Cohen, N.A., Snyder, S.H. & Sabatini, D.M. RAFT1 phosphorylation of the translational regulators p70 S6 kinase and 4E-BP1. *Proc Natl Acad Sci U S A* **95**, 1432-1437 (1998).
28. Brown, E.J., *et al.* Control of p70 s6 kinase by kinase activity of FRAP in vivo. *Nature* **377**, 441-446 (1995).
29. Bierer, B.E., Somers, P.K., Wandless, T.J., Burakoff, S.J. & Schreiber, S.L. Probing immunosuppressant action with a nonnatural immunophilin ligand. *Science* **250**, 556-559 (1990).
30. Schmelzle, T. & Hall, M.N. TOR, a central controller of cell growth. *Cell* **103**, 253-262 (2000).
31. Ravikumar, B., *et al.* Inhibition of mTOR induces autophagy and reduces toxicity of polyglutamine expansions in fly and mouse models of Huntington disease. *Nat Genet* **36**, 585-595 (2004).
32. Hunt, S., Pak, S., Bridges, M., Gray, P., Sleigh, M. . Chinese hamster ovary cells produce sufficient recombinant insulin-like growth factor I to support growth in serum-free medium. Serum-free growth of IGF-I-producing CHO cells. *Cytotechnology* **24**, 55-64 (1997).
33. Wu, J., *et al.* Molecular cloning and characterization of rat LC3A and LC3B--two novel markers of autophagosome. *Biochem Biophys Res Commun* **339**, 437-442 (2006).
34. Chang, H.C., Hung, W.C., Chuang, Y.J. & Jong, Y.J. Degradation of survival motor neuron (SMN) protein is mediated via the ubiquitin/proteasome pathway. *Neurochem Int* **45**, 1107-1112 (2004).
35. Liu, H., Wang, P., Song, W. & Sun, X. Degradation of regulator of calcineurin 1 (RCAN1) is mediated by both chaperone-mediated autophagy and ubiquitin proteasome pathways. *FASEB J* **23**, 3383-3392 (2009).
36. Geng, Y., Kohli, L., Klocke, B.J. & Roth, K.A. Chloroquine-induced autophagic vacuole accumulation and cell death in glioma cells is p53 independent. *Neuro Oncol* **12**, 473-481 (2010).
37. Lee, D.H. & Goldberg, A.L. Proteasome inhibitors: valuable new tools for cell biologists. *Trends Cell Biol* **8**, 397-403 (1998).
38. Capell, A., *et al.* Rescue of progranulin deficiency associated with frontotemporal lobar degeneration by alkalizing reagents and inhibition of vacuolar ATPase. *J Neurosci* **31**, 1885-1894 (2011).

39. Sobota, J.A., Back, N., Eipper, B.A. & Mains, R.E. Inhibitors of the V0 subunit of the vacuolar H⁺-ATPase prevent segregation of lysosomal- and secretory-pathway proteins. *J Cell Sci* **122**, 3542-3553 (2009).
40. Wolan, D.W., Zorn, J.A., Gray, D.C. & Wells, J.A. Small-molecule activators of a proenzyme. *Science* **326**, 853-858 (2009).
41. Huang, L., Ho, P. & Chen, C.H. Activation and inhibition of the proteasome by betulinic acid and its derivatives. *FEBS Lett* **581**, 4955-4959 (2007).
42. Grimm, C., *et al.* Small molecule activators of TRPML3. *Chem Biol* **17**, 135-148 (2010).
43. Mruk, K. & Kobertz, W.R. Discovery of a novel activator of KCNQ1-KCNE1 K channel complexes. *PLoS One* **4**, e4236 (2009).
44. Hopkins, A.L. & Groom, C.R. The druggable genome. *Nat Rev Drug Discov* **1**, 727-730 (2002).
45. Segalat, L. Loss-of-function genetic diseases and the concept of pharmaceutical targets. *Orphanet J Rare Dis* **2**, 30 (2007).
46. Pellizzoni, L., Kataoka, N., Charroux, B. & Dreyfuss, G. A novel function for SMN, the spinal muscular atrophy disease gene product, in pre-mRNA splicing. *Cell* **95**, 615-624 (1998).
47. Rossoll, W., *et al.* Smn, the spinal muscular atrophy-determining gene product, modulates axon growth and localization of beta-actin mRNA in growth cones of motoneurons. *J Cell Biol* **163**, 801-812 (2003).
48. Lefebvre, S., *et al.* Correlation between severity and SMN protein level in spinal muscular atrophy. *Nat Genet* **16**, 265-269 (1997).
49. Sonenberg, N. & Hinnebusch, A.G. Regulation of translation initiation in eukaryotes: mechanisms and biological targets. *Cell* **136**, 731-745 (2009).
50. Long, X., *et al.* TOR deficiency in *C. elegans* causes developmental arrest and intestinal atrophy by inhibition of mRNA translation. *Curr Biol* **12**, 1448-1461 (2002).
51. Miron, M. & Sonenberg, N. Regulation of translation via TOR signaling: insights from *Drosophila melanogaster*. *J Nutr* **131**, 2988S-2993S (2001).
52. Barbet, N.C., *et al.* TOR controls translation initiation and early G1 progression in yeast. *Mol Biol Cell* **7**, 25-42 (1996).

53. Carracedo, A., *et al.* Inhibition of mTORC1 leads to MAPK pathway activation through a PI3K-dependent feedback loop in human cancer. *J Clin Invest* **118**, 3065-3074 (2008).
54. O'Reilly, K.E., *et al.* mTOR inhibition induces upstream receptor tyrosine kinase signaling and activates Akt. *Cancer Res* **66**, 1500-1508 (2006).
55. Segal, R.A. & Greenberg, M.E. Intracellular signaling pathways activated by neurotrophic factors. *Annu Rev Neurosci* **19**, 463-489 (1996).
56. Borasio, G.D., *et al.* ras p21 protein promotes survival and fiber outgrowth of cultured embryonic neurons. *Neuron* **2**, 1087-1096 (1989).
57. Heumann, R., *et al.* Transgenic activation of Ras in neurons promotes hypertrophy and protects from lesion-induced degeneration. *J Cell Biol* **151**, 1537-1548 (2000).

Chapter 3. High-throughput screening hit validation for Huntington's Disease

Phenotypic small molecule screening in neurodegenerative diseases

Phenotypic small molecule screening is often the appropriate option when searching for small molecule modulators of diseases with complex physiopathology. This applies especially to neurodegenerative diseases, as they are often pleiotropic and inherently difficult to study, due to the complex and interconnected nature of the nervous system. Cell culture models of these disease states, while rarely recapitulating all aspects of a diseased organism, are a simpler and more cost-effective way to study cell death in poorly-understood neurodegenerative disorders ¹. The combination of phenotypic small molecule screening and cell culture models of neurodegenerative diseases has the potential to reveal novel insights into the mechanisms of cell death relevant to these disease states.

Pathogenesis of Huntington's disease

A strong example of the value of small molecule screening in a cell culture model of a neurodegenerative disease is reported in work by Hoffstrom and colleagues. The focus of this screen was to identify small molecule inhibitors of cell death caused by the gene responsible for Huntington's disease (HD), the mutant *huntingtin* (*htt*) gene. Huntington's disease is an autosomal dominant neurodegenerative disease caused by expansion of the polyglutamine stretch

in exon 1 of the *htt* gene². Wild-type *htt* contains between 6 and 35 CAG triplicates, which code for glutamines, however expansion above 36 repeats results in disease³. The age of onset and speed of disease progression correlate strongly with the length of the polyglutamine expansion. Expression of a mutant allele of *htt* in an organism results in degeneration of neurons, mainly in the basal ganglia and cortex^{4,5}. As the basal ganglia is responsible for sending inhibitory signals to the motor cortex, this pattern of neuronal loss causes chorea, involuntary dance-like movements, characteristic of Huntington's patients⁴.

Huntingtin protein

Htt is an essential gene highly expressed in neuronal tissues⁶⁻⁷. Normal Htt protein is approximately 350kDa, with no significant homology to other proteins. It has been suggested to be involved in clathrin-mediated endocytosis⁸, intracellular vesicle trafficking⁹ and has been shown to be highly concentrated on microtubules¹⁰, however its exact cellular functions remain unclear.

Mutant huntingtin protein, similar to other proteins containing expanded polyglutamine tracts, is toxic to specific neuronal subpopulations, most predominantly the medium spiny neurons of the striatum. The mutant form of *Htt* has been implicated in the alteration of many functions of key importance in neurons, including cytoskeletal integrity¹¹, gene expression¹², response to excitotoxicity¹³, translation¹⁴ and signaling¹⁵.

Although mutant Htt affects many vital cellular pathways, the mechanism resulting in selective neuronal death is unknown. Several studies for cell death markers in animal models and

human patients, however, have provided strong evidence implicating activation of the apoptotic pathway¹⁶⁻²⁰. However, there is no clear link between mutant Htt and apoptotic cell death. In order to gain more information about the connection between mutant Htt expression and cell death, Hoffstrom, *et al.* screened 47,000 compounds in the search for inhibitors of polyglutamine-induced cell death in a cell culture model of Huntington's disease²¹. The neuronal-like cell line utilized for screening, rat pheochromocytoma (PC12) cells, stably express an ecdysone-inducible pathogenic *htt* mutant with 103 glutamines in its polyglutamine tract (Q103). These cells faithfully replicate mutant Htt-induced cell death²². From this screen, five structurally distinct inhibitors of polyglutamine-induced apoptosis were identified (Figures 14 and 15). These compounds not only rescue cell viability, they also restore normal cell morphology.

The small molecule inhibitors of mutant Htt-induced cell death were utilized as probes in target identification studies, in efforts to identify the missing link between polyglutamine expression and cell death. The target of these inhibitors was identified as protein disulfide isomerase (PDI), an oxidoreductase chaperone protein which catalyzes disulfide bond formation and rearrangement²³⁻²⁴.

Protein misfolding and chaperones in neurodegenerative disease

PDI is a well-described chaperone protein generally residing in the endoplasmic reticulum (ER)²⁵. The ER is responsible for the proper folding of its many substrate proteins in eukaryotic cells. In addition to housing the chaperone proteins required for protein folding,

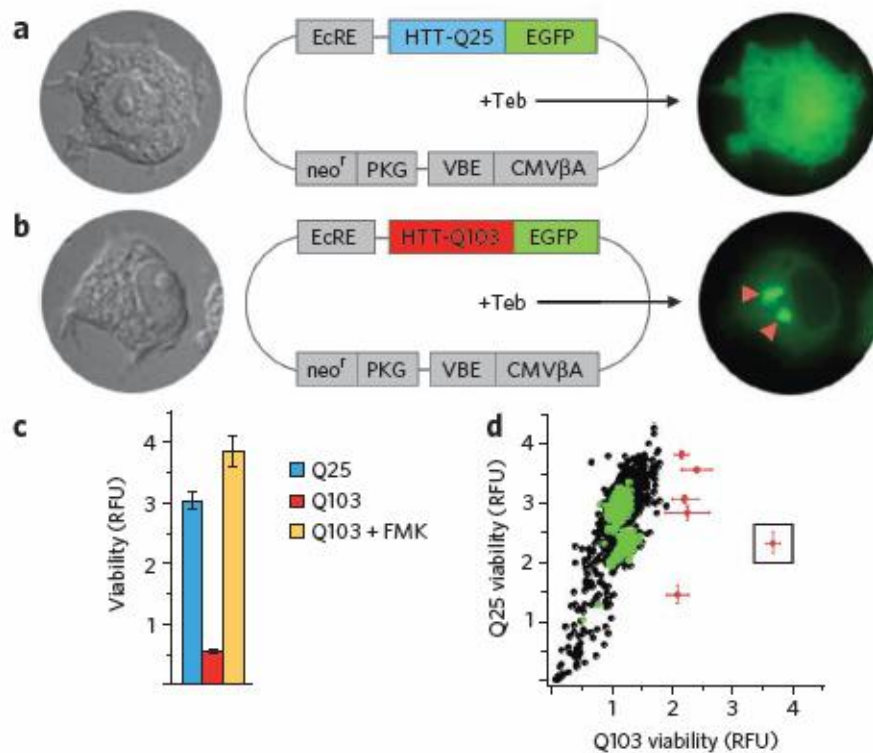


Figure 14. Cell based (PC12) model of mutant huntingtin protein misfolding and cell toxicity. (a) Cells transfected with an inducible plasmid containing wild-type huntingtin exon 1 (HTT-Q25) show diffuse protein expression throughout the cytosol (24 h post-induction with the ecdysone analog tebufenozide, Teb). EcRE, ecdysone responsive element; VBE, VP16-ecdysone receptor chimera; CMV-βA, cytomegalovirus enhancer-β-actin promoter, neo^r-PKG, neomycin resistance. (b) Cells transfected with the same plasmid containing mutant, polyQ huntingtin exon 1 (HTT-Q103) show perinuclear inclusion bodies at 24 h post-induction (red arrows). (c) Cell viability of mutant huntingtin-expressing cells (measured by Alamar Blue fluorescence at 48 h post-induction). Cell death induced by HTT-Q103 can be rescued by treatment with a general caspase inhibitor, Boc-D-FMK (FMK; 50μM). (d) Primary screening results of 2,036 compounds showing effects on cell viability of induced Q25 and Q103 cells. Putative hit

compounds that rescue Q103-induced cell death are shown in red; confirmed hit (thiomuscimol) is boxed; DMSO-treated controls are shown in green. (Reproduced from ²¹.)

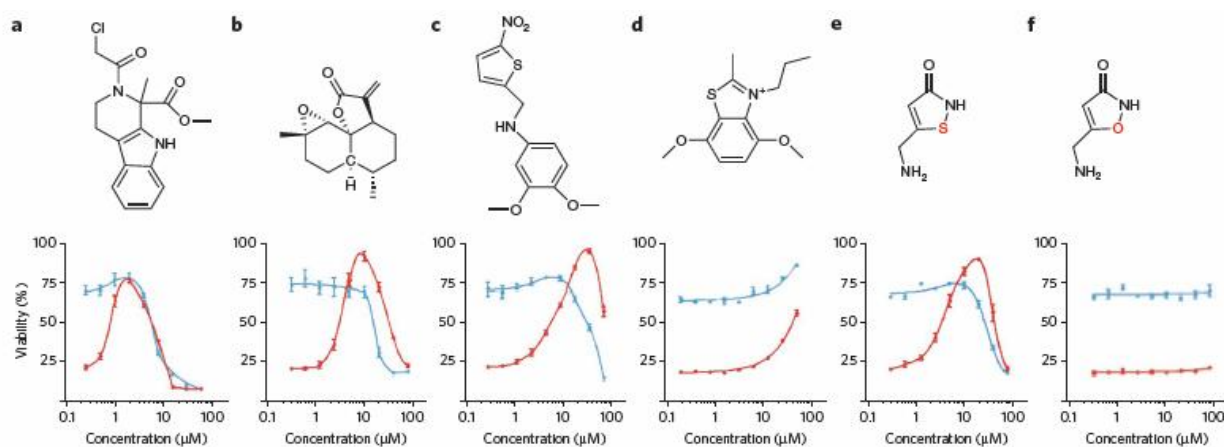


Figure 15. Dose-response curves for hit compounds that suppress Q103-induced apoptosis.

The viability of tebufenozide-induced HTT-Q25 (blue) and HTT-Q103 (red) cells was detected by Alamar Blue fluorescence and plotted as a percentage of uninduced cells at 48 h post-induction. (a) 16F16, (b) arteannuin B, (c) BBC7M13 (D13), (d) BBC7E8, (e) thiomuscimol, (f) muscimol (inactive analog of thiomuscimol; single atom substitution shown in red in compound structures). (Reproduced from ²¹.)

the ER also contains mechanisms by which to monitor the fidelity of folding. These quality control mechanisms only release correctly folded protein through the secretory pathway while targeting misfolded proteins for degradation, via a process termed ER-associated protein degradation (ERAD) ²⁶. When the ER quality control systems have determined that a protein is terminally misfolded, the target protein is retrotranslocated into the cytosol for proteolytic degradation by the ubiquitin-proteasome system ²⁷. The ER can respond dynamically to cellular alterations which affect the thermodynamic stability of protein folding, in a process called the unfolded protein response (UPR) ²⁸. UPR is triggered upon the accumulation of unfolded protein in the ER lumen, which initiates a coordinated set of signaling pathways designed to attenuate protein synthesis and modify transcription ²⁹. This process provides a feedback loop to increase the ER's ability to cope with maintaining proper protein folding under changing cellular conditions ³⁰. Poor ER quality control mechanisms, resulting in activation of UPR, have been associated with neurodegenerative disease ³¹ and this pathway has been associated with neuronal death ³².

Protein disulfide isomerase in Huntington's disease

PDI is a member of the thioredoxin superfamily ³³, and consists of six domains: a, b, b', x, a' and c ³⁴⁻³⁵. Each of these domains, with the exception of x, contain the active site CXXC motif characteristic of thioredoxin family members, however only two (a and a') have been shown to be catalytically active ³⁶. The b and b' domains are considered to be important for substrate recognition ³⁷. Although many groups have attempted to solve the structure of full-length mammalian PDI, only the smaller yeast Pdi1p orthologue (PDB: 2b5e) has been

successfully crystallized³⁸. The structures of the individual domains of mammalian PDI have been solved, however, although mainly through the use of solution NMR. These include the a domain (PDB: 1mek)³⁹⁻⁴⁰, b domain (PDB: 2bjx)^{36,41}, b'x domains (PDB: 3bj5)⁴² as well as bb' domains (PDB: 2kl8)⁴³ and a' domain (PDB: 1x5c)²⁵. Together, these structures provide an overall framework describing the structure of full-length PDI.

PDI contains a classic KDEL ER-retention sequence and is highly enriched within the endoplasmic reticulum⁴⁴, however it has been observed to present in other cellular compartments^{24,45-46} and has even been shown to be actively exported from the ER in certain cell types⁴⁷. The functions of PDI outside of the ER are poorly understood, however it was found to re-localize to ER-mitochondrial junction points upon induction of mutant Htt expression and induce mitochondrial outer membrane permeabilization (MOMP)²¹. MOMP initiates an intrinsic apoptotic pathway via release of cytochrome c and Smac/DIABLO from the mitochondria, which in turn activate caspase-mediated cell death⁴⁸. Activation of MOMP is governed by the Bcl-2 family proteins; oligomerization of the pro-apoptotic proteins Bax and Bak promote the release of apoptotic factors, while the anti-apoptotic Bcl-2 can inhibit the activation of these proteins and subsequent activation of apoptosis⁴⁹⁻⁵².

While the mechanism resulting in induction of apoptosis is unexpected, in retrospect, it is not altogether surprising that an ER chaperone protein would be involved in mediating mutant Htt-induced apoptosis. Expanded polyglutamine proteins are generally considered misfolded and have a tendency to aggregate, causing ER stress by activating the ER quality control mechanisms. ER stress, in turn, can activate MOMP⁵³. Stimulation of the unfolded protein response (UPR) has been observed HD models⁵⁴⁻⁵⁵, as well as mutant Htt-induced impairment of

the endoplasmic reticulum associated protein degradation (ERAD) pathway⁵⁶. Furthermore, ER stress has been implicated in HD pathogenesis⁵⁷, and has been shown to upregulate the levels of PDI protein⁵⁸. It is possible that extended activation of UPR, results in the pathway switching from a protective function to an active cell death mechanism, and that the UPR-responsive protein PDI mediates this pro-apoptotic function.

My efforts in this project were aimed at elucidating the mechanism linking poly-Q *htt* to apoptosis via PDI. This included validating apoptosis as the death pathway relevant to PDI-induced cell death in the PC12 HD model used in our assays, and demonstrating that increased PDI expression could directly result in cell death, in order to complement the *in vitro* studies which demonstrated PDI-induced MOMP in isolated mitochondria. Lastly, we began crystallization studies in order to identify the binding mode of the PDI inhibitors identified in the high-throughput screen for small molecule inhibitors of mutant Htt-induced cell death. Although the crystallization trials have yet to offer any solid results, these studies have assisted in validating the role of PDI in a pro-apoptotic, mitochondrial-mediated pathway relevant to polyglutamine-induced cell death.

Validation of PDI as a mitochondrial-mediated pro-apoptotic stimuli

Rescue of mutant Htt-induced cell death by Bcl-2

Although the cellular pathway by which expanded polyglutamine Htt induces cell death remains unclear, several models of Huntington's disease as well as studies of HD patient tissues

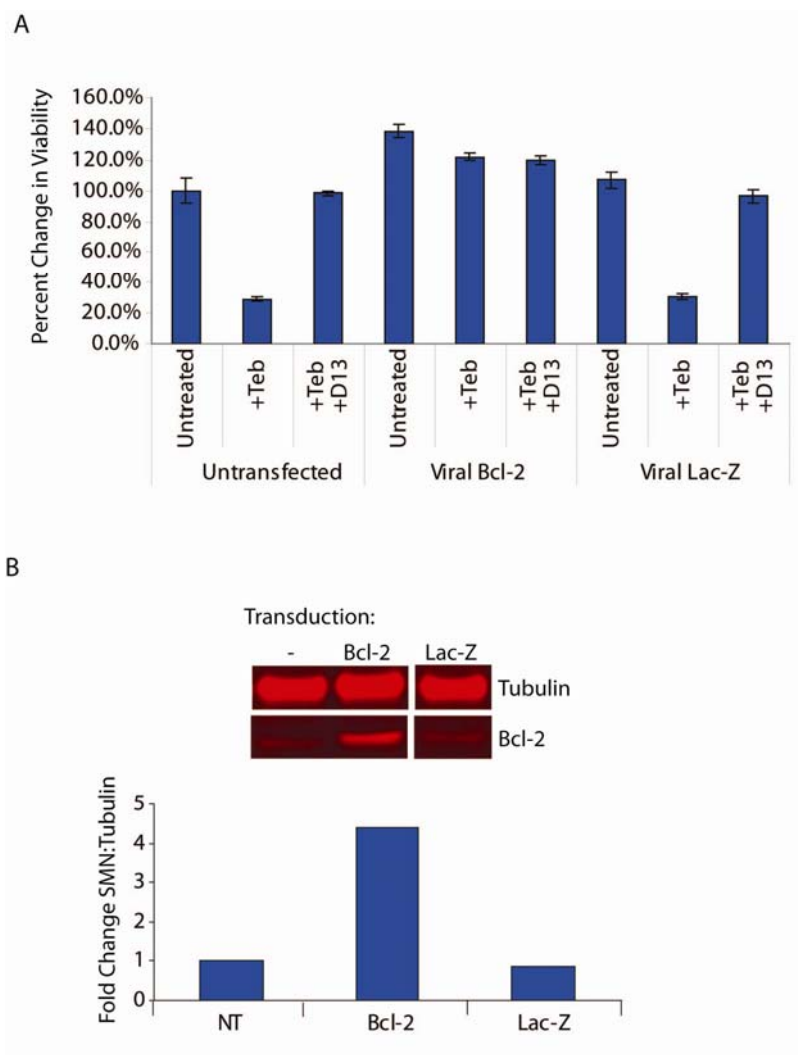


Figure 16. Overexpression of the anti-apoptotic protein Bcl-2 rescues from mutant Q103-HTT induced cell death. (A) Cell viability of Q103-HTT expressing cells, measured by Alamar Blue fluorescence at 48 h post-induction with tebufenozide (Teb). Overexpression of Bcl-2, by viral transduction of a Bcl-2 expression plasmid, rescues cell death. Expression of a control protein, Lac-Z, has no effect. Bcl-2 expression rescues to a similar extent as the small molecule PDI inhibitor D13 (BBC7M13;10 μ g/mL), and does not show additive rescue upon co-treatment with D13. **(B)** Western blot and graph quantifying the level of Bcl-2 protein in each cell line.

have supported apoptosis as a mechanism involved in the pathogenesis of HD¹⁶⁻²⁰. To determine whether mutant Htt protein expression induces apoptosis in the PC12 cell line used in our assays, we overexpressed the anti-apoptotic protein Bcl-2 and examined its effect on mutant Htt-induced cell death. Overexpression of Bcl-2 in the Q103 PC12 background resulted in an 88% rescue of viability from tebufenazide-induced expression of mutant Htt protein (Figure 16A). In comparison, the negative control Lac-Z demonstrated no rescue in comparison to the untransfected control, but could be rescued by the small molecule PDI inhibitor D13. Viral transduction increased Bcl-2 expression levels approximately 4-fold (Figure 16B). Bcl-2 overexpression rescued both cell viability, as well as cell morphology (Figure 17). Inhibition of mutant Htt-induced cell death by the classical anti-apoptotic protein indicates that induced Q103 PC12 cell death is mediated by apoptosis. Further studies using RNAi to deplete the levels of the pro-apoptotic proteins Bak and Bax confirmed the importance of apoptosis for mediating cell death in this cell line²¹.

Next, we wanted to determine whether the small molecule PDI inhibitors identified in the screen prevented Q103 Htt-mediated apoptosis by acting via the same pathway as Bcl-2. If the two factors acted independently, co-treatment should result in a higher level of rescue than Bcl-2 overexpression alone. If the two factors affect the same pathway however, no additional rescue should be observed upon co-treatment. The level of rescue observed with Bcl-2 overexpression was not increased by addition of the small molecule PDI inhibitor D13 (Figure 16A), suggesting that these two factors rescue mutant Htt-induced cell death via the same cellular pathway leading to inhibition of apoptosis.

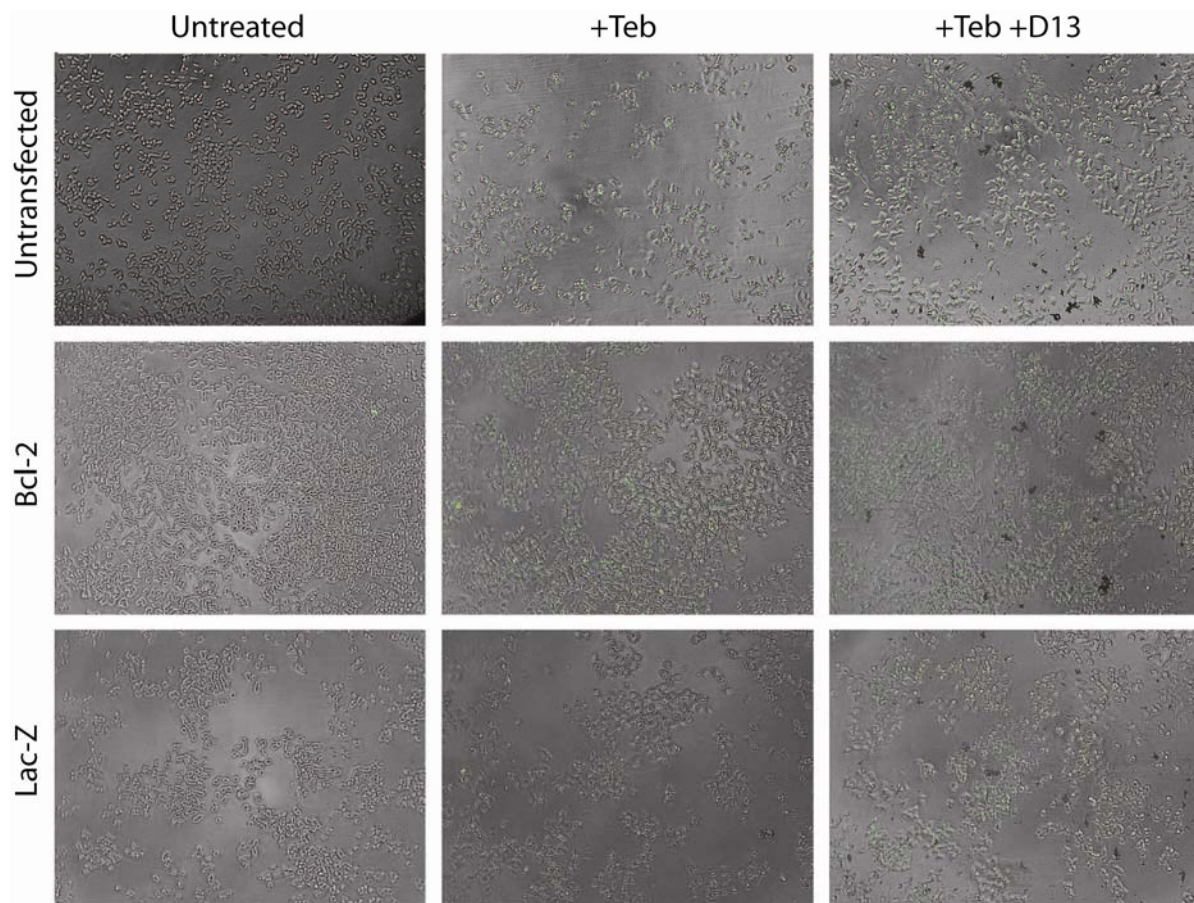


Figure 17. Overexpression of the anti-apoptotic protein Bcl-2 rescues morphology as well as viability from mutant Q103-HTT induced cell death. PC12 cells transfected with an inducible plasmid containing the pathogenic Q103-HTT mutant fused to GFP display shrunken morphology and cell death 48 h post-induction of protein expression with tebufenozide (Teb). Overexpression of the anti-apoptotic protein Bcl-2 rescues both cell numbers and normal cell morphology, indicating complete rescue from cell death. The level of rescue is similar to that seen upon treatment with the small molecule PDI inhibitor D13 (BBC7M13;10 μ g/mL).

Overexpression of PDI isoforms A1 and A3

Previous studies determined that the small molecule inhibitors of expanded polyglutamine Huntingtin (Q103-Htt) protein-induced cell death were acting via inhibition of protein disulfide isomerase (PDI) ²¹. As expression of Q103-Htt in the PC12 cell line was hypothesized to result in cell death by activation of a pro-apoptotic activity of PDI, we examined the possibility that the increased levels of PDI achieved by ectopic overexpression would be sufficient to induce cell death. PC12 cells containing an ecdysone-regulated pathogenic Q103-Htt fragment were transfected with Blasticidin-selectable plasmids expressing either PDI A1, PDI A3 or Lac-Z as negative control. Transfected cells were seeded into 384-well assay plates and selected with Blasticidin at 36 hours post- transfection. At 48 hours post-transfection, Alamar Blue, a viability dye, was added to wells. Alamar Blue is metabolized by live cells, and viability can be quantified by measurement of fluorescence of the metabolized dye. Cells were incubated with Alamar Blue for 18-24 hours before fluorescence quantification. Transfection with either PDI A1 or PDI A3 resulted in approximately 70% decrease in viability, compared to transfection with the LacZ negative control (Figure 18). As these cells are uninduced, this indicates that PDI toxicity is a downstream effect of mutant Htt expression. PDI-induced cell death could be dose-dependently rescued by treatment with the PDI inhibitors 141 and 16F16, thereby confirming that increased levels of PDI are sufficient to cause cell death in a cultured neuronal cell model and that these small molecules can rescue cells from PDI-induced cell death (Figure 18). Interestingly, this effect was not isoform-specific, suggesting a level of redundancy in the pro-apoptotic function of PDI.

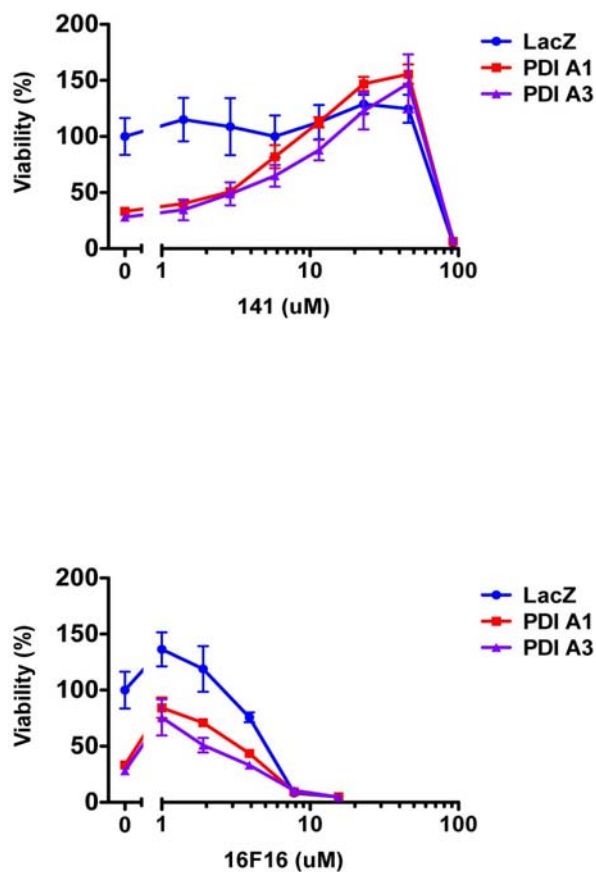


Figure 18. Overexpression of PDI leads to loss of cell viability in Q103-PC12 cells.

Transfection of Q103-PC12 cells (uninduced) with plasmids expressing either the PDI A1 or A3 isoform leads to 70% loss of cell viability (measured by Alamar Blue fluorescence 48 h post-transfection), compared to cells expressing the control protein Lac-Z. Loss of cell viability can be rescued dose-dependently upon treatment with the small molecule PDI inhibitors 141 or 16F16.

Mitochondrial outer membrane permeabilization (MOMP)

Previous work had demonstrated that during Q103 Htt-induced death, PDI re-localizes to accumulate on or near the mitochondria²¹. Further investigations lead to the discovery that purified PDI could induce mitochondrial outer membrane permeabilization (MOMP), a hallmark of apoptosis^{51,59}, in isolated mitochondria. To determine whether PDI-induced MOMP proceeded through the Bax/Bak-mediated apoptotic pathway⁶⁰, I isolated mitochondria from Q103 PC12 cells and the same cell line stably expressing Bcl-2, an anti-apoptotic protein able to antagonize Bax/Bak, to investigate Bcl-2's activity in a MOMP assay. While Q103 PC12 cells demonstrated strong activation of MOMP upon incubation with PDI, Bcl-2 overexpressing cells were resistant to PDI-induced MOMP (Figure 19). This result indicates that the mechanism by which PDI induces MOMP is an active pathway involving the BH3 domain-containing Bcl-2 family proteins, and further strengthens the connection between PDI and apoptotic cell death in this cell culture model of Huntington's disease.

Crystallization condition screening for the a domain of PDI isoforms A1 and A3

Screening efforts have identified several small molecule inhibitors of PDI's activation of mitochondrial-mediated apoptosis in the PC12 model of Huntington's disease, however the

mechanism by which these compounds bind to and inhibit PDI remained unclear. The ideal method to elucidate the binding mode of these small molecules would be co-crystallization with

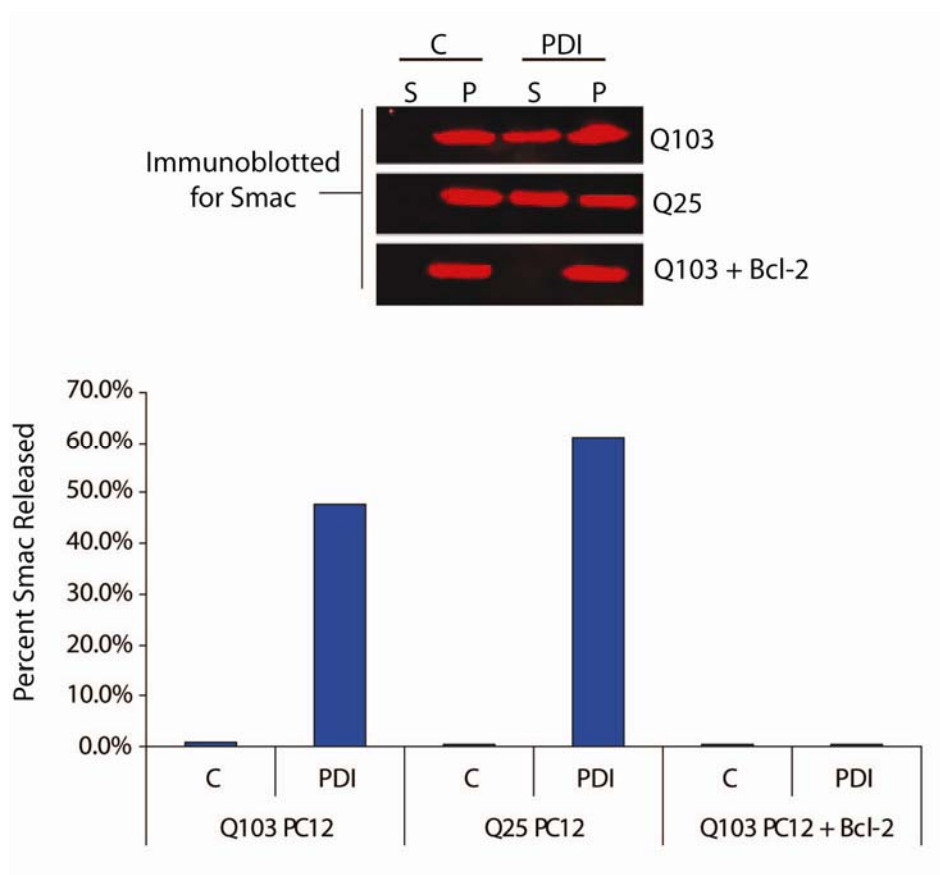


Figure 19. Overexpression of Bcl-2 rescues from PDI-induced MOMP in isolated mitochondria. PC12 cells transfected with inducible plasmids expressing either the pathogenic Q103-HTT or wild-type Q25-HTT huntingtin protein undergo mitochondrial outer membrane permeabilization (MOMP) upon 1.5 h incubation with 6U purified PDI. MOMP was assessed by release of the inner membrane protein Smac/DIABLO from the isolated mitochondria. Control samples, treated with 1mg/ml BSA, demonstrate no release of Smac, however PDI-treated samples show 50-60% release of Smac. Mitochondria isolated from Q103-PC12 cells overexpressing Bcl-2 show complete resistance to PDI-induced MOMP.

their target. However, as expression and purification tests of full-length PDI were not yielding protein of sufficient quality, we chose to test a catalytic domain of PDI, the a domain. As the catalytically active domains of PDI were identified as the likely mediators of PDI's pro-apoptotic activity²¹, we endeavored to identify favorable conditions for crystallization of the a domain of the PDI isoforms A1 and A3. Bacterial expression plasmids expressing His-tagged a domains of PDI A1 and A3 were created, expressed in BL-21 *E. coli* and the resulting protein was isolated via affinity purification followed by size-exclusion chromatography (see *Methods*) (Figure 20). These plasmids demonstrated moderate expression, and post-purification yields were on average 6mg/L culture. Some yield was lost to oligomers during size-exclusion chromatography, however the high concentrations required for crystallization were attainable, as the His-tagged a domains of PDI A1 and A3 were highly soluble, remaining in solution at concentrations of 120mg/mL. This protein may be able to be further concentrated, however higher concentrations were not tested. The purified proteins (at 40-100mg/ml) were seeded into sitting-drop crystallization trays containing commercially available crystallization solutions, utilizing a Mosquito nanoliter liquid handling system. However, after regular observation over a period of eight months, no crystals were detected in any of the conditions, likely due to the extremely high solubility of this protein domain.

Proteins with more stable structures are more likely to crystallize, therefore we attempted to stabilize the protein utilizing small molecules inhibitors of PDI. Several small molecules were tested, including phenylarsine oxide (PAO)⁶¹, 5,5'-Dithiobis(2-nitrobenzoic acid) (DNTB)⁶²,

and cystamine, which has been shown to ameliorate the phenotype of several animal models of HD⁶³⁻⁶⁵ and has demonstrated PDI inhibition in our PDI activity assays²¹. Unfortunately, the

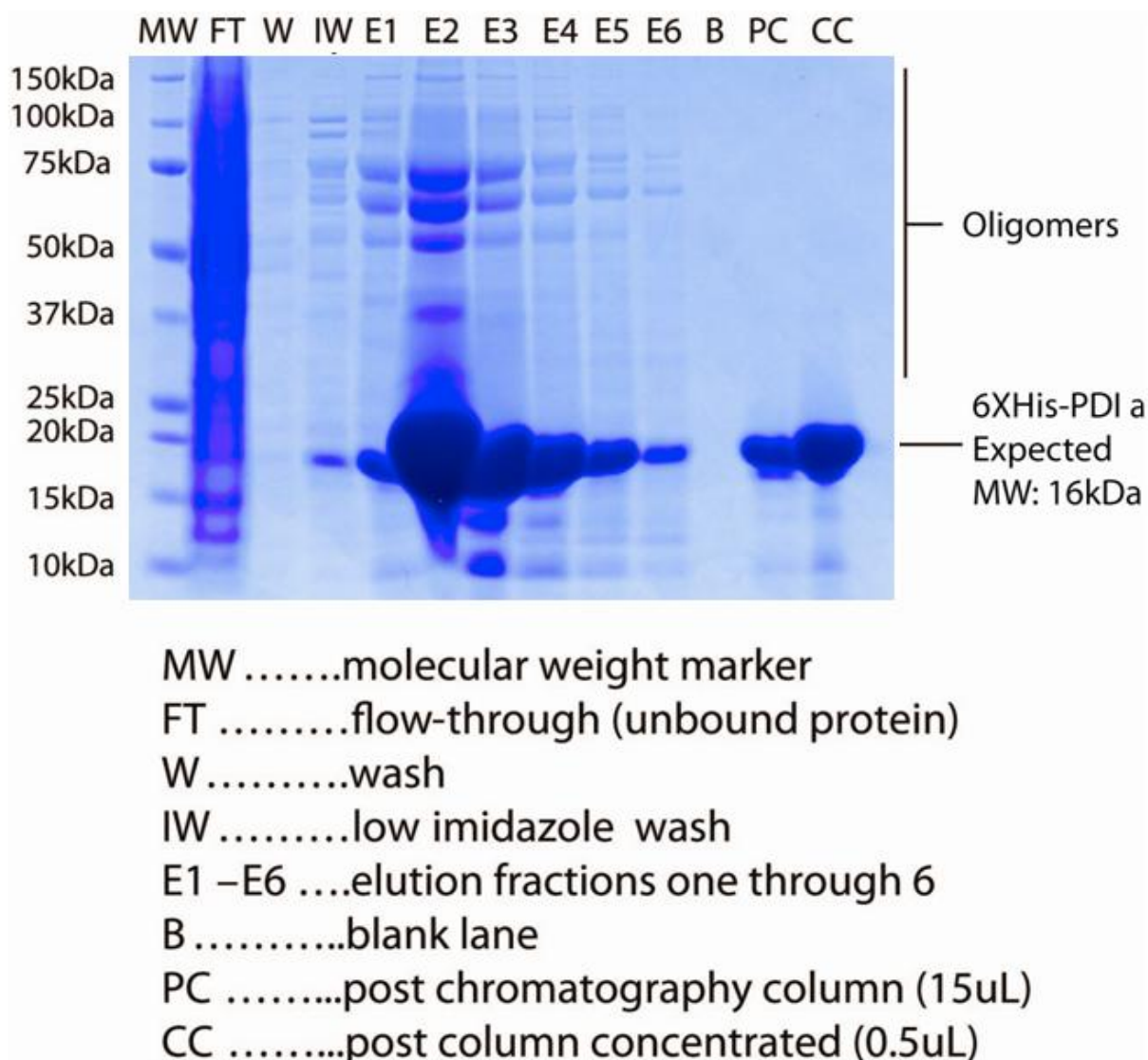


Figure 20. Expression and purification of the PDI A1 a domain for crystallization trials.

Samples from several stages of protein purification were separated on a SDS-PAGE gel which was Coomassie-stained. Protein was harvested from *E. coli* BL21 cells expressing the 6XHis-PDI A1 a domain (expected MW: 16kDa). Protein purification stages include lysis, affinity

purification on agarose-Ni²⁺ resin, size-exclusion chromatography and final concentration of purified protein for crystallization trials. Multiple oligomers of the PDI a domain are visible post affinity purification, however they are removed upon size-exclusion chromatography.

purified PDI a domains precipitated out of solution upon addition of dimethyl sulfoxide (DMSO) to final concentrations as low as 0.1%. As PAO demonstrated limited solubility in aqueous solutions, and could reach only moderate concentrations in DMSO (25mg/ml), it could not be used for crystallization trials. DNTB and cystamine were both highly soluble in aqueous conditions, and cystamine was selected for crystallization trials as it had shown strong activity in various PDI inhibition assays²¹.

The crystallization trays containing the commercially available solution sets Cryo I, Cryo II and Wizard II were selected for cystamine co-treatment crystallization trials, as these trays had shown the highest level of PDI a domain precipitation in past trials. PDI A1 a domain at 100mg/mL was co-seeded with 1mM cystamine into sitting drop crystallization trays. However, after regular observation over a period of six months, no crystal formation was detected. In fact, addition of cystamine appeared to solubilize the protein further, as some conditions which had resulted in protein precipitation in previous trials were now clear of precipitate, and no conditions showed enhanced precipitation. Although we have been unable to identify conditions favorable for crystallization of the a domains of the PDI A1 and A3 isoforms, the optimization of protein isolation conditions and the production of highly stable, soluble PDI constructs can be put to good use in future NMR experiments aimed at detecting PDI-ligand interactions.

Discussion

Defects in protein folding have been linked to many neurodegenerative diseases⁶⁶⁻⁶⁸, in particular diseases associated with expression of mutant polyglutamine proteins⁶⁹⁻⁷⁰. However, the connection between protein misfolding and neuronal cell death remains enigmatic. In order to investigate this mechanism, small molecule screen was performed in a cell culture model of Huntington's disease (HD). HD is caused by an expansion in the trinucleotide CAG repeat in exon 1 of the *huntingtin (HTT)* gene. The polyglutamine expansion (polyQ) causes the protein to misfold and aggregate, leading to neuronal cell death via an unknown mechanism⁷¹. Human and animal studies have implicated apoptosis as the death-inducing pathway^{16,72-73}, however little connection had been made between misfolded polyQ proteins and initiation of the apoptotic cascade.

Investigations into the targets of the small molecule inhibitors of mutant polyQ Htt-induced cell death identified protein disulfide isomerase (PDI) as their target. PDI has been extensively demonstrated to be one of the chaperone proteins involved in the endoplasmic reticulum (ER) protein folding quality control mechanisms^{26,74}. Induction of chaperone proteins, such as PDI, has been suggested to be beneficial in models of polyglutamine diseases^{16,75-77}. However our investigations propose that extended induction of pathways responding to protein misfolding results in initiation of a pro-apoptotic effect of PDI.

Expression of pathogenic polyQ-Htt was shown to result in concentration of PDI at the ER-mitochondrial junction points, where it may initiate apoptosis via a yet-undefined mechanism. *In vitro* evidence of a pro-apoptotic effect of PDI was demonstrated in isolated mitochondria, which underwent mitochondrial outer membrane permeabilization (MOMP) upon

incubation with purified PDI. MOMP is part of an intrinsic apoptosis-initiating cellular pathway; permeabilization of the mitochondrial membrane results in release of cytochrome c, Smac and other factors which activate caspases and initiate the apoptotic cascade⁴⁸. PDI-induced MOMP was prevented in mitochondria isolated from cells overexpressing the anti-apoptotic protein Bcl-2⁷⁸, indicating this effect was both specific and mediated via the classical mitochondrial outer membrane Bcl family proteins. Overexpression of Bcl-2 also rescued from cell death due to pathogenic polyQ-Htt expression, demonstrating the relevance of this pathway to HD.

As preliminary studies of the novel PDI inhibitors in a model of Alzheimer's disease appeared positive²¹, further study of this novel pro-apoptotic mechanism linking protein misfolding and cell death may prove to be of interest to a wide range of neurodegenerative diseases.

Methods

Cell lines and reagents

PC12 cells stably expressing a geneticin-selectable plasmid expressing Q103 Htt exon 1 fused to GFP under control of an ecdysone-regulated promoter, allowing induction of the toxic protein by addition of the ecdysone analog tebufenazide. Cells were propagated in PC12 cell media (DMEM (Invitrogen/#12430-047), 10% Cosmic Calf Serum (Fisher/#SH3008703), 2 mM L-glutamine (Invitrogen/#25030-081), and antibiotics (100,000 units penicillin/L MEM, 100 mg

streptomycin/L MEM) (Invitrogen/#15140-122) and 500 μ g/mL geneticin) at 37°C and 9.5% CO₂.

Q103 PC12 plate-based viability assay

Trypsinized Q103 PC12 cells were resuspended at 250,000 cells/mL in PC12 cell media. 40 μ L/well of cell suspension was pipetted into 384-well assay plates (Corning/#3712). Cells were incubated with desired treatment for two days, after which the viability dye Alamar Blue (Invitrogen/#DAL1100) was added to assay plates to a final concentration of 10%. Cells were incubated with Alamar Blue for an additional 16-24 hours. Alamar Blue fluorescence was read on a PerkinElmer Victor³ platreader at 590nm (530nm excitation, 0.1 second integration). Cell viability was normalized to control cells.

PDI overexpression

PC12-Q103 cells (2×10^6 cells) were transfected with pLenti6 plasmid (Invitrogen/#V496-10) expressing either PDI A1, PDI A3 or LacZ using the Amaxa nucleofection system (Amaxa nucleofection reagent V, program U-29). Immediately following transfection, cells were seeded into 384-well assay plates (10,000 cells/well) and incubated for 36 hours (37°C, 9.5% CO₂) prior to selection with Blasticidin (5 μ g/mL) and addition of a 2-fold, 7-point dilution of each compound into triplicate assay wells. Alamar Blue was added to a final concentration of 10% and incubated for an additional 18-24 hours. Cell viability was scored by Alamar Blue

fluorescence. Statistical significance of compound rescue was determined by ANOVA and Dunnett's post hoc comparison test at 0.01 confidence.

Bcl-2 overexpression

Cells (PC12-Q103) were transfected with pLenti6-Bcl-2 or pLenti6-LacZ cDNA via Amaxa nucleofection (5×10^5 cells, Amaxa nucleofection reagent V, program U-23 or G-13) or lentiviral infection (two serial spinning infections, 10 μ l polybrene, 1.5hrs, 2,250rpm, 37°C). Cells were selected for 1-2 weeks with Blasticidin (5 μ g/ml) prior to viability assays, which were performed as described previously.

Mitochondrial isolation

Mitochondria were isolated from 1×10^7 cells per experiment. Cells were harvested by trypsinization, centrifugation at 1,000rpm for 5 minutes, washed once in 10mL PBS and centrifuged again. Pellet was resuspended in 250 μ L extraction buffer (250mM sucrose, 0.1% bovine serum albumin, 10mM HEPES (pH 7.5), 5mM KCl, 1.5mM MgCl₂, 1mM EGTA and 1mM EDTA), and cells were allowed to swell on ice for 3 minutes. Cells were lysed by trituration through a 30G needle for approximately 15 strokes. Samples were incubated on ice for 15 minutes and then centrifuged at 700rpm for 5 minutes to pellet unlysed cells and nuclei. Supernatant was transferred to a fresh eppendorf tube and centrifuged at 10,000rpm for 15 minutes at 4°C to pellet the mitochondria. Pellet was washed in 300 μ L extraction buffer and

resuspended in 100 μ L of extraction buffer. Mitochondrial concentration was determined by absorbance at 280nm.

MOMP assay

Isolated mitochondria were normalized to 12 μ g/ μ L, and 17 μ L of mitochondrial suspension (~200 μ g) were utilized per sample. For samples at a different pH than 7.5, mitochondrial aliquots were centrifuged at 10,000rpm for 15 minutes at 4°C, and resuspended in extraction buffer at desired pH. To each sample, either BSA (1mg/mL) or PDI (6U) were added, volumes were normalized with extraction buffer. Samples were incubated in a 36°C water bath for 90 minutes. After incubation with enzyme, samples were centrifuged at 10,000rpm for 15 minutes at 4°C. Supernatants were transferred to a fresh centrifuge tube containing 10 μ L 5X SDS-PAGE sample buffer. To the pellet, 40 μ L of 1X SDS-PAGE sample buffer was added. Samples were incubated at RT for 15 minutes prior to boiling to allow thorough solubilization of the lipid-rich mitochondrial pellets. Samples were separated on 4-12% Bis-Tris NuPage gel in 1X NuPage MES running buffer. Transfer and immunoblotting were performed as described earlier. Degree of MOMP was calculated by Western blot for Smac released from the mitochondrial pellet (P) into the supernatant (S). Antibodies: mouse anti-Smac/DIABLO (BD Biosciences/#612244)(1:1,000).

Expression and purification of PDI A1 and A3 a' domains

BL-21 DE3 *E. coli* cells (Stratagene/#230132) were transformed with pET-15b plasmids (EMD Biosciences/#69661-3) containing the catalytic a domain of either PDI A1 or PDI A3. Transformed cells were grown in liquid culture at 37°C to an O.D. of approximately 0.4, after which the temperature was decreased to 25°C. Once the culture reached O.D. of 0.6, protein production was induced by adding Isopropyl β -D-1-thiogalactopyranoside (IPTG) to a final concentration of 1mM. After overnight induction, the cells were harvested by centrifugation at 4,000 rpm for 25 minutes at 4°C. The pellet was resuspended in 35mL RS buffer (50mM Tris-HCl, pH 8.0, 150mM NaCl and 2mM β -mercaptoethanol) per liter of culture, and magnesium chloride was added to a final concentration of 5mM. The cell suspension was sonicated on ice (tip limit 8, 50% duty cycle, 10-15 cycles of 20 seconds on and 20 seconds pause). Insoluble materials in the cell lysate were cleared by centrifugation at 13,000 rpm for 30 minutes at 4°C. Cleared lysates were added to 2mL of Ni²⁺-agarose bead slurry (Sigma/#P6611) washed with 10mL RS buffer and rotated for 1 hour at 4°C to permit binding of the His-tagged protein to the Ni²⁺ beads. After batch binding, beads were separated from lysate using a gravity column. Beads were washed with 40mL of RS buffer, and 20mL Low Imidazole Buffer (RS buffer + 10mM imidazole) to remove loosely bound proteins. His-tagged protein was eluted with Elution Buffer (RS buffer + 250mM imidazole); final volumes ranged from 3mL to 7mL of eluted protein solution.

Eluted protein solution was concentrated to approximately 4mL using centrifugal filtration devices with a molecular weight cut-off of 10kDa (Millipore/#42406) prior to loading onto a S300 column equilibrated with Column Buffer (20mM tris-HCl, pH 8.0 and 150mM NaCl). Fractions containing the protein of interest were collected, and purified protein solution

was concentrated to the desired level utilizing larger volume centrifugal filter units with a 10kDa MW-cutoff (Fisher/#2997).

Crystallization condition screening

Commercially available crystallization solutions were utilized: Index (Hampton Research/#HR2-144), SaltRx (Hampton Research/#HR2-108), Natrix (Hampton Research/#HR2-116), PEG/Ion Screen (Hampton Research/#HR2-126), PEG/Ion Screen 2 (Hampton Research/#HR2-098), Crystal Screen (Hampton Research/#HR2-110), Crystal Screen 2 (Hampton Research/#HR2-112), Crystal Screen Cryo (Hampton Research/#HR2-122), Crystal Screen Lite (Hampton Research/#HR2-128), Wizard I (Emerald BioSystems/#EBS-WIZ-1), Wizard II (Emerald BioSystems/#EBS-WIZ-2), Cryo I (Emerald BioSystems/#EBS-CRYO-1), Cryo II (Emerald BioSystems/#EBS-CRYO-2) JCSG Core Suite I (Qiagen/#130924) and JCSG Core Suite II (Qiagen#130925). These sets total 918 crystallization conditions, although they may not all be unique. Crystallization solutions were formatted into 96-well plates, and 80 μ L per well was utilized for screening in 96-well Crystal Ex plates (Corning/#3785). Using an automated nanoliter pipetting system (mosquito, TTP Labtech), for each well 0.5 μ L of purified protein was combined with 0.5 μ L well solution and deposited into the drop well of sitting drop crystallization. For samples including cystamine, cystamine dihydrochloride (Sigma/#C121509) was added to the protein solution for a final concentration of 1mM. Plates were sealed, incubated at 20°C, and observed regularly over a period of six to eight months.

References

1. Varma, H., Lo, D.C. & Stockwell, B.R. High throughput screening for neurodegeneration and complex disease phenotypes. *Comb Chem High Throughput Screen* **11**, 238-248 (2008).
2. Tobin, A.J. & Signer, E.R. Huntington's disease: the challenge for cell biologists. *Trends Cell Biol* **10**, 531-536 (2000).
3. Nance, M.A., Mathias-Hagen, V., Breningstall, G., Wick, M.J. & McGlennen, R.C. Analysis of a very large trinucleotide repeat in a patient with juvenile Huntington's disease. *Neurology* **52**, 392-394 (1999).
4. Walker, F.O. Huntington's disease. *Lancet* **369**, 218-228 (2007).
5. Ross, C.A. Huntington's disease: new paths to pathogenesis. *Cell* **118**, 4-7 (2004).
6. Nasir, J., *et al.* Targeted disruption of the Huntington's disease gene results in embryonic lethality and behavioral and morphological changes in heterozygotes. *Cell* **81**, 811-823 (1995).
7. Cattaneo, E., Zuccato, C. & Tartari, M. Normal huntingtin function: an alternative approach to Huntington's disease. *Nat Rev Neurosci* **6**, 919-930 (2005).
8. Velier, J., *et al.* Wild-type and mutant huntingtins function in vesicle trafficking in the secretory and endocytic pathways. *Exp Neurol* **152**, 34-40 (1998).
9. Caviston, J.P. & Holzbaur, E.L. Huntingtin as an essential integrator of intracellular vesicular trafficking. *Trends Cell Biol* **19**, 147-155 (2009).
10. Hoffner, G., Kahlem, P. & Djian, P. Perinuclear localization of huntingtin as a consequence of its binding to microtubules through an interaction with beta-tubulin: relevance to Huntington's disease. *J Cell Sci* **115**, 941-948 (2002).
11. Varma, H., Yamamoto, A., Sarantos, M.R., Hughes, R.E. & Stockwell, B.R. Mutant huntingtin alters cell fate in response to microtubule depolymerization via the GEF-H1-RhoA-ERK pathway. *J Biol Chem* **285**, 37445-37457 (2010).
12. Cha, J.H. Transcriptional signatures in Huntington's disease. *Prog Neurobiol* **83**, 228-248 (2007).
13. Zuchner, T. & Brundin, P. Mutant huntingtin can paradoxically protect neurons from death. *Cell Death Differ* **15**, 435-442 (2008).
14. Tauber, E., *et al.* Functional gene expression profiling in yeast implicates translational dysfunction in mutant huntingtin toxicity. *J Biol Chem* **286**, 410-419 (2011).
15. Gines, S., Ivanova, E., Seong, I.S., Saura, C.A. & MacDonald, M.E. Enhanced Akt signaling is an early pro-survival response that reflects N-methyl-D-aspartate receptor activation in Huntington's disease knock-in striatal cells. *J Biol Chem* **278**, 50514-50522 (2003).
16. Kiechle, T., *et al.* Cytochrome C and caspase-9 expression in Huntington's disease. *Neuromolecular Med* **1**, 183-195 (2002).
17. Hickey, M.A. & Chesselet, M.F. Apoptosis in Huntington's disease. *Prog Neuropsychopharmacol Biol Psychiatry* **27**, 255-265 (2003).
18. Almeida, S., Sarmiento-Ribeiro, A.B., Januario, C., Rego, A.C. & Oliveira, C.R. Evidence of apoptosis and mitochondrial abnormalities in peripheral blood cells of Huntington's disease patients. *Biochem Biophys Res Commun* **374**, 599-603 (2008).

19. Teles, A.V., *et al.* Increase in bax expression and apoptosis are associated in Huntington's disease progression. *Neurosci Lett* **438**, 59-63 (2008).
20. Garcia-Martinez, J.M., *et al.* BH3-only proteins Bid and Bim(EL) are differentially involved in neuronal dysfunction in mouse models of Huntington's disease. *J Neurosci Res* **85**, 2756-2769 (2007).
21. Hoffstrom, B.G., *et al.* Inhibitors of protein disulfide isomerase suppress apoptosis induced by misfolded proteins. *Nat Chem Biol* **6**, 900-906 (2010).
22. Aiken, C.T., Tobin, A.J. & Schweitzer, E.S. A cell-based screen for drugs to treat Huntington's disease. *Neurobiol Dis* **16**, 546-555 (2004).
23. Gruber, C.W., Cemazar, M., Heras, B., Martin, J.L. & Craik, D.J. Protein disulfide isomerase: the structure of oxidative folding. *Trends Biochem Sci* **31**, 455-464 (2006).
24. Wilkinson, B. & Gilbert, H.F. Protein disulfide isomerase. *Biochim Biophys Acta* **1699**, 35-44 (2004).
25. Hatahet, F. & Ruddock, L.W. Protein disulfide isomerase: a critical evaluation of its function in disulfide bond formation. *Antioxid Redox Signal* **11**, 2807-2850 (2009).
26. Nishikawa, S., Brodsky, J.L. & Nakatsukasa, K. Roles of molecular chaperones in endoplasmic reticulum (ER) quality control and ER-associated degradation (ERAD). *J Biochem* **137**, 551-555 (2005).
27. Vembar, S.S. & Brodsky, J.L. One step at a time: endoplasmic reticulum-associated degradation. *Nat Rev Mol Cell Biol* **9**, 944-957 (2008).
28. Ron, D. & Walter, P. Signal integration in the endoplasmic reticulum unfolded protein response. *Nat Rev Mol Cell Biol* **8**, 519-529 (2007).
29. Harding, H.P., Calton, M., Urano, F., Novoa, I. & Ron, D. Transcriptional and translational control in the Mammalian unfolded protein response. *Annu Rev Cell Dev Biol* **18**, 575-599 (2002).
30. Travers, K.J., *et al.* Functional and genomic analyses reveal an essential coordination between the unfolded protein response and ER-associated degradation. *Cell* **101**, 249-258 (2000).
31. Atkin, J.D., *et al.* Endoplasmic reticulum stress and induction of the unfolded protein response in human sporadic amyotrophic lateral sclerosis. *Neurobiol Dis* **30**, 400-407 (2008).
32. Wang, M., *et al.* Essential role of the unfolded protein response regulator GRP78/BiP in protection from neuronal apoptosis. *Cell Death Differ* **17**, 488-498 (2010).
33. Ferrari, D.M. & Soling, H.D. The protein disulphide-isomerase family: unravelling a string of folds. *Biochem J* **339** (Pt 1), 1-10 (1999).
34. Darby, N.J., Kemmink, J. & Creighton, T.E. Identifying and characterizing a structural domain of protein disulfide isomerase. *Biochemistry* **35**, 10517-10528 (1996).
35. Darby, N.J., van Straaten, M., Penka, E., Vincentelli, R. & Kemmink, J. Identifying and characterizing a second structural domain of protein disulfide isomerase. *FEBS Lett* **448**, 167-172 (1999).
36. Kemmink, J., Darby, N.J., Dijkstra, K., Nilges, M. & Creighton, T.E. The folding catalyst protein disulfide isomerase is constructed of active and inactive thioredoxin modules. *Curr Biol* **7**, 239-245 (1997).

37. Pineskoski, A., *et al.* Molecular characterization of the principal substrate binding site of the ubiquitous folding catalyst protein disulfide isomerase. *J Biol Chem* **279**, 10374-10381 (2004).
38. Tian, G., Xiang, S., Noiva, R., Lennarz, W.J. & Schindelin, H. The crystal structure of yeast protein disulfide isomerase suggests cooperativity between its active sites. *Cell* **124**, 61-73 (2006).
39. Kemmink, J., Darby, N.J., Dijkstra, K., Nilges, M. & Creighton, T.E. Structure determination of the N-terminal thioredoxin-like domain of protein disulfide isomerase using multidimensional heteronuclear ¹³C/¹⁵N NMR spectroscopy. *Biochemistry* **35**, 7684-7691 (1996).
40. Kemmink, J., Darby, N.J., Dijkstra, K., Scheek, R.M. & Creighton, T.E. Nuclear magnetic resonance characterization of the N-terminal thioredoxin-like domain of protein disulfide isomerase. *Protein Sci* **4**, 2587-2593 (1995).
41. Kemmink, J., *et al.* The structure in solution of the b domain of protein disulfide isomerase. *J Biomol NMR* **13**, 357-368 (1999).
42. Nguyen, V.D., *et al.* Alternative conformations of the x region of human protein disulphide-isomerase modulate exposure of the substrate binding b' domain. *J Mol Biol* **383**, 1144-1155 (2008).
43. Denisov, A.Y., *et al.* Solution structure of the bb' domains of human protein disulfide isomerase. *FEBS J* **276**, 1440-1449 (2009).
44. Munro, S. & Pelham, H.R. A C-terminal signal prevents secretion of luminal ER proteins. *Cell* **48**, 899-907 (1987).
45. Turano, C., Coppari, S., Altieri, F. & Ferraro, A. Proteins of the PDI family: unpredicted non-ER locations and functions. *J Cell Physiol* **193**, 154-163 (2002).
46. Rigobello, M.P., Donella-Deana, A., Cesaro, L. & Bindoli, A. Distribution of protein disulphide isomerase in rat liver mitochondria. *Biochem J* **356**, 567-570 (2001).
47. Yoshimori, T., *et al.* Protein disulfide-isomerase in rat exocrine pancreatic cells is exported from the endoplasmic reticulum despite possessing the retention signal. *J Biol Chem* **265**, 15984-15990 (1990).
48. Jiang, X. & Wang, X. Cytochrome C-mediated apoptosis. *Annu Rev Biochem* **73**, 87-106 (2004).
49. Dlugosz, P.J., *et al.* Bcl-2 changes conformation to inhibit Bax oligomerization. *EMBO J* **25**, 2287-2296 (2006).
50. Dejean, L.M., Martinez-Caballero, S., Manon, S. & Kinnally, K.W. Regulation of the mitochondrial apoptosis-induced channel, MAC, by BCL-2 family proteins. *Biochim Biophys Acta* **1762**, 191-201 (2006).
51. Chipuk, J.E. & Green, D.R. How do BCL-2 proteins induce mitochondrial outer membrane permeabilization? *Trends Cell Biol* **18**, 157-164 (2008).
52. Leber, B., Lin, J. & Andrews, D.W. Embedded together: the life and death consequences of interaction of the Bcl-2 family with membranes. *Apoptosis* **12**, 897-911 (2007).
53. Gupta, S., *et al.* Mechanisms of ER Stress-Mediated Mitochondrial Membrane Permeabilization. *Int J Cell Biol* **2010**, 170215 (2010).
54. Kouroku, Y., *et al.* Polyglutamine aggregates stimulate ER stress signals and caspase-12 activation. *Hum Mol Genet* **11**, 1505-1515 (2002).

55. Nishitoh, H., *et al.* ASK1 is essential for endoplasmic reticulum stress-induced neuronal cell death triggered by expanded polyglutamine repeats. *Genes Dev* **16**, 1345-1355 (2002).
56. Duennwald, M.L. & Lindquist, S. Impaired ERAD and ER stress are early and specific events in polyglutamine toxicity. *Genes Dev* **22**, 3308-3319 (2008).
57. Yang, H., *et al.* Huntingtin interacts with the cue domain of gp78 and inhibits gp78 binding to ubiquitin and p97/VCP. *PLoS One* **5**, e8905 (2010).
58. Nundlall, S., *et al.* An unfolded protein response is the initial cellular response to the expression of mutant matrilin-3 in a mouse model of multiple epiphyseal dysplasia. *Cell Stress Chaperones* **15**, 835-849 (2010).
59. Dewson, G. & Kluck, R.M. Mechanisms by which Bak and Bax permeabilise mitochondria during apoptosis. *J Cell Sci* **122**, 2801-2808 (2009).
60. Lomonosova, E. & Chinnadurai, G. BH3-only proteins in apoptosis and beyond: an overview. *Oncogene* **27 Suppl 1**, S2-19 (2008).
61. Root, P., Sliskovic, I. & Mutus, B. Platelet cell-surface protein disulphide-isomerase mediated S-nitrosoglutathione consumption. *Biochem J* **382**, 575-580 (2004).
62. Ryser, H.J., Levy, E.M., Mandel, R. & DiSciullo, G.J. Inhibition of human immunodeficiency virus infection by agents that interfere with thiol-disulfide interchange upon virus-receptor interaction. *Proc Natl Acad Sci U S A* **91**, 4559-4563 (1994).
63. Dedeoglu, A., *et al.* Therapeutic effects of cystamine in a murine model of Huntington's disease. *J Neurosci* **22**, 8942-8950 (2002).
64. Karpuj, M.V., *et al.* Prolonged survival and decreased abnormal movements in transgenic model of Huntington disease, with administration of the transglutaminase inhibitor cystamine. *Nat Med* **8**, 143-149 (2002).
65. Van Raamsdonk, J.M., *et al.* Cystamine treatment is neuroprotective in the YAC128 mouse model of Huntington disease. *J Neurochem* **95**, 210-220 (2005).
66. Kupfer, L., Hinrichs, W. & Groschup, M.H. Prion protein misfolding. *Curr Mol Med* **9**, 826-835 (2009).
67. Tan, J.M., Wong, E.S. & Lim, K.L. Protein misfolding and aggregation in Parkinson's disease. *Antioxid Redox Signal* **11**, 2119-2134 (2009).
68. Nakamura, T. & Lipton, S.A. Cell death: protein misfolding and neurodegenerative diseases. *Apoptosis* **14**, 455-468 (2009).
69. Kang, S. & Hong, S. Molecular pathogenesis of spinocerebellar ataxia type 1 disease. *Mol Cells* **27**, 621-627 (2009).
70. Williams, A.J. & Paulson, H.L. Polyglutamine neurodegeneration: protein misfolding revisited. *Trends Neurosci* **31**, 521-528 (2008).
71. Montoya, A., Price, B.H., Menear, M. & Lepage, M. Brain imaging and cognitive dysfunctions in Huntington's disease. *J Psychiatry Neurosci* **31**, 21-29 (2006).
72. Thomas, L.B., *et al.* DNA end labeling (TUNEL) in Huntington's disease and other neuropathological conditions. *Exp Neurol* **133**, 265-272 (1995).
73. Ciammola, A., *et al.* Increased apoptosis, Huntingtin inclusions and altered differentiation in muscle cell cultures from Huntington's disease subjects. *Cell Death Differ* **13**, 2068-2078 (2006).
74. Appenzeller-Herzog, C. & Ellgaard, L. The human PDI family: versatility packed into a single fold. *Biochim Biophys Acta* **1783**, 535-548 (2008).

75. Arawaka, S., Machiya, Y. & Kato, T. Heat shock proteins as suppressors of accumulation of toxic prefibrillar intermediates and misfolded proteins in neurodegenerative diseases. *Curr Pharm Biotechnol* **11**, 158-166 (2010).
76. Nagai, Y., Fujikake, N., Popiel, H.A. & Wada, K. Induction of molecular chaperones as a therapeutic strategy for the polyglutamine diseases. *Curr Pharm Biotechnol* **11**, 188-197 (2010).
77. Sittler, A., *et al.* Geldanamycin activates a heat shock response and inhibits huntingtin aggregation in a cell culture model of Huntington's disease. *Hum Mol Genet* **10**, 1307-1315 (2001).
78. Reed, J.C. Double identity for proteins of the Bcl-2 family. *Nature* **387**, 773-776 (1997).

Chapter 4. Conclusions and Future Directions

This thesis presents the use of small molecule probes in the investigation of the neurodegenerative diseases Spinal Muscular Atrophy and Huntington's Disease. Work performed on Spinal Muscular Atrophy identified a small molecule upregulator of the disease gene product, Survival of Motor Neuron (SMN). Investigation into its mechanism of action revealed regulation of SMN protein levels by the small GTPase Ras and the nutrient-sensing translational regulator mammalian target of rapamycin (mTOR) kinase. Work performed on Huntington's Disease (HD) were aimed at validation of the mechanism of action of a HD-mediated cell death inhibitor.

I. Spinal Muscular Atrophy

Ia. Summary

The neurodegenerative disease Spinal Muscular Atrophy is caused by decreased levels of the Survival of Motor Neuron protein, however the cellular pathways regulating its levels are largely undefined. Therefore we developed, optimized and implemented a screen to identify novel small molecule upregulators of the Survival of Motor Neuron protein. The optimal hit from this screen, Chemical Upregulator of SMN-1 (cuspin-1), was utilized as a chemical probe in efforts to identify the cellular pathways being modulated resulting in increased SMN protein levels. Mechanistic studies revealed modulation of Ras signaling, and confirmatory studies lead to the discovery that expression of an oncogenic isoform of Ras resulted in a robust three-fold upregulation of

SMN protein levels via increased translation. The involvement of altered translation led us to investigate the role of the mammalian target of rapamycin (mTOR) in this Ras-mediated effect, and identified mTOR as an important positive regulator of SMN protein levels.

Ib. Significance

Neurodegenerative diseases tend to be inherently difficult to study, due to a general inability to acquire the disease cells for experimentation as well as the complex nature of neuronal systems. Reductionist methods, such as utilizing cell culture models of disease states, can offer great insight into the cellular mechanisms underlying disease. We have used fibroblasts from human SMA patients to identify novel small molecules and pathways regulating the levels of the disease gene product, SMN protein. While preliminary studies suggest that these modulators may act positively in the disease tissue, motor neurons, more work is needed to conclusively determine their effect. Additionally, as increased Ras signaling has been shown to rescue neuronal cell death due to various neurodegenerative insults, identifying the downstream effector pathways of Ras responsible for SMN protein upregulation may identify cellular factors that could be modulated to benefit not only the SMA phenotype, but other neurodegenerative diseases as well.

Ic. Future Directions

The future directions for this project are two-pronged: first, determine the relevance of these pathways in motor neurons and second, to define the mechanism by

which Ras activation upregulates SMN protein levels. To determine the relevance of these pathways, we would like to test the effect of cuspin-1 and expression of Ras isoforms on the tissue of interest in Spinal Muscular Atrophy, namely human motor neurons. Due to the development of robust methods for the differentiation of motor neurons from embryonic stem cells, we are hopeful that we may be able to test our hypothesis in SMA motor neurons as well. As expression of Ras has been shown to be beneficial in various models of neuronal outgrowth and damage¹⁻², it is possible that activation of Ras could rescue SMA-induced neuronal outgrowth defects. However, it will require significant effort to identify whether these effects are due to re-establishment of sufficient levels of SMN protein, or due to an alternate mechanism.

If these mechanisms prove to be beneficial to motor neuron outgrowth in culture, we may endeavor to test the effect of Ras pathway activation in mouse models of SMA. As cuspin-1 has not shown activity in mouse cells, it is unlikely that it will prove functional in an animal model. Therefore, activation of Ras via expression of an oncogenic isoform will likely prove to be the preferable method for testing our hypothesis. As organism-wide expression of oncogenic Ras would likely cause significant undesired side effects³, a mouse line expressing activated Ras in a neuron-specific manner, such as described Heumann and colleagues² would be preferred. Observing the phenotype of mice generated by crossing a line expressing an activated isoform of Ras in a neuron-specific manner with an SMA mouse model should provide valuable information on the efficacy of Ras activation in rescuing the motor neuron degeneration evident in SMA.

Secondly, we would like to investigate the mechanism by which cuspin-1 activates Ras as well as how increased Ras signaling results in SMN protein upregulation. Therefore, identification of the target of cuspin-1 would be of great interest. One method by which to identify cuspin-1's target is via affinity purification, utilizing click chemistry. Click chemistry, also known as copper-mediated Huisgen 1,3,-dipolar cycloaddition ⁴, allows a small molecule with a terminal alkyne moiety to be selectively attacked in a bio-orthogonal manner by an azide-coupled affinity tag. For target identification, the small molecule of interest must be first modified to include a terminal alkyne. While modifying the structure of cuspin-1 without loss of activity has been problematic, some degree of freedom in changing the molecular makeup has been identified at the methyl group. Alteration of this functional group to an ethynyl group may provide the needed 'handle' without loss of efficacy. The alkyne-modified compound can then be incubated with cell lysate to allow binding to the target, and the cyclo-addition reaction is performed to bind the target protein-small molecule complex covalently to the affinity tag. The tag can then be affinity purified, and the proteins remaining with the tag, presumably including the target, can be identified by mass spectrometry. This technique has been utilized successfully by members of our group ⁵ as well as others ⁶⁻⁷.

As we have identified cuspin-1 as an activator of Ras signaling, potential targets include Ras guanine nucleotide exchange factors (Ras-GEF) and Ras GTPase activating proteins (Ras-GAP), which activate ⁸ and inactivate Ras signaling ⁹⁻¹⁰, respectively. However, activation of proteins involved in upstream signaling from various growth factors is also a possibility.

If a potential target is found via click chemistry, follow-up studies will be required to confirm the compound's mechanism of action. These include knockdown and overexpression studies in order to determine that the potential target has the relevant cellular activity, and confirmation of direct binding of cuspin-1 to the purified target protein via *in vitro* binding assays.

We would also like to address the issue of specificity for SMN protein upregulation upon Ras activation. To gain a global view of the mRNAs whose translational activities are affected by either cuspin-1 or oncogenic Ras expression, we will perform a polysomal microarray, in conjunction with the Sonenberg Laboratory at McGill University. This technique involves sucrose gradient fractionation of cell lysates in order to separate mRNAs bound by one or two ribosomes, indicating they are being translated at a low rate, from mRNAs bound by several ribosomes (termed a polysome), which are producing multiple copies of the protein product. The mRNAs in each fraction can then be extracted and identified by microarray. The shift of an mRNA from the low-ribosomal fraction to a high-ribosomal fraction upon treatment with cuspin-1 or Ras expression would indicate an increase in its translation rate, and we can thereby identify, in a global manner, the mRNAs targeted by cuspin-1 or oncogenic Ras.

Although preliminary work attempting to identify the relevant downstream Ras effector utilizing small molecule inhibitors and overexpression studies has been negative to date, alternate methods may yet prove successful. Creation of Ras point mutants, which have been demonstrated to inhibit specific Ras-effector binding events, while preserving others¹¹, may prove informative. The Ras interacting partners that can be discriminated between by this method are Raf, PI3K and Ral-GEF. Raf is essential for

activation of the Raf/MEK/Erk pathway, however preliminary studies indicate that this is not the relevant pathway leading to SMN protein upregulation. The Ras^{E37G} mutant is unable to interact with and activate Raf or PI3K, but maintains Ral-GEF binding. The Ras^{T35S} mutation inhibits activation of PI3K or Ral-GEF, but can activate Raf. Lastly, the Ras^{Y40C} mutant activates PI3K, but not Raf or Ral-GEF. While these reagents may not be perfect, they will help determine the role, if any, that these pathways play in Ras-mediated upregulation of SMN protein levels.

Several lines of investigation have pointed towards an important role for translational regulation in SMN protein upregulation, including the identification that the upregulation is caused by an increase in translation rate and the involvement of the translational regulator mTOR. Therefore, another potential mediator of SMN upregulation is the eukaryotic initiation factor 4E (eIF4E), a major regulator of cap dependent translation¹². The activity level of eIF4E is regulated in large part by its availability¹³, therefore we will overexpress eIF4E and determine its effect on SMN protein levels. To determine whether eIF4E is the downstream effector of Ras activation which results in upregulation of SMN protein levels, we will overexpress the translational repressor eIF4E-binding protein 1 (4E-BP1), which binds to eIF4E and thereby reduces its effective cellular concentration¹⁴. If overexpression of 4E-BP1 prevents the increase in SMN protein levels upon Ras activation, this will suggest that eIF4E is a relevant downstream effector leading to upregulation of SMN protein levels.

II. Huntington's Disease

IIa. Summary

Huntington's Disease (HD) is caused by an expanded polyglutamine (polyQ) repeat in the N-terminus of the *huntingtin* (*HTT*) gene, resulting in striatal cell death by an unknown mechanism. A screen for small molecule inhibitors of polyQ Htt-induced cell death discovered several compounds which could rescue mutant huntingtin-induced cell death in a cell culture model of HD. Affinity purification studies identified the target of the compounds as the oxidoreductase protein disulfide isomerase (PDI), however mechanisms connecting PDI to cell death were lacking. Identification of re-localization of PDI to the membrane junctions between the endoplasmic reticulum and the mitochondria suggested a mitochondrial function for this normally ER-resident protein. The application of purified PDI to isolated mitochondria was determined to result in mitochondrial outer membrane permeabilization (MOMP), an initiating step in mitochondrially-mediated apoptosis. We utilized the anti-apoptotic protein Bcl-2 to validate the role of apoptosis in polyQ Htt-induced death in our HD cell culture model, as well as in PDI-induced MOMP in isolated mitochondria. Studies aimed at determining the binding mode of the small molecule cell death inhibitors to PDI were initiated, however as we have been unable to crystallize PDI to date, we have turned to solution NMR for these studies.

IIb. Significance

Many neurodegenerative diseases have been linked to expression of misfolded mutant proteins with expanded polyglutamine regions, however the mechanism by which these mutant proteins result in cell death remains unclear. We have identified and validated a cell death pathway linking the chaperone protein PDI to apoptotic cell death in HD model. Additionally, modification of this pathway has shown promise in other protein misfolding diseases, suggesting that this mechanism associating protein misfolding and apoptotic cell death may have relevance to a broader range of neurodegenerative diseases.

IIc. Future Directions

First and foremost, we would like to identify the binding mode of the small molecule inhibitors to PDI. Efforts aimed at crystallization of the catalytic a domain of PDI have proven unsuccessful to date, likely due to the high solubility of the purified protein. To take advantage of this solubility, solution NMR structure studies have been initiated. Since a solution NMR structure of the PDI a domain has been published¹⁵, this should facilitate studies to determine the residues interacting with the small molecules. Comparison of solution NMRs of the protein with and without compound should demonstrate spectral shifts in the residues responsible for binding to the inhibitors, and allow computer-aided modeling of the binding mode of these small molecules.

Next we would like to determine whether the enzymatic activity of PDI is required for its pro-apoptotic function. For these studies, we will create inactive PDI

mutants and test their efficacy in both the cell culture model of HD and in the MOMP assay. Additionally, we should identify whether additional effector proteins are involved in PDI-induced MOMP. One method for identification of PDI-interacting proteins is to fractionate mitochondria to isolate the mitochondrial membranes, and flow this purified fraction over a column containing resin-immobilized PDI. Proteins binding to PDI can then be identified by mass spectrometry. As an alternative or confirmatory method, we can use shRNAs targeting mitochondrial outer membrane proteins to screen for proteins involved in PDI-induced MOMP. Mitochondria can be isolated from these cell lines, and can be tested for their ability to undergo MOMP upon incubation with purified PDI. Knockdowns which result in loss of PDI-induced MOMP will be candidates for follow-up testing.

Next, as these PDI inhibitors have shown efficacy in models of both HD and Alzheimer's disease ⁵, medicinal chemistry efforts should be undertaken in order to perform animal studies. Our laboratory has established protocols for testing the efficacy of small molecules in a *C. elegans* model of HD in collaboration with the laboratory of Dr. Anne Hart ¹⁶. To perform studies in the R6/2 mouse model of HD ¹⁷ we must first determine and optimize the solubility, pharmacokinetic parameters, metabolic stability and blood-brain barrier penetration capability of these compounds. The activity of compounds produced in this medicinal chemistry effort should be confirmed in our cell culture and *in vitro* assays for PDI inhibition. These studies will enable optimization of these small molecule inhibitors of PDI in order to determine their efficacy in a mammalian HD model. If these compounds prove effective, they could be tested in

animal models of other neurodegenerative diseases resulting from protein misfolding, potentially increasing the scope of diseases that can be ameliorated via PDI inhibition.

References

1. Borasio, G.D., *et al.* ras p21 protein promotes survival and fiber outgrowth of cultured embryonic neurons. *Neuron* 2, 1087-1096 (1989).
2. Heumann, R., *et al.* Transgenic activation of Ras in neurons promotes hypertrophy and protects from lesion-induced degeneration. *J Cell Biol* 151, 1537-1548 (2000).
3. Johnson, L., *et al.* Somatic activation of the K-ras oncogene causes early onset lung cancer in mice. *Nature* 410, 1111-1116 (2001).
4. Rostovtsev, V.V., Green, L.G., Fokin, V.V. & Sharpless, K.B. A stepwise Huisgen cycloaddition process: copper(I)-catalyzed regioselective "ligation" of azides and terminal alkynes. *Angew Chem Int Ed Engl* 41, 2596-2599 (2002).
5. Hoffstrom, B.G., *et al.* Inhibitors of protein disulfide isomerase suppress apoptosis induced by misfolded proteins. *Nat Chem Biol* 6, 900-906 (2010).
6. Leslie, B.J. & Hergenrother, P.J. Identification of the cellular targets of bioactive small organic molecules using affinity reagents. *Chem Soc Rev* 37, 1347-1360 (2008).
7. Speers, A.E. & Cravatt, B.F. Profiling enzyme activities in vivo using click chemistry methods. *Chem Biol* 11, 535-546 (2004).
8. Bos, J.L., Rehmann, H. & Wittinghofer, A. GEFs and GAPs: critical elements in the control of small G proteins. *Cell* 129, 865-877 (2007).
9. Skinner, R.H., *et al.* Use of the Glu-Glu-Phe C-terminal epitope for rapid purification of the catalytic domain of normal and mutant ras GTPase-activating proteins. *J Biol Chem* 266, 14163-14166 (1991).
10. Tcherkezian, J. & Lamarche-Vane, N. Current knowledge of the large RhoGAP family of proteins. *Biol Cell* 99, 67-86 (2007).
11. Rangarajan, A., Hong, S.J., Gifford, A. & Weinberg, R.A. Species- and cell type-specific requirements for cellular transformation. *Cancer Cell* 6, 171-183 (2004).
12. Sonenberg, N. & Gingras, A.C. The mRNA 5' cap-binding protein eIF4E and control of cell growth. *Curr Opin Cell Biol* 10, 268-275 (1998).
13. Svitkin, Y.V., *et al.* Eukaryotic translation initiation factor 4E availability controls the switch between cap-dependent and internal ribosomal entry site-mediated translation. *Mol Cell Biol* 25, 10556-10565 (2005).
14. Haghghat, A., Mader, S., Pause, A. & Sonenberg, N. Repression of cap-dependent translation by 4E-binding protein 1: competition with p220 for binding to eukaryotic initiation factor-4E. *EMBO J* 14, 5701-5709 (1995).
15. Kemmink, J., Darby, N.J., Dijkstra, K., Nilges, M. & Creighton, T.E. Structure determination of the N-terminal thioredoxin-like domain of protein disulfide

- isomerase using multidimensional heteronuclear $^{13}\text{C}/^{15}\text{N}$ NMR spectroscopy. *Biochemistry* 35, 7684-7691 (1996).
16. Varma, H., Cheng, R., Voisine, C., Hart, A.C. & Stockwell, B.R. Inhibitors of metabolism rescue cell death in Huntington's disease models. *Proc Natl Acad Sci U S A* 104, 14525-14530 (2007).
 17. Mangiarini, L., *et al.* Exon 1 of the HD gene with an expanded CAG repeat is sufficient to cause a progressive neurological phenotype in transgenic mice. *Cell* 87, 493-506 (1996).